

NACA RM L54B09

NACA

RESEARCH MEMORANDUM

THE EFFECT OF A CHANGE IN BODY SHAPE ON THE
LOADING OF A 45° SWEEPBACK WING-BODY
COMBINATION AT TRANSONIC SPEEDS

By Donald L. Loving

Langley Aeronautical Laboratory
~~CONFIDENTIAL~~ Langley Field, Va.

UNCLASSIFIED

To _____

By authority of NACA Res also Date effective
+ RN-125 Feb. 26, 1958
AMT 3-20-58

CLASSIFIED DOCUMENT

This material contains information affecting the National Defense of the United States within the meaning of the espionage laws, Title 18, U.S.C., Secs. 793 and 794, the transmission or revelation of which in any manner to an unauthorized person is prohibited by law.

NATIONAL ADVISORY COMMITTEE FOR AERONAUTICS

WASHINGTON

April 2, 1954

NATIONAL ADVISORY COMMITTEE FOR AERONAUTICS

RESEARCH MEMORANDUM

THE EFFECT OF A CHANGE IN BODY SHAPE ON THE
LOADING OF A 45° SWEEPBACK WING-BODY
COMBINATION AT TRANSONIC SPEEDS

By Donald L. Loving

SUMMARY

An investigation was made in the Langley 8-foot transonic tunnel of the pressure distribution on a wing-body combination having a 45° swept-back wing with aspect ratio 4, taper ratio 0.6, and NACA 65A006 airfoil sections parallel to the plane of symmetry. The body had an afterbody which was cylindrical from the region of the leading edge of the wing-body juncture rearward to the base. Data were obtained at Mach numbers from 0.60 to 1.13. The test Reynolds numbers ranged from 1.74×10^6 to 2.03×10^6 . In order to determine the effects on loads of a change in body shape, the results of this investigation are compared with similar data previously obtained for the same wing in combination with a body that was curved from the nose to the base.

The chordwise pressure distributions, which were determined at various spanwise stations, indicate that the flow about the two configurations is the same. Trends in the changes in pressure on the combinations are noticeable with change in body shape even though the changes are small. At subsonic Mach numbers the wing pressures are generally more positive, a condition which indicates less separation as a result of lower induced velocities about the cylindrical body combination. At supersonic Mach numbers, the reduced induced velocities alter the location of the shock-wave system about the cylindrical body combination so that reduced loadings are obtained at the trailing edge of the wing, especially outboard in the region of the usual control surface.

On the body in combination with the wing, changes in pressure of the same magnitude as for the wing resulted from the change in body shape from curved to cylindrical. A decrease in the influence of the wing on the body resulted in less negative pressure coefficients in the region of the wing-body juncture. The pressure coefficients on the afterbody of the cylindrical body were more positive than those on the curved body.

INTRODUCTION

The study of the effect of a change in body shape on the loading on a 45° sweptback wing-body combination was instigated as a result of the observation of the pronounced influence that a precise body shape has on the flow and shock-wave pattern at a Mach number of 1.00. A difference in the flow field extending an appreciable distance away from the body near the speed of sound, as affected by a body shape which was curved toward the rear, has been reported in reference 1.

During the investigation of wing-body interference, a systematic series of body shapes was tested in combination with a 45° sweptback wing in the Langley 8-foot transonic tunnel. On the basis of the results of this investigation, which have been reported in reference 2, it was decided to investigate the effect on loads of the body which, in combination with the wing, produced the lowest drag values and should have caused the largest changes in the flow and shock-wave pattern about the configuration. The results of previous loads investigations for the same wing in combination with a body of different profile shape have been reported in references 3 to 5. A comparison of the data obtained from these investigations provides the material for the study of the effect of a change in body shape on the loading of the wing-body combination.

For the present investigation the pressure measurements were obtained on the wing-body combination having the cylindrical body at angles of attack of 0° , 4° , 8° , 12° , and 20° for a Mach number range from 0.60 to 1.13.

SYMBOLS

b	wing span
c	airfoil section chord, parallel to plane of symmetry
\bar{c}	average wing chord, S/b
c'	mean aerodynamic chord, $\frac{2}{S} \int_0^{b/2} c^2 dy$
d	body section diameter
d_{\max}	body maximum diameter

M	Mach number
P_0	free-stream static pressure
P_1	local static pressure
P	pressure coefficient, $\frac{P_1 - P_0}{q}$
q	free-stream dynamic pressure, $\frac{1}{2} \rho V^2$
R	Reynolds number, $\frac{\rho V c'}{\mu}$
r	body section radius
r_{\max}	body maximum radius
S	total wing area
V	velocity in undisturbed stream
y	distance measured perpendicular to the plane of symmetry in spanwise direction
α	angle of attack of body center line
ρ	mass density in undisturbed stream
μ	coefficient of viscosity in undisturbed stream
C_b	bending-moment coefficient of the exposed wing about the wing-body juncture, $\frac{1}{b(b - d_{\max})} \int_{r_{\max}}^{b/2} \frac{c_n c}{c} (y - r_{\max}) dy$
c_n	wing-section normal-force coefficient, $\frac{1}{c} \int_0^c (P_L - P_U) dx$
$\frac{c_n c}{c}$	section normal-loading coefficient
c_{n_F}	body cross-section normal-force coefficient, $\frac{1}{r} \int_0^r (P_L - P_U) dy$

$\frac{c_{n_f} d}{d_{\max}}$	body cross-section normal-loading coefficient
C_{N_B}	normal-force coefficient of body in presence of wing
C_{N_W}	normal-force coefficient of exposed wing
$C_{N_{WB}}$	total normal-force coefficient of wing-body combination
$\Delta C_{N_{BW}}$	load carryover from wing to body, $C_{N_B} - C_{N_{\text{body alone}}}$
C_{m_W}	pitching-moment coefficient of exposed wing about 25-percent mean-aerodynamic-chord position
$C_{m_{WB}}$	pitching-moment coefficient of wing-body combination about 25-percent mean-aerodynamic-chord position
$C_{T_c}/4$	twisting-moment coefficient about line through 25-percent chord of wing sections

Subscripts:

f	body cross section
L	lower surface of section
U	upper surface of section

APPARATUS

Tunnel.— A description of the Langley 8-foot transonic tunnel giving details of the slotted transonic test section is presented in reference 6. In this facility, the test-section Mach number can be varied continuously from about 0.2 to 1.14 simply by varying the drive power; no discontinuity in operation is experienced at sonic speed. Figure 1 presents the details of the test section of the Langley 8-foot transonic tunnel. The locations of the two models discussed in this report are indicated in terms of the distance from the test-section slot origin to the nose of the bodies.

Model.— The wing used in this investigation had a steel core with a tin-bismuth covering and was the same wing as that used in the previous loads investigations of references 3 to 5. This wing had 45° of sweepback

of the quarter-chord line, an aspect ratio of 4, and was 6 percent thick. As shown in figure 2, the curved body of references 1, 3, 4, and 5, and referred to as body A in reference 2, had a curved profile from the nose to the base. The cylindrical body of the present investigation was developed by extending the curved forebody forward a distance equal to twice the maximum diameter and then making the body cylindrical from the leading edge of the wing to a plane behind the trailing edge of the wing tip, which is equivalent to making an infinite-fineness-ratio body. This body was referred to as body D in reference 2. The wing remained in approximately the same position relative to the base of the body for both investigations. (See fig. 2.) The steel cylindrical body had 156 static-pressure orifices distributed among 6 meridians on the body, designated by the angular displacements of the meridians 0° , 45° , 75° , 105° , 135° , and 180° from the upper to the lower surface (fig. 2).

An attempt was made to maintain the model aerodynamically smooth throughout the investigation. Details of the manner in which the models were sting supported are presented in figure 1. A photograph of the curved body model mounted in the slotted test section of the tunnel is presented as figure 3.

MEASUREMENTS AND ACCURACY

The tests were made for a Mach number range from 0.60 to 1.13 at angles of attack of 0° , 4° , 8° , 12° , and 20° . The average Reynolds number varied between 1.74×10^6 and 2.03×10^6 for these tests as shown in figure 4.

The accuracy of the pressure coefficients, based on repeatability of data, is believed to be ± 0.006 and the free-stream Mach number is believed to be accurate to within ± 0.003 .

The angle of attack of the model was derived from the sting angle (an electrical strain-gage unit was mounted in the sting) and a correction was obtained by determining the deflection of the model under applied normal load and pitching moments. The angle-of-attack measurements, also corrected for air-stream angularity, are believed to be accurate to within $\pm 0.10^\circ$.

RESULTS AND DISCUSSION

All data presented are for the wing in combination with the body or the body in combination with the wing and therefore include the mutual

effect of one on the other. The terms "cylindrical body" and "curved body" serve to identify the two wing-body combinations studied.

Basic Pressure Measurements

Wing section characteristics.- The chordwise pressure distributions for the wing in combination with the cylindrical body presented in figure 5 illustrate the variations in the upper- and lower-surface pressure coefficients at five spanwise stations for angles of attack of 0° , 4° , 8° , 12° , and 20° throughout the test Mach number range from 0.60 to 1.13. Included in the figures for purposes of comparison are the chordwise pressure distributions for the same wing in combination with the curved body at the same angles of attack and for Mach numbers of 0.60, 0.94, 0.99, and 1.13. These data were obtained from references 3 and 4.

The chordwise pressure coefficients for these four Mach numbers indicate that a change in body shape from curved to cylindrical produced only small changes in pressure loading over the wing throughout the Mach number range investigated. As shown by the data at angles of attack of 0° , 4° , and 8° and subsonic speeds at Mach numbers from 0.60 to 0.95 (figs. 5(a) to 5(e)), the changes were in the form of small adjustments, mostly in a positive direction, in the level of negative pressure coefficients. This trend is indicative of less separation over the wing panel as a result of reductions in induced velocities in the flow field about the cylindrical body compared with the curved body. At 12° angle of attack, separation was so severe over the exposed wing that the trend toward lower section loads is noticeable only on the most inboard station of the wing on the cylindrical body. For some unknown reason, at 20° angle of attack, slightly higher loads were obtained on the wing in combination with the cylindrical body than with the curved body.

At supersonic speeds, the small changes in wing pressures were due mainly to the changes in the location of the shock-wave system as the result of the decrease in the induced velocities associated with the flow about the cylindrical body. The most pronounced of these slight changes at supersonic speeds may be seen in the region of the trailing edge on the outer part of the wing and hence would have an effect on any control surfaces located in this region. For example, at an angle of attack of 8° and Mach numbers of 1.00 and 1.13, the largest changes in wing pressure are mainly at the tip region of the wing. A shock pattern, similar to that described in references 1 and 4, occurred across the span near the trailing edge and caused separation as shown by the flat pressure distributions toward the tip. Primarily because of body shape, the shock pattern of the cylindrical body was shifted forward slightly and the separation effects were less extensive on the outboard stations.

Body section characteristics.- The longitudinal pressure distributions for the cylindrical body in combination with the wing along each of six meridian lines, as illustrated in figure 2, are given in figure 6 for angles of attack of 0° , 4° , 8° , 12° , and 20° at Mach numbers from 0.60 to 1.13. Again, for purposes of comparison, longitudinal pressures on the curved body as obtained from references 3 and 4 are included for the same angles of attack and for Mach numbers of 0.60, 0.94, 0.99, and 1.13. The pressure coefficients on the body at the wing-body juncture are affected in approximately the same manner as that shown for the wing by the change in body shape from curved to cylindrical. The distribution of pressure coefficients on the cylindrical body in the region of the wing has the same shape and trend with increase in angle of attack and Mach number as shown in reference 4 for the curved body. The values of pressure coefficient are more positive for the cylindrical-body combination, however, throughout the test Mach number range, a condition which leads to reductions in local loading in the region of the wing-body juncture at all angles of attack except 20° . At this angle of attack, the pressure coefficients were more positive on the lower half of the body in the region of the wing, and more negative for some of the meridians on the upper half of the body, a condition which leads to greater total loading on the cylindrical body than on the curved body.

As might be expected, the pressure coefficients on the two afterbodies are different (more positive on the cylindrical body) because of the change in body shape. The more negative pressure coefficients on the curved body are directly associated with drag-producing energy losses which occur in the stream at a distance out from the configuration. The more positive pressure coefficients for the cylindrical body are an indication that the energy losses in the stream are not as severe as for the curved body and therefore a lower drag rise may be expected. This condition is especially true for the data at Mach numbers of 1.00 and 1.13 which show large decreases in the level of negative pressure coefficient when the body shape is changed from curved to cylindrical. These findings are in complete agreement with the concepts of the transonic drag-rise rule (ref. 7) and indicate the flow associated with the lower drag rise obtained for the cylindrical-body combination compared with the curved-body combination as reported in reference 2.

The more negative pressure coefficients at the base of the cylindrical body compared with those of the curved body are the result of accelerated flow around the sharp cornered discontinuity at the model base in the region of the simulated juncture of the model support sting and body. (See fig. 2.)

Loading and Aerodynamic Characteristics

Spanwise loading characteristics.- A comparison of the spanwise loading distributions obtained from the integrated pressure distributions

for the wing in combination with the cylindrical body and the curved body are given in figure 7 for total normal-force coefficients of 0.2, 0.4, 0.6, and 0.8 and Mach numbers of 0.60, 0.95, 1.00, and 1.13. The data at Mach numbers of 0.95 and 1.00 for the curved body were obtained from interpolation of the results presented in references 3 to 5. Included in this figure is the average of the total section loadings on the body which were obtained by integrating over the body length the previously integrated body axial section loads. As might be expected from the discussion of the pressure distributions, the variations in spanwise loading due to a change in body shape are small. The shapes of the curves of the spanwise loading distribution are approximately the same for both wing-body combinations being considered. On the other hand, several definite trends are noted in the level of spanwise loading with change in body shape: (1) At a normal-force coefficient of 0.6, the loading is less at Mach numbers of 0.95 and 1.00 for the outboard portion of the wing on the cylindrical body than on the curved body. This result can be traced to the decrease in the level of negative pressure coefficients on the upper surface of the outboard wing sections as a result of the reduced induced velocities associated with the cylindrical body. (2) At a normal-force coefficient of 0.8, the loading is noticeably less on the 20-percent-semispan station of the wing on the cylindrical body throughout the Mach number range. As explained in the discussion of the pressure distributions, separation was severe on the outboard sections of the wing at an angle of attack of 12° , which corresponds to a normal-force coefficient of approximately 0.8. Therefore, the effect of a change in body shape was confined to the inboard section of the wing. (3) At a Mach number of 1.13 and for any given normal-force coefficient from 0.2 to 0.8, the loading for the wing on the cylindrical-body configuration is uniformly less across the span than for the curved-body configuration. This reduction in loading may be explained by the fact that for a given total normal-force coefficient at supersonic speeds, a greater portion of the load is carried by the body than at subsonic speeds and, for the cylindrical-body configuration, an even greater percentage of the load is carried by the body than for the curved-body case.

Normal-force characteristics.- The variation of angle of attack and exposed wing normal-force coefficient with total normal-force coefficient, as shown in figure 8, indicates that the trends in loading with angle of attack and Mach number for the cylindrical-body and curved-body configurations are practically the same. The results of figure 8 indicate that the percentage of total load carried by the cylindrical body is slightly greater than for the curved body at Mach numbers of 0.60, 1.00, and 1.13. This result is substantiated in figure 9. The average of the total load carried by the bodies is between 15 and 16 percent up to a total normal-force coefficient of approximately 0.65. Thereafter the rate at which the percentage of total load carried by the body varies with increase in total normal-force coefficient decreases progressively with increase in Mach number from 0.60 to 1.13.

The influence of the change in body shape on the load carryover from the wing to the body is indicated in figure 10. The results were obtained by subtracting the load on the body alone from the load on the body when in combination with the wing for both configurations. Data for the cylindrical body alone were obtained from reference 8. The effect of wing-body interference appears to increase with increase in angle of attack, but to remain fairly constant throughout the Mach number range for a given angle of attack. The data indicate that the interference from the wing on the cylindrical body is slightly less than that for the wing on the curved body. The largest reduction in interference occurred at an angle of attack of 20° . The results of longitudinal loading on the body shown in figure 11 for a Mach number of 1.00 indicate that the reduction in interference at angles of attack of 4° , 8° , and 12° is due mainly to a reduction in the lift carryover from the wing to the body in the region of the wing-body juncture. It is shown also in figure 11 that the reduction in interference at 20° angle of attack was due primarily to the influence of the wing on the load ahead of the wing and the reduction of separation effects over the cylindrical afterbody.

Lateral position of center of pressure.- In figure 12, it is shown that for a given exposed wing normal-force coefficient, very little change in the lateral position of the center of pressure resulted from a change in body shape. Except for a slight outboard shift in center of pressure for the wing on the cylindrical body at a Mach number of 0.95 and between normal-force coefficients of 0.50 and 0.71, the general trend with a change in body shape from curved to cylindrical was a small but definite inboard shift in the center of pressure. The largest shift occurred at a Mach number of 0.95 and a normal-force coefficient of 0.24 amounting to approximately 3 percent of the semispan.

Bending-moment characteristics.- It was reported in reference 9 that the most outboard location of the spanwise center of pressure generally represents the critical conditions for maximum root bending moments.

Additional study of the data herein indicates that the bending-moment coefficients do not necessarily decrease after the lateral position of the center of pressure moves inboard from its most outboard location. Actually, it increases again as shown in figure 13. The inflection in the curves is noted at all subsonic Mach numbers and is most pronounced at a Mach number of 0.95. At supersonic Mach numbers of 1.03, 1.08, and 1.10 data were not obtained at angles of attack high enough to show the nature of the curve beyond the point of nonlinearity, but it is assumed that the variation with exposed-wing normal-force coefficient would be similar to that shown for Mach numbers of 1.00 and 1.13. Therefore, if, as was discussed in reference 10, the airplane experiences pitch-up and inadvertently overshoots the upper limit of the V-g diagram

in normal use, the bending moments will increase, exceed the design limits, and become more critical.

The change in body shape from curved to cylindrical produced only small changes in bending-moment coefficient. Of these small changes, the most noticeable is in the form of a decrease in bending-moment coefficient at the high values of wing loading.

Pitching-moment characteristics.- The effect of the change in body shape from curved to cylindrical resulted in slightly larger changes in the stability characteristics between the two configurations than in the loading characteristics. Mainly, the degree of stability was affected as shown in figure 14. The wing on the cylindrical body exhibited less stable characteristics than the wing on the curved body as a result of the decrease in loading at the trailing edge of the wing. This decrease in loading at the trailing edge produced a forward shift in the chordwise center of pressure as shown in figure 15. This effect appears to be more pronounced at low values of normal-force coefficient up to a Mach number of 1.00 and at the higher values of normal-force coefficient at a Mach number of 1.13.

The pitch-up characteristics appeared to be affected only at a Mach number of 0.60. The use of the cylindrical body tended to alleviate the pitch-up associated with the curved-body combination at this Mach number.

The variation of pitching-moment coefficient with normal-force coefficient for the wing-body combination indicates that the cylindrical-body contribution to the stability characteristics of the combination generally was in the direction of more positive pitching-moment coefficients for a given total normal-force coefficient.

Twisting-moment characteristics.- The difference in the twisting-moment coefficient between the curved-body and cylindrical-body combinations as shown in figure 16 is small, but a definite trend may be noted. Negative values indicate a washout tendency at the tips. At moderate subsonic Mach numbers, the negative twisting-moment coefficient was larger for the wing on the cylindrical body. This effect is a result of the small reductions in loading which occurred on the forward portion of the wing at these subsonic speeds as shown by the more positive pressure coefficients on the forward portion of the wing upper surface for the cylindrical-body combination compared to the curved-body combination. The results at the transonic and supersonic Mach numbers indicate that the load at the trailing edge of the sections is less for the wing on the cylindrical body than on the curved body. Apparently, the largest difference in twisting-moment coefficient occurs between Mach numbers of 0.85 and 0.95, a condition which results in a maximum decrease of 0.01 when the body shape is changed from curved to cylindrical.

CONCLUDING REMARKS

An investigation was made in the Langley 8-foot transonic tunnel of the pressure distribution on a wing-body combination having a 45° swept-back wing with aspect ratio 4, taper ratio 0.6, and NACA 65A006 airfoil sections parallel to the plane of symmetry. The body had an afterbody which was cylindrical from the region of the leading edge of the wing-body juncture rearward to the base. Data were obtained at Mach numbers from 0.60 to 1.13. The test Reynolds numbers ranged from 1.74×10^6 to 2.03×10^6 . In order to determine the effects on loads of a change in body shape, the results of this investigation were compared with similar data previously obtained for the same wing in combination with a body that was curved from the nose to the base.

The results of the investigation indicate that the changes in loading were small with the loading generally being less on the cylindrical-body combination than on the curved-body combination. At subsonic speeds, the small changes were due to reduced induced velocities about the cylindrical-body combination. At transonic and supersonic speeds, the reduced loadings were mainly at the trailing edge and toward the tip of the wing on the cylindrical body and resulted from changes in the position of the shock-wave pattern and reductions in flow separation near the wing trailing edge.

On the body in combination with the wing, changes in pressure of the same magnitude as for the wing resulted from the change in body shape from curved to cylindrical. A decrease in the influence of the wing on the cylindrical body resulted in less negative pressure coefficients in the region of the wing-body juncture. The pressure coefficients on the afterbody of the cylindrical body were more positive than those on the curved body.

Langley Aeronautical Laboratory,
National Advisory Committee for Aeronautics,
Langley Field, Va., January 26, 1954.

REFERENCES

1. Whitcomb, Richard T., and Kelly, Thomas C.: A Study of the Flow Over a 45° Sweptback Wing-Fuselage Combination at Transonic Mach Numbers. NACA RM L52D01, 1952.
2. Loving, Donald L., and Wornom, Dewey E.: Transonic Wind-Tunnel Investigation of the Interference Between a 45° Sweptback Wing and a Systematic Series of Four Bodies. NACA RM L52J01, 1952.
3. Loving, Donald L., and Estabrooks, Bruce B.: Transonic-Wing Investigation in the Langley 8-Foot High-Speed Tunnel at High Subsonic Mach Numbers and at a Mach Number of 1.2. Analysis of Pressure Distribution of Wing-Fuselage Configuration Having a Wing of 45° Sweepback, Aspect Ratio 4, Taper Ratio 0.6, and NACA 65A006 Airfoil Section. NACA RM L51F07, 1951.
4. Loving, Donald L., and Williams, Claude V.: Basic Pressure Measurements on a Fuselage and a 45° Sweptback Wing-Fuselage Combination at Transonic Speeds in the Slotted Test Section of the Langley 8-Foot High-Speed Tunnel. NACA RM L51F05, 1951.
5. Loving, Donald L., and Williams, Claude V.: Aerodynamic Loading Characteristics of a Wing-Fuselage Combination Having a Wing of 45° Sweepback Measured in the Langley 8-Foot Transonic Tunnel. NACA RM L52B27, 1952.
6. Ritchie, Virgil S., and Pearson, Albin O.: Calibration of the Slotted Test Section of the Langley 8-Foot Transonic Tunnel and Preliminary Experimental Investigation of Boundary-Reflected Disturbances. NACA RM L51K14, 1952.
7. Whitcomb, Richard T.: A Study of the Zero-Lift Drag-Rise Characteristics of Wing-Body Combinations Near the Speed of Sound. NACA RM L52H08, 1952.
8. Robinson, Harold L.: Pressures and Associated Aerodynamic and Load Characteristics for Two Bodies of Revolution at Transonic Speeds. NACA RM L53L28a, 1953.
9. Williams, Claude V., and Kuhn, Richard E.: A Study of Aerodynamic Loads on Sweptback Wings at Transonic Speeds. NACA RM L53E08b, 1953.
10. Campbell, George S., and Weil, Joseph: The Interpretation of Nonlinear Pitching Moments in Relation to the Pitch-Up Problem. NACA RM L53I02, 1953.

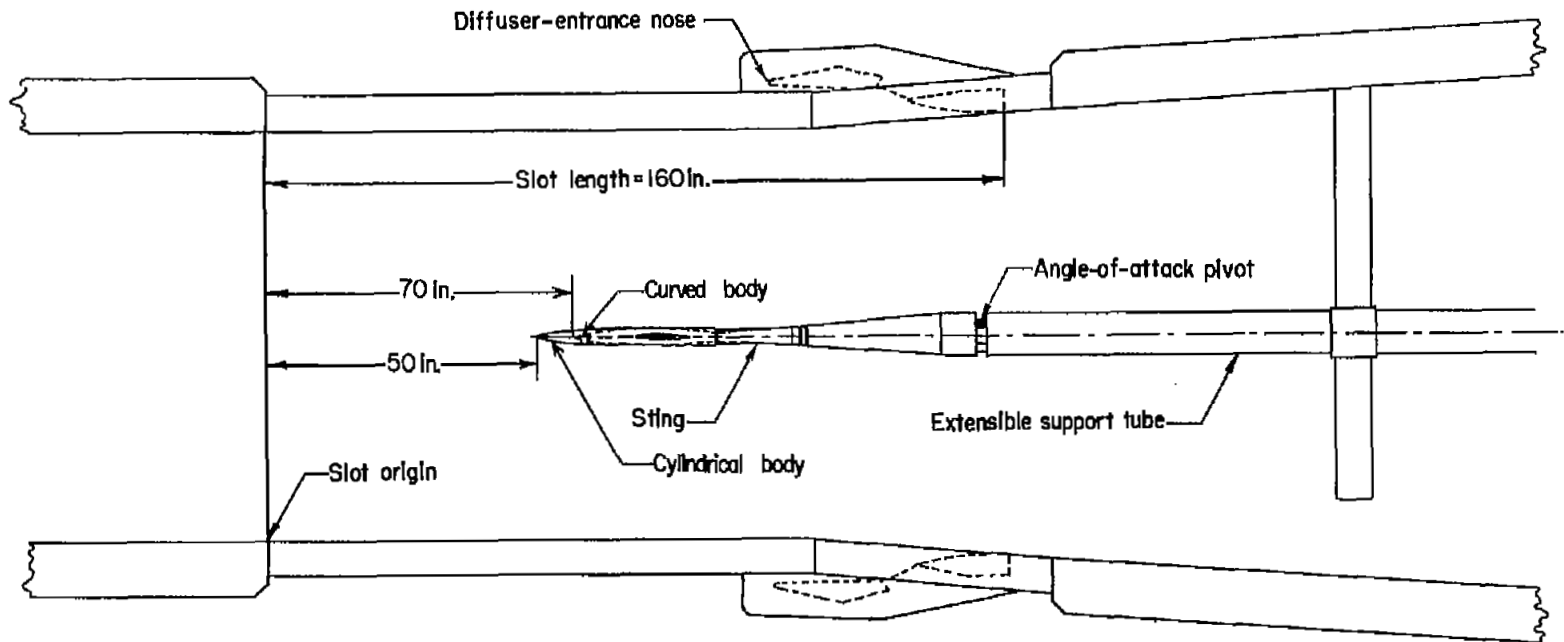


Figure 1.- Details of test section and location of model in Langley 8-foot transonic tunnel.

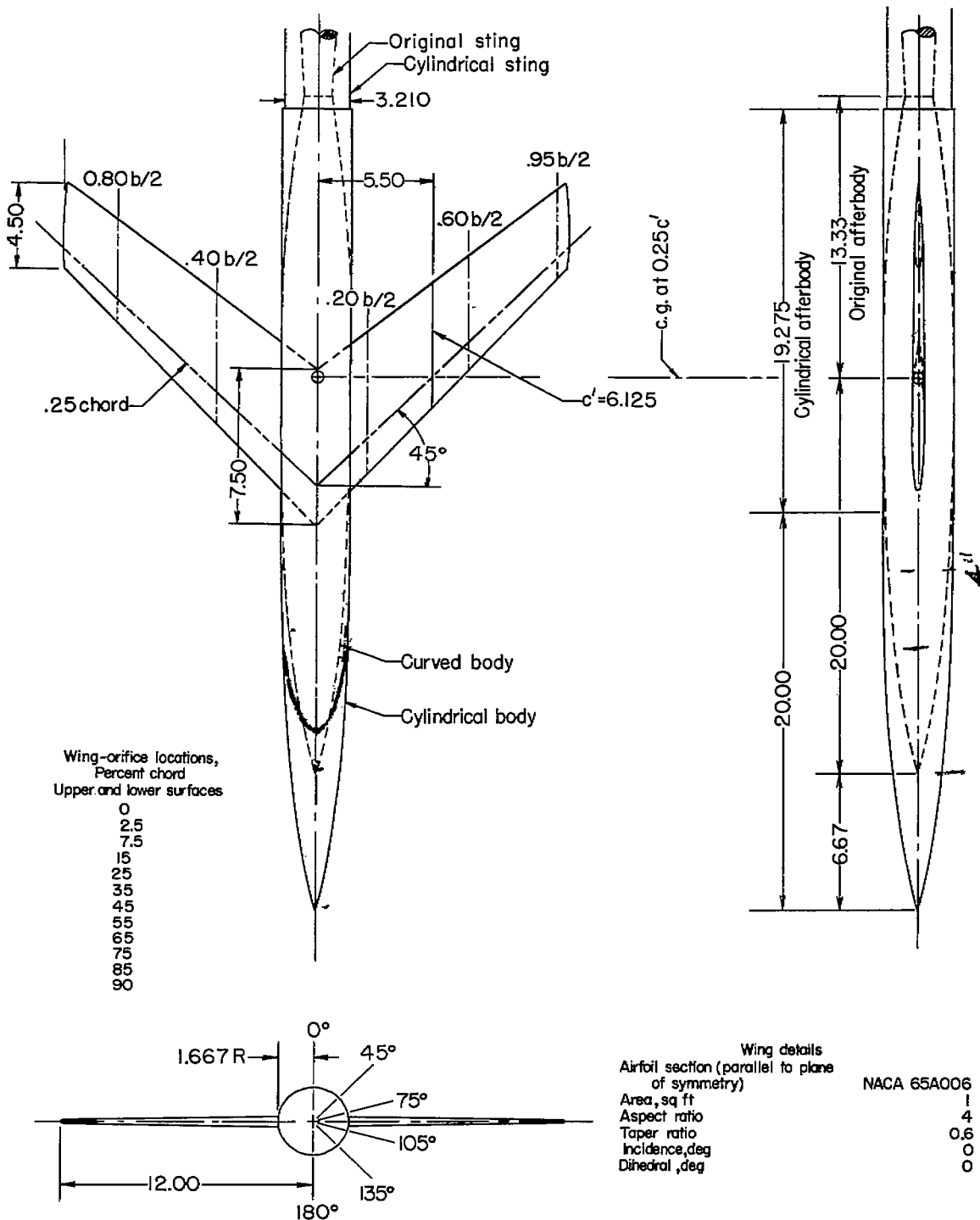


Figure 2.- General arrangement of test models and pressure orifice stations.
(All dimensions are in inches except as otherwise noted.)



L-68983

Figure 3.- Typical installation of model (curved body) in Langley 8-foot transonic tunnel.

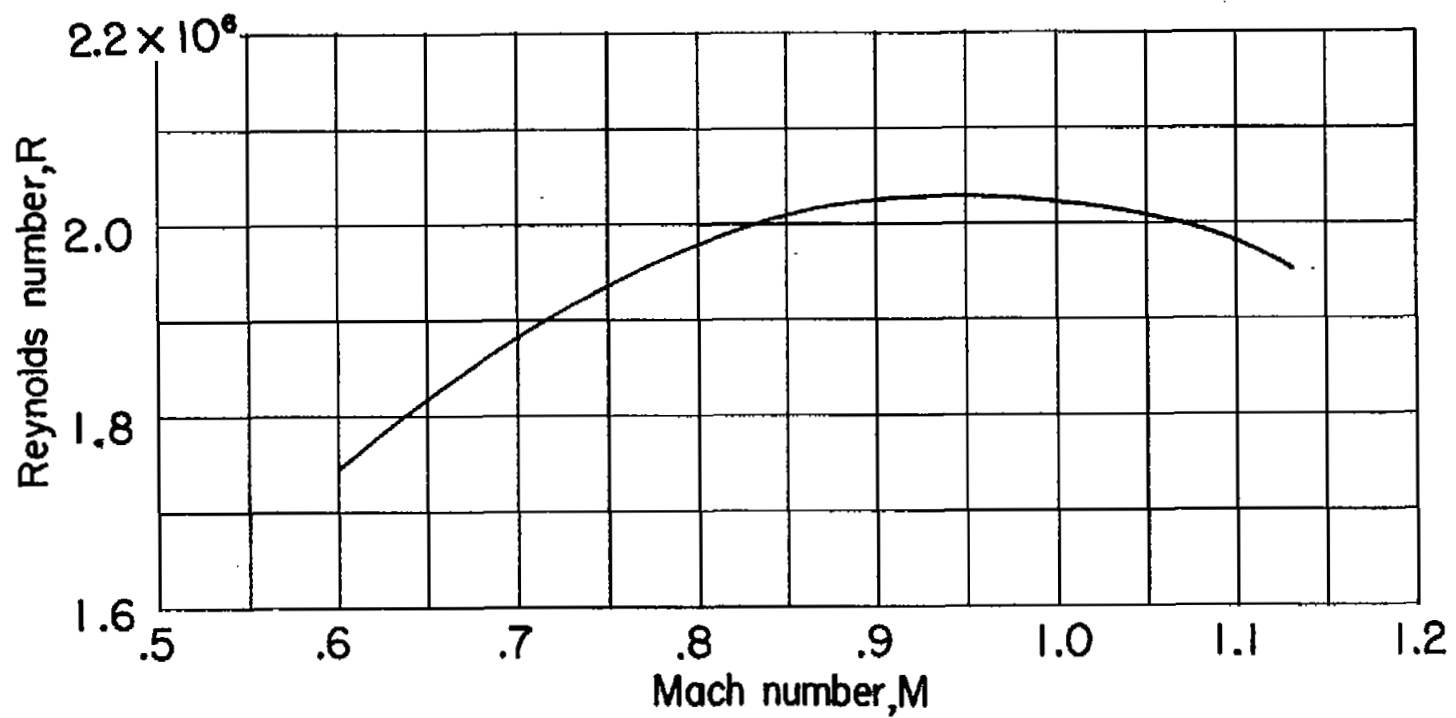
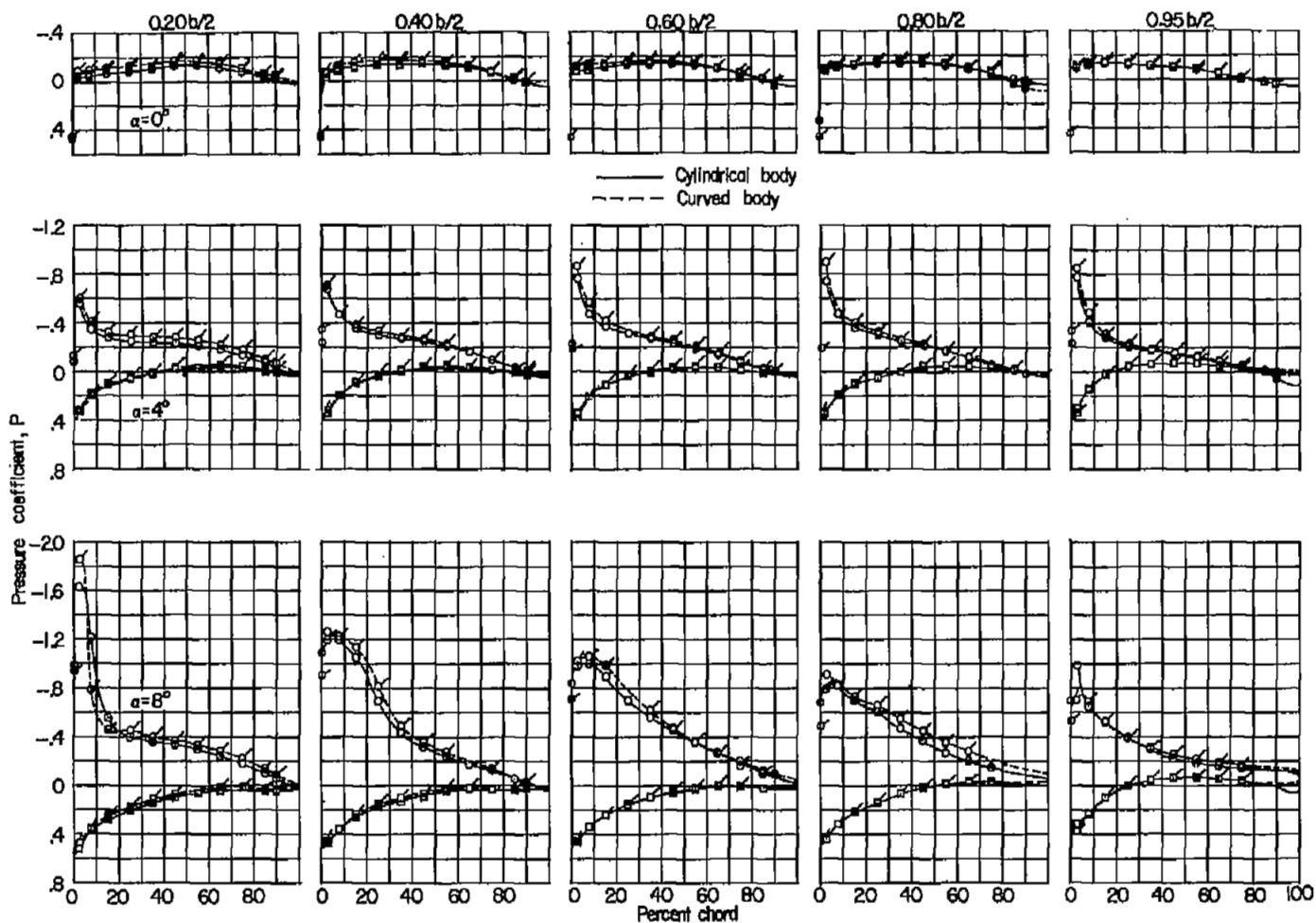
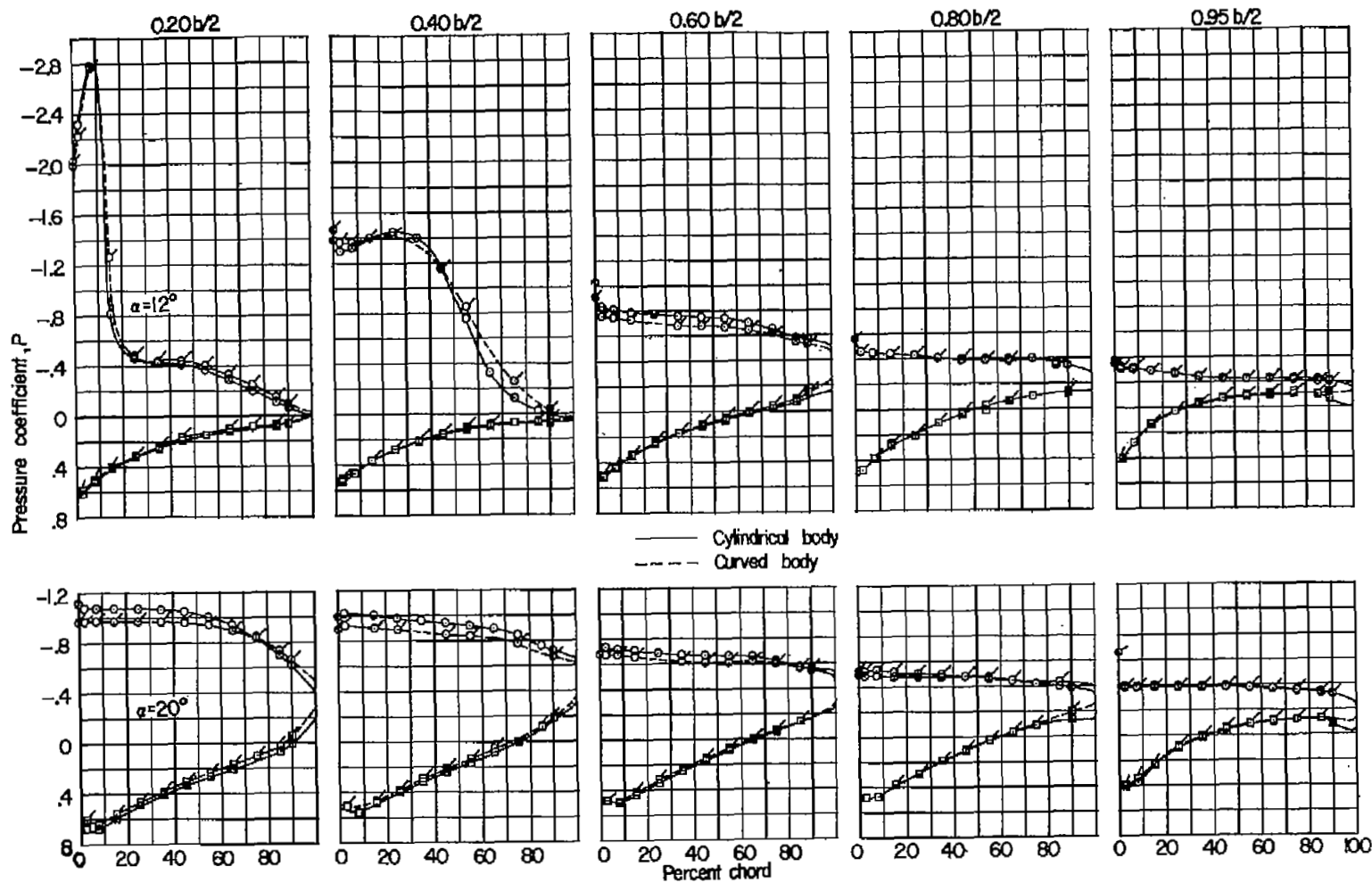


Figure 4.- Variation with Mach number of average test Reynolds number based on mean aerodynamic chord of 6.125 inches.



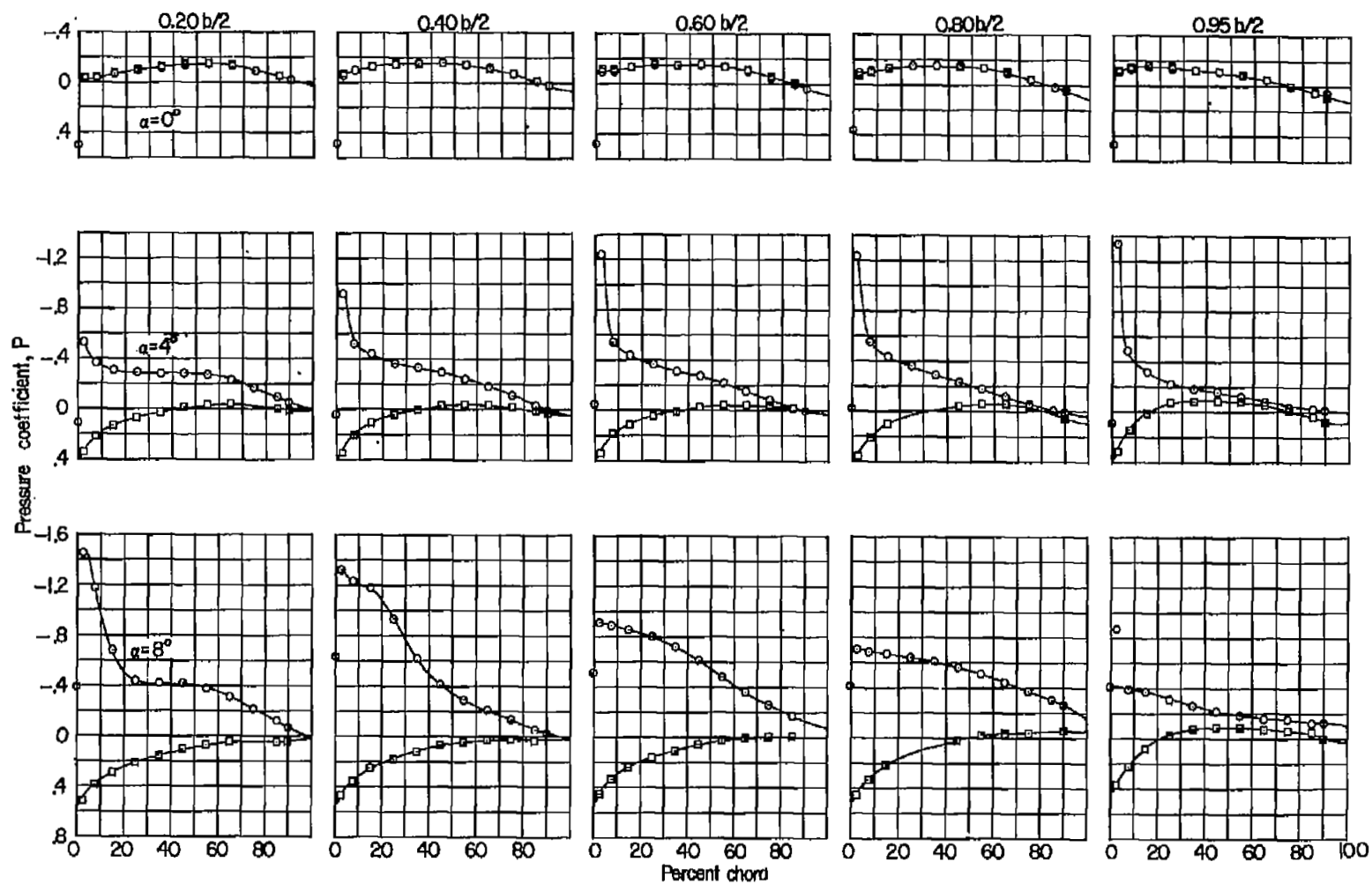
(a) $M = 0.60$; $\alpha = 0^\circ$, 4° , and 8° .

Figure 5.- Chordwise pressure distribution at five spanwise stations on wing in combination with cylindrical body for various angles of attack. Flagged symbols indicate curved-body configuration.



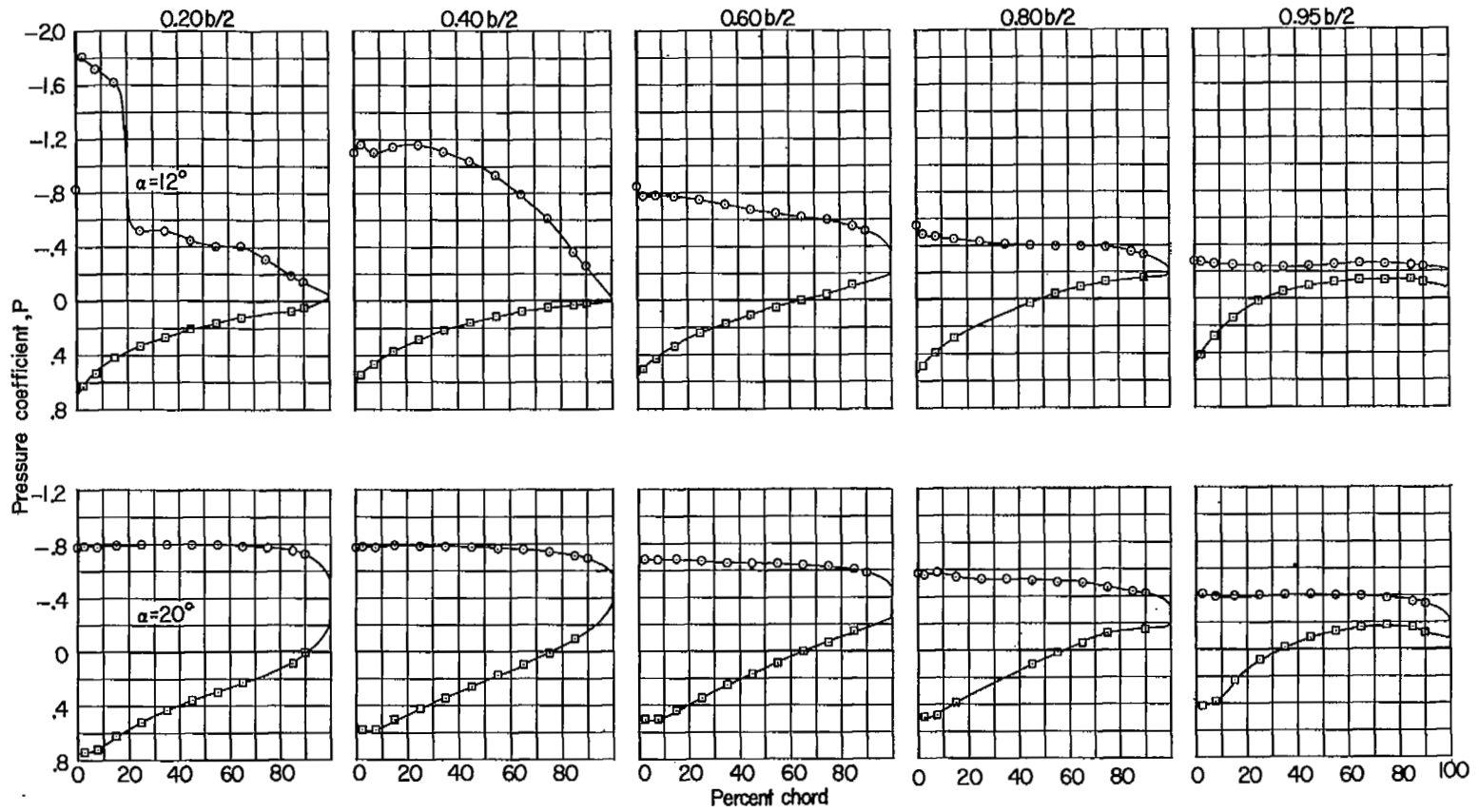
(a) $M = 0.60$; $\alpha = 12^\circ$ and 20° . Concluded.

Figure 5.- Continued.



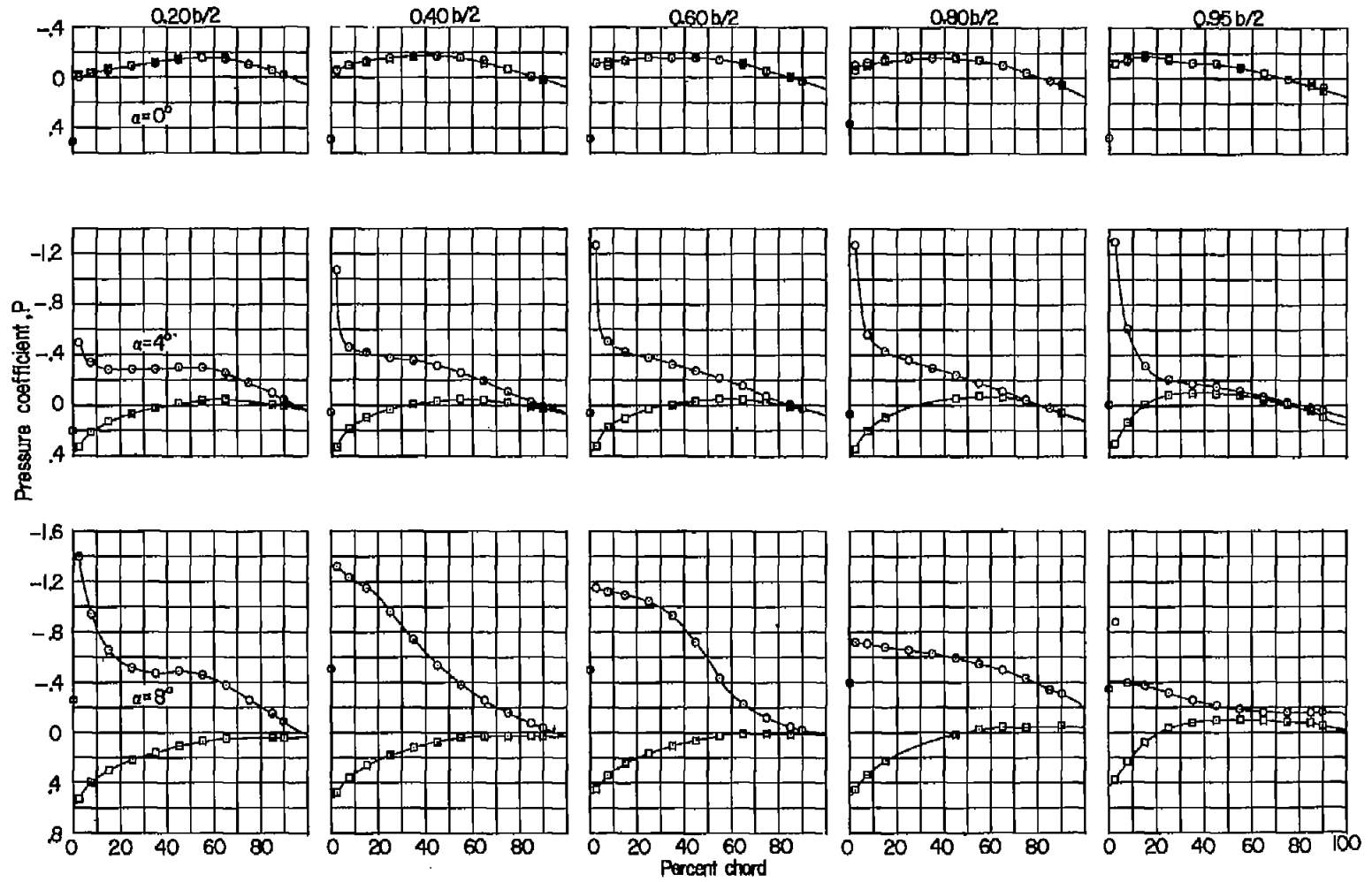
(b) $M = 0.80$; $\alpha = 0^\circ, 4^\circ, \text{ and } 8^\circ$.

Figure 5.- Continued.



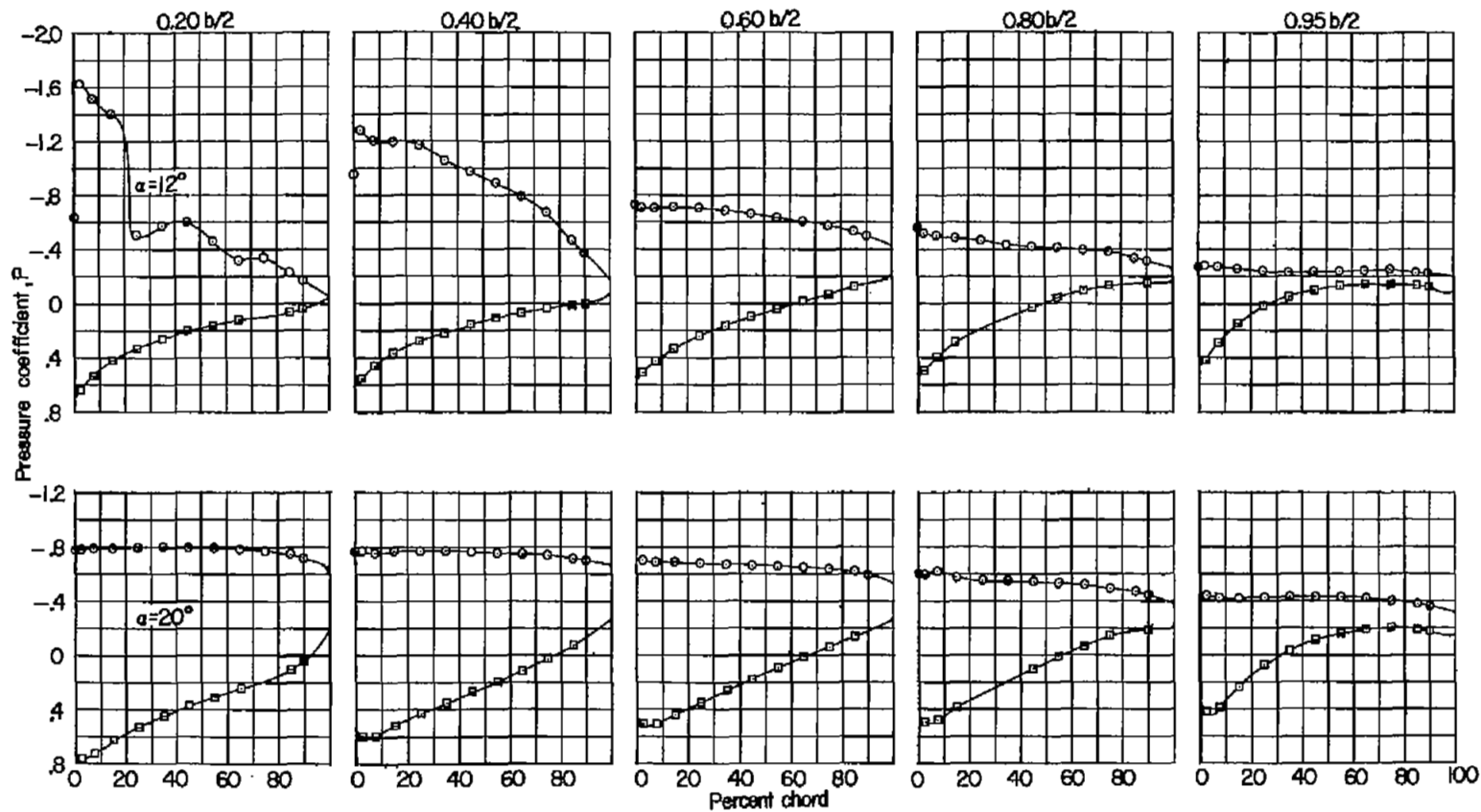
(b) $M = 0.80$; $\alpha = 12^\circ$ and 20° . Concluded.

Figure 5.- Continued.



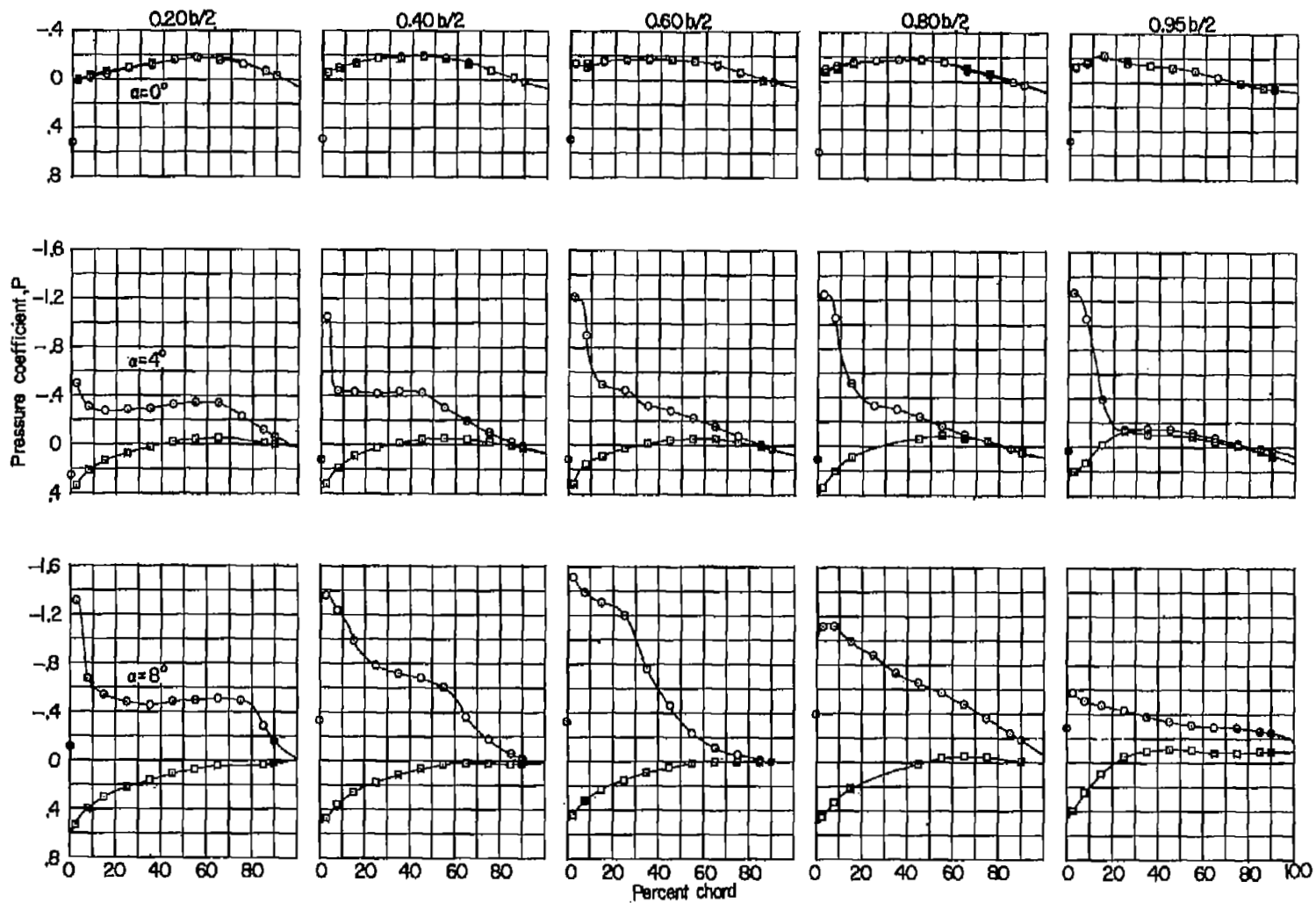
(c) $M = 0.85$; $\alpha = 0^\circ, 4^\circ, \text{ and } 8^\circ$.

Figure 5.- Continued.



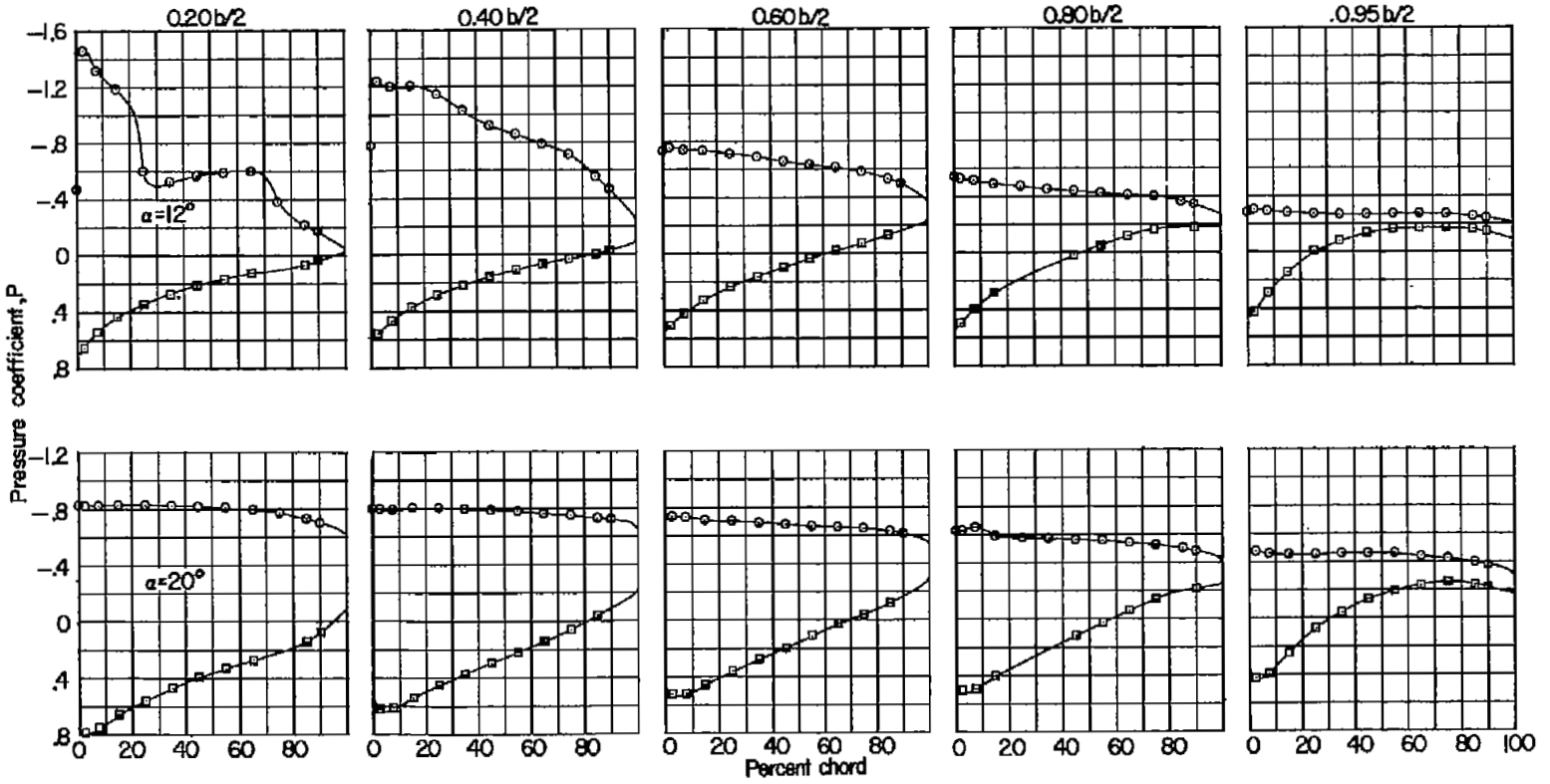
(c) $M = 0.85$; $\alpha = 12^\circ$ and 20° . Concluded.

Figure 5.- Continued.



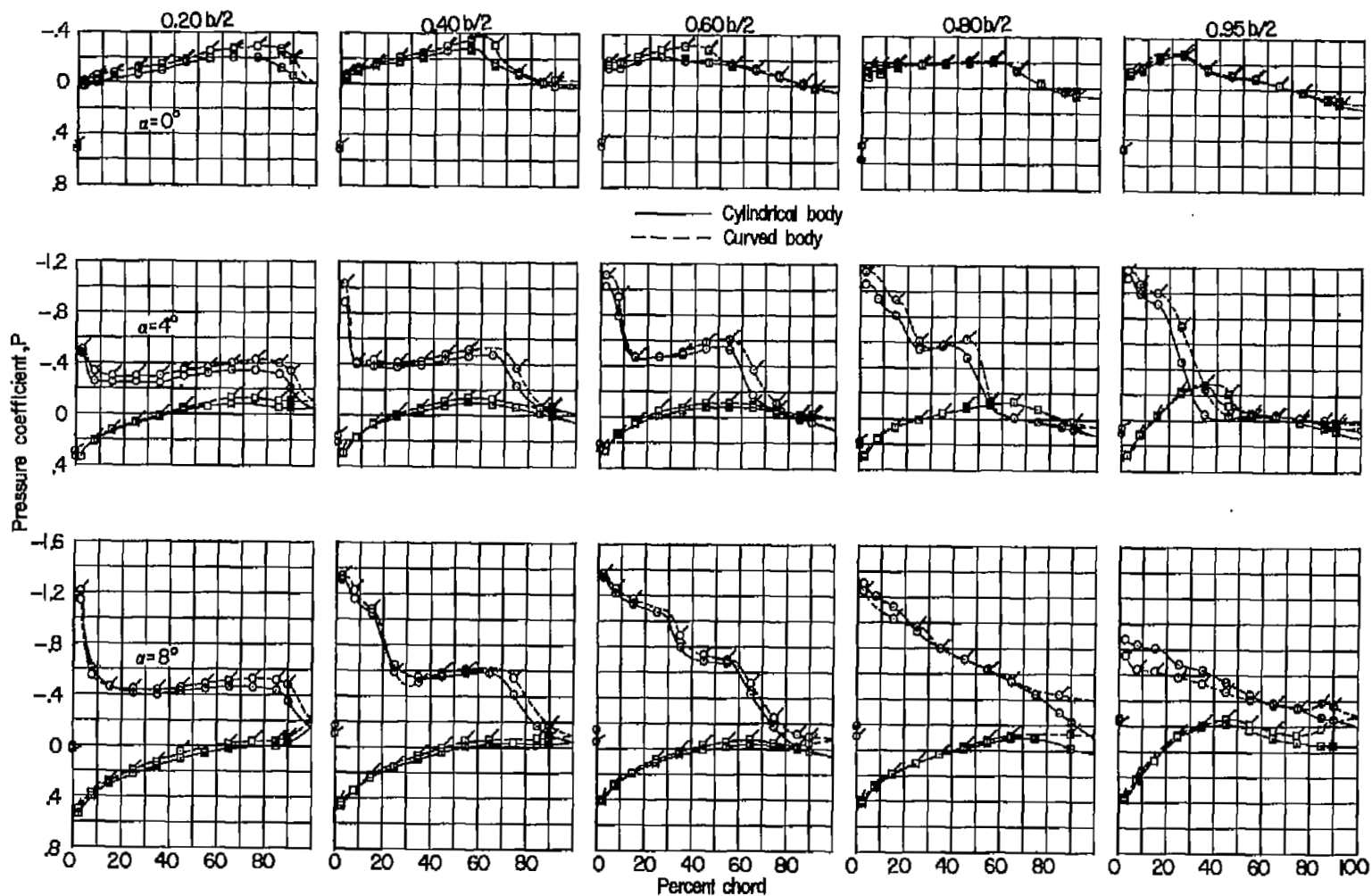
(d) $M = 0.90$; $\alpha = 0^\circ, 4^\circ, \text{ and } 8^\circ$.

Figure 5.- Continued.



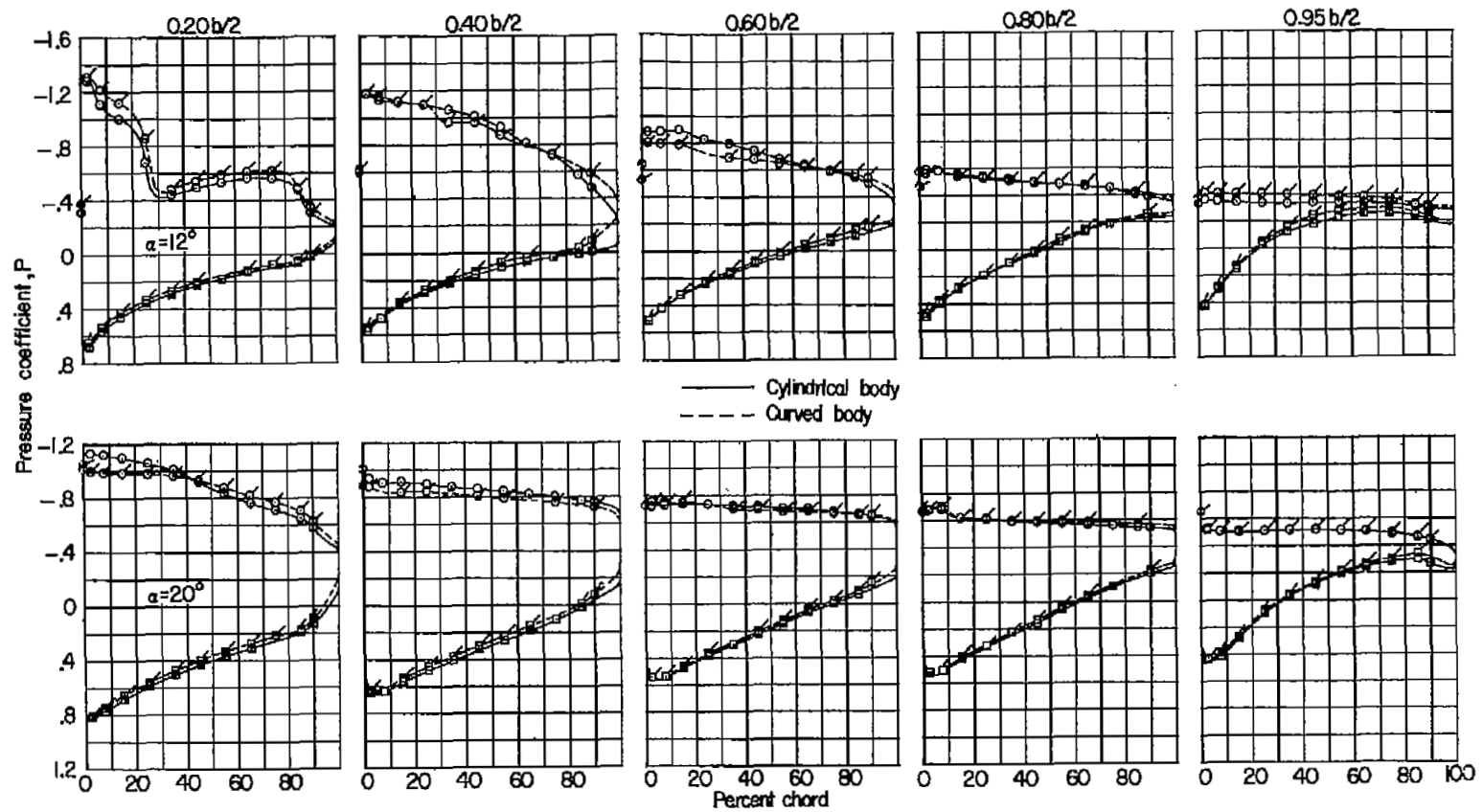
(d) $M = 0.90$; $\alpha = 12^\circ$ and 20° . Concluded.

Figure 5.- Continued.



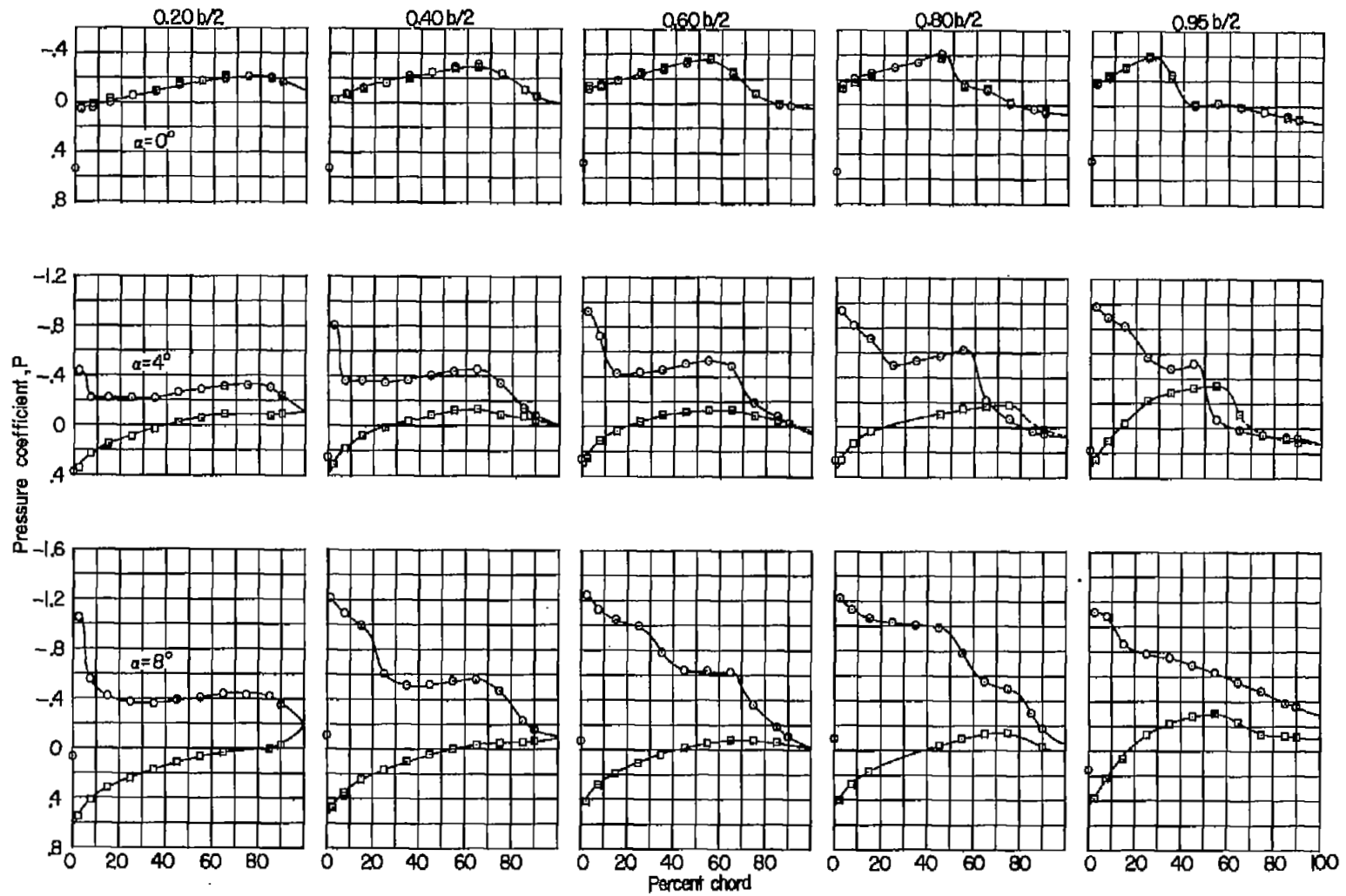
(e) Cylindrical body, $M = 0.95$; curved body, $M = 0.94$; $\alpha = 0^\circ$, 4° , and 8° .

Figure 5.- Continued.



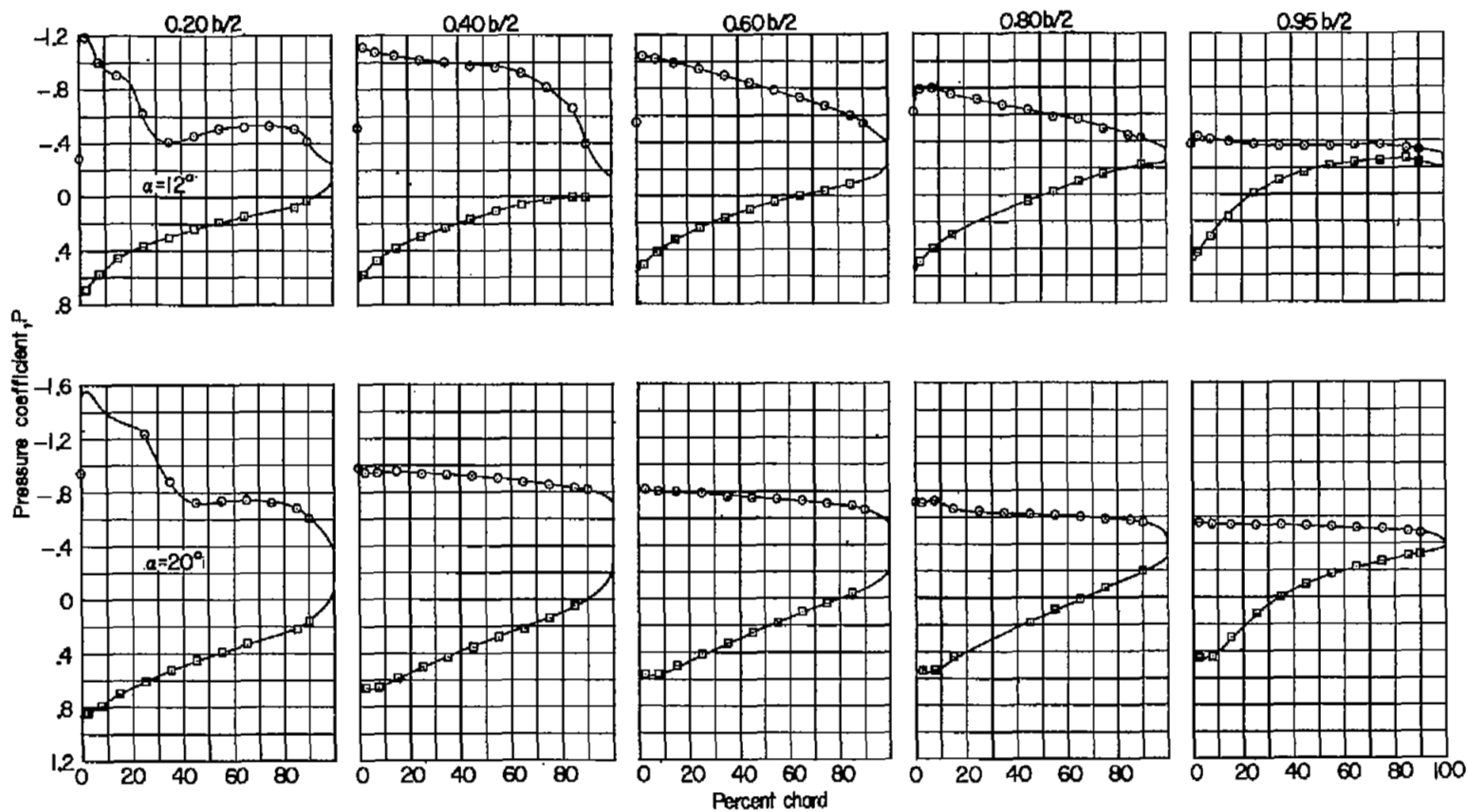
(e) Cylindrical body, $M = 0.95$; curved body, $M = 0.94$; $\alpha = 12^\circ$ and 20° .
Concluded.

Figure 5.- Continued.



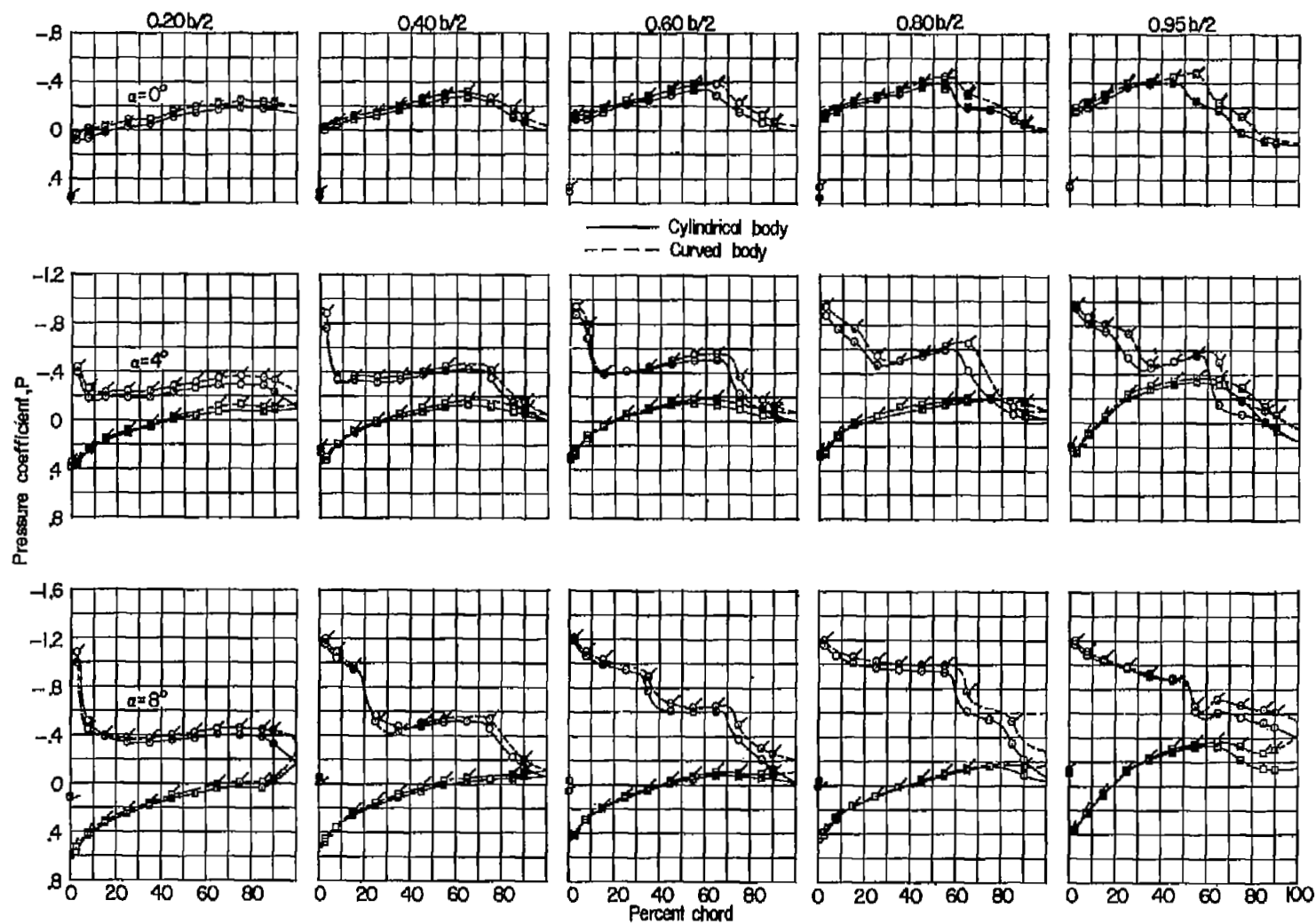
(f) $M = 0.98$; $\alpha = 0^\circ, 4^\circ, \text{ and } 8^\circ$.

Figure 5.- Continued.



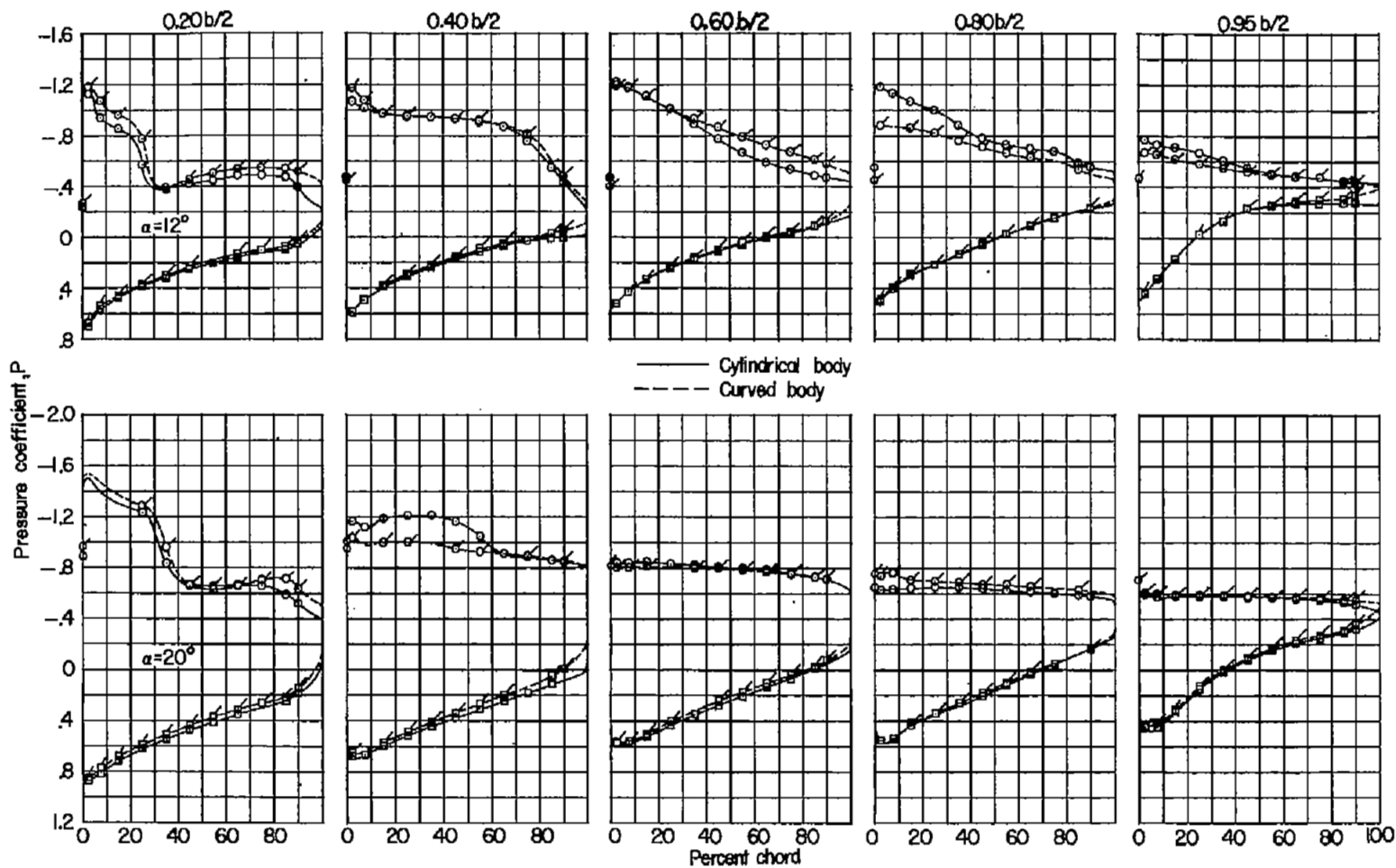
(f) $M = 0.98$; $\alpha = 12^\circ$ and 20° . Concluded.

Figure 5.- Continued.



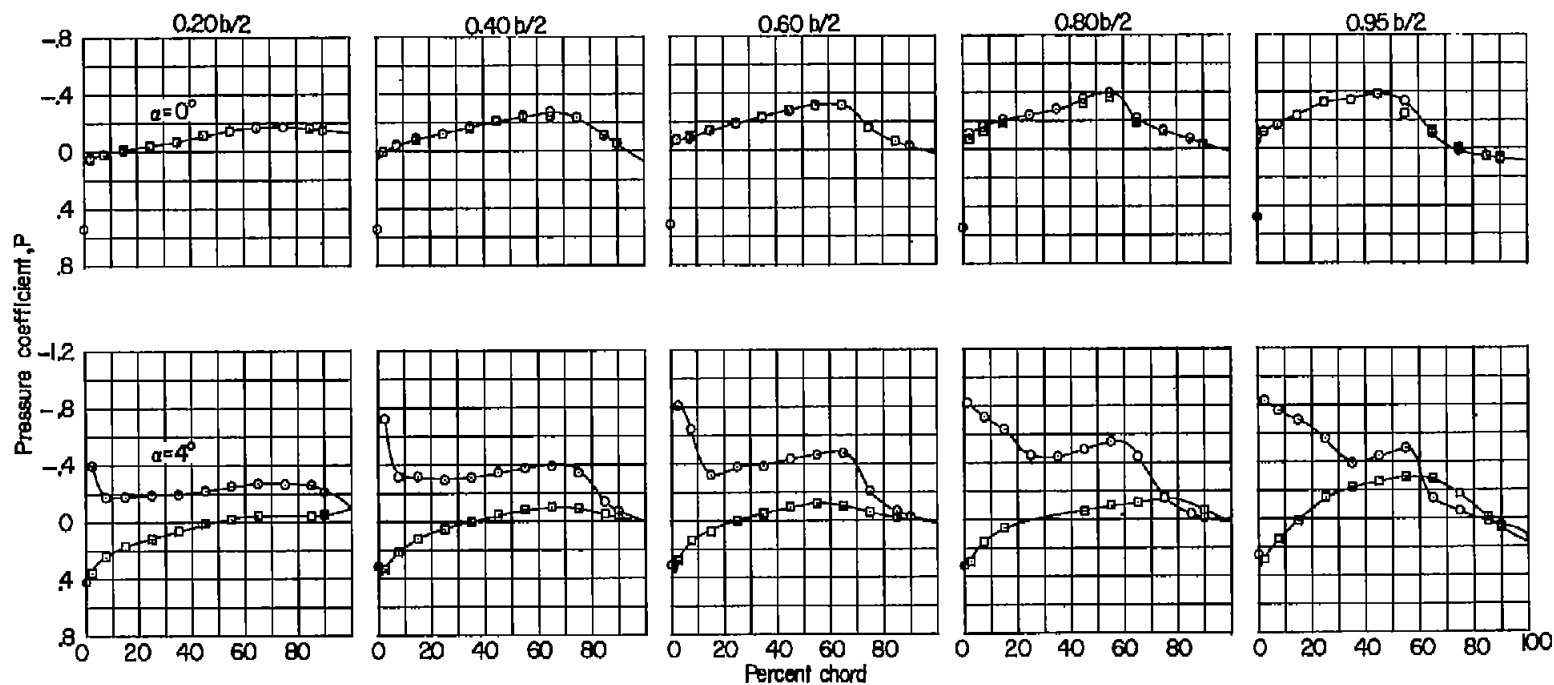
(g) Cylindrical body, $M = 1.00$; curved body, $M = 0.99$; $\alpha = 0^\circ, 4^\circ, \text{ and } 8^\circ$.

Figure 5.- Continued.



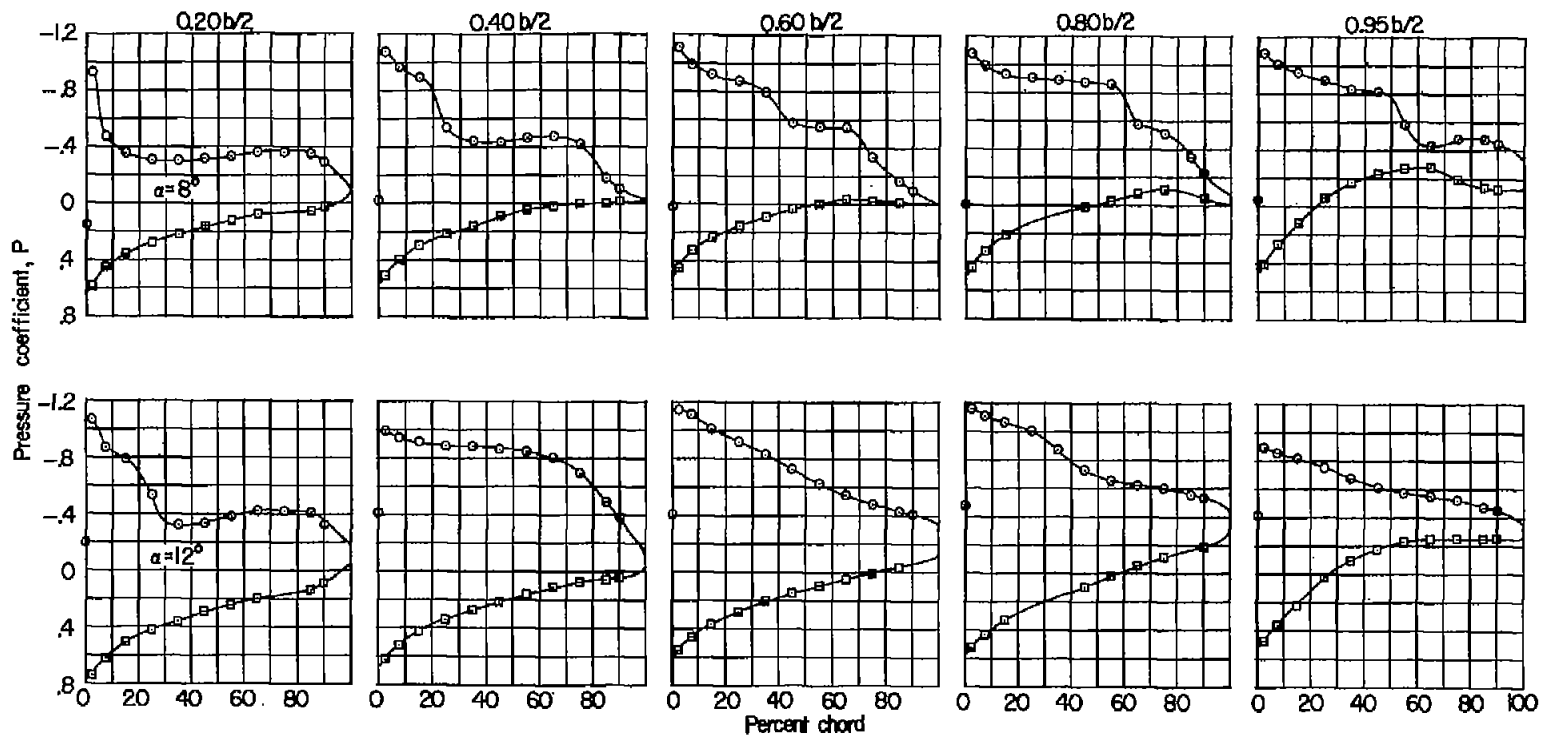
(g) Cylindrical body, $M = 1.00$; curved body, $M = 0.99$; $\alpha = 12^\circ$ and 20° .
Concluded.

Figure 5.- Continued.



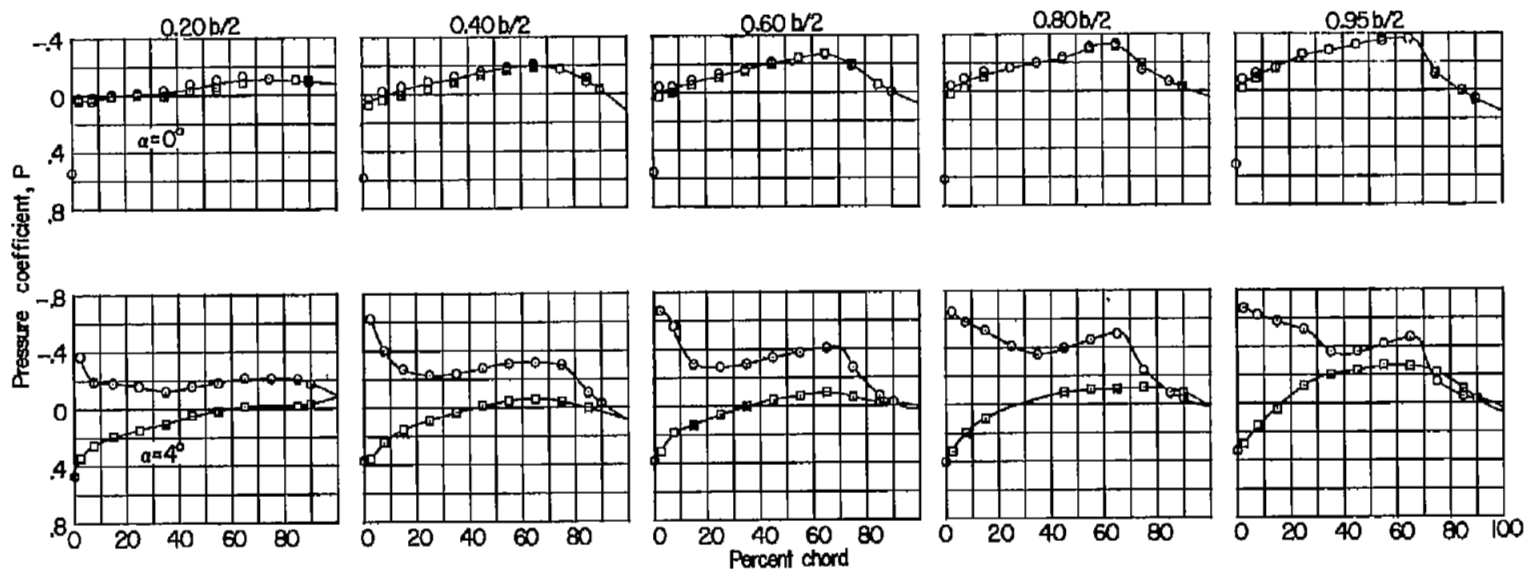
(h) $M = 1.03$; $\alpha = 0^\circ$ and 4° .

Figure 5.- Continued.



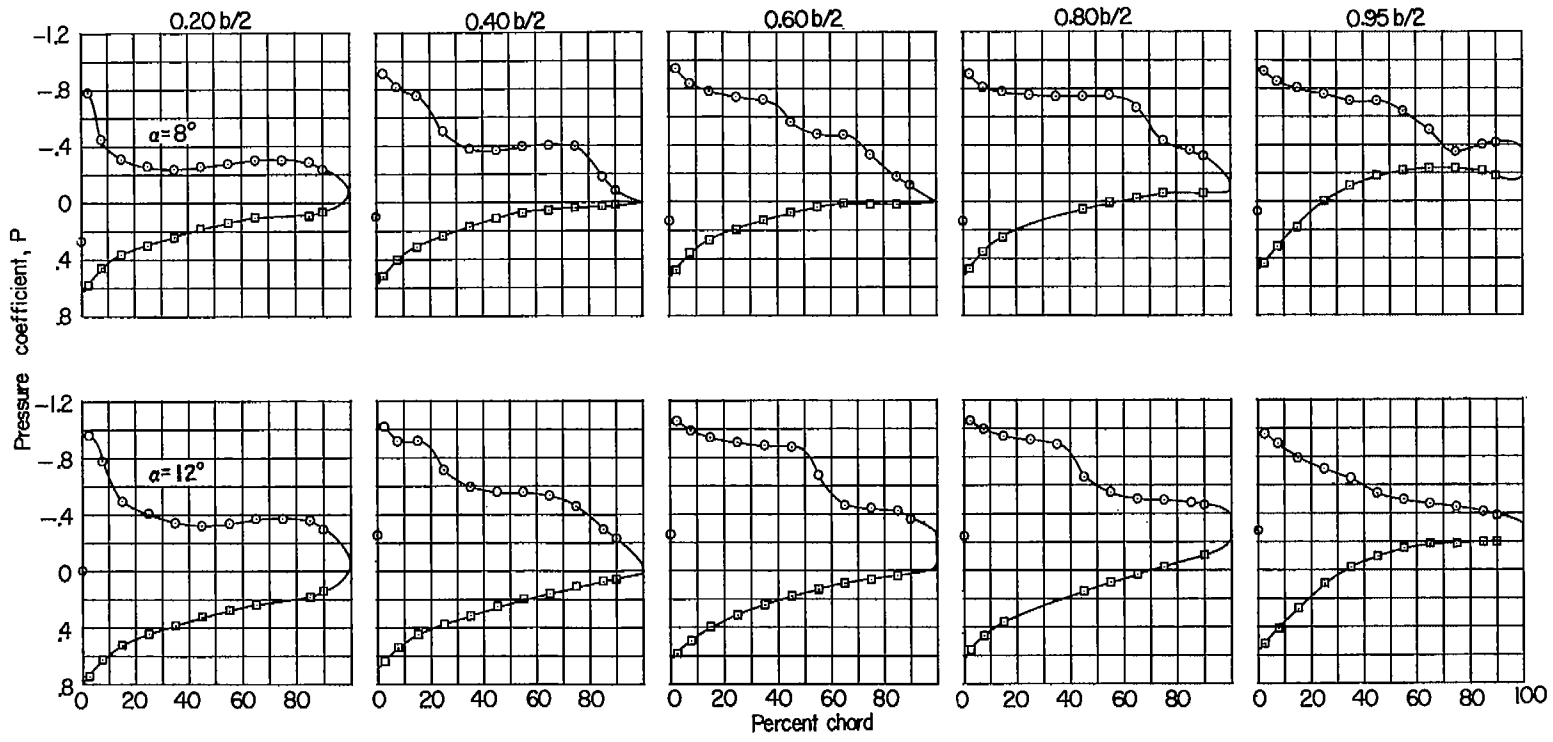
(h) $M = 1.03$; $\alpha = 8^\circ$ and 12° . Concluded.

Figure 5.- Continued.



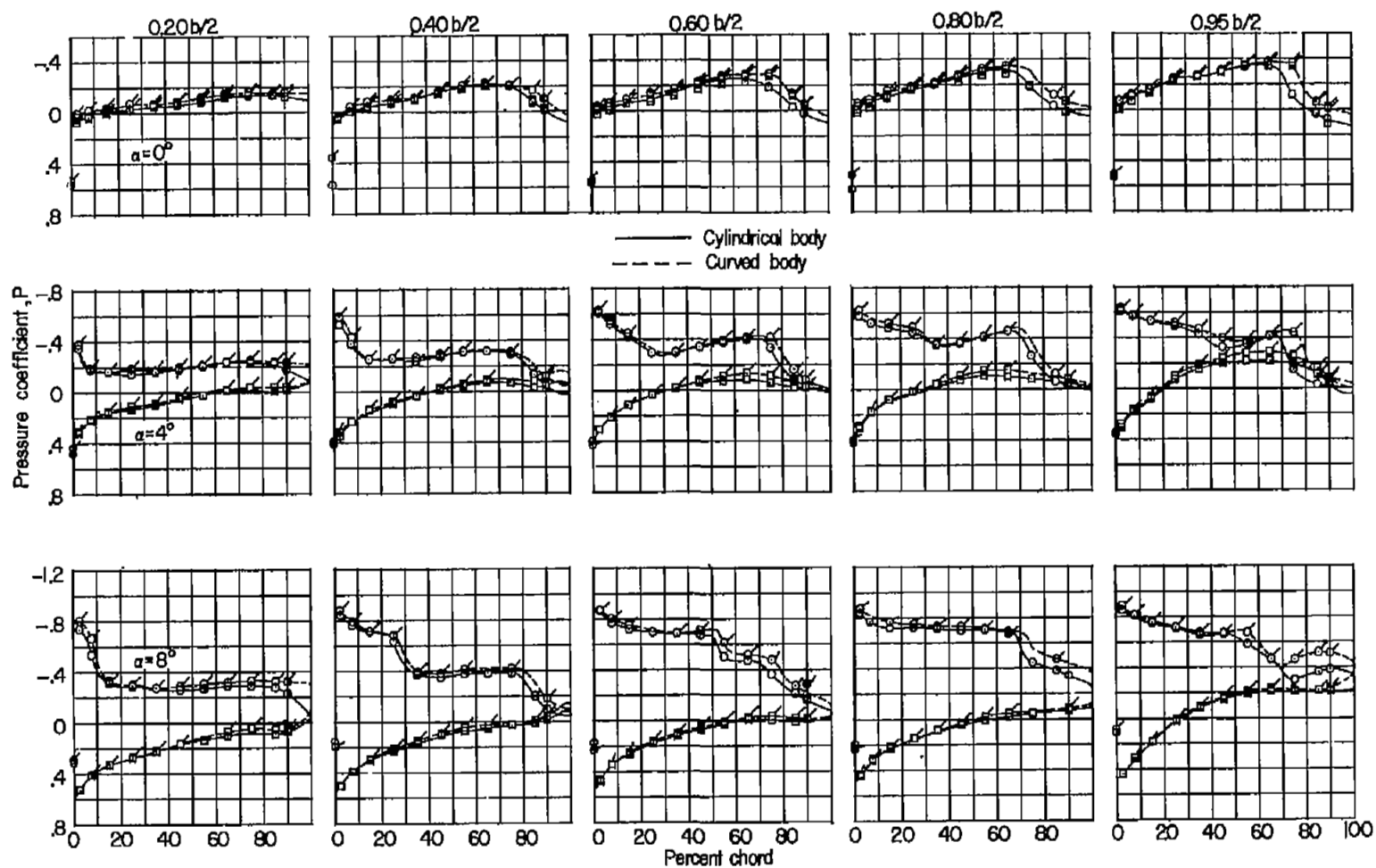
(1) $M = 1.10$; $\alpha = 0^\circ$ and 4° .

Figure 5.- Continued.



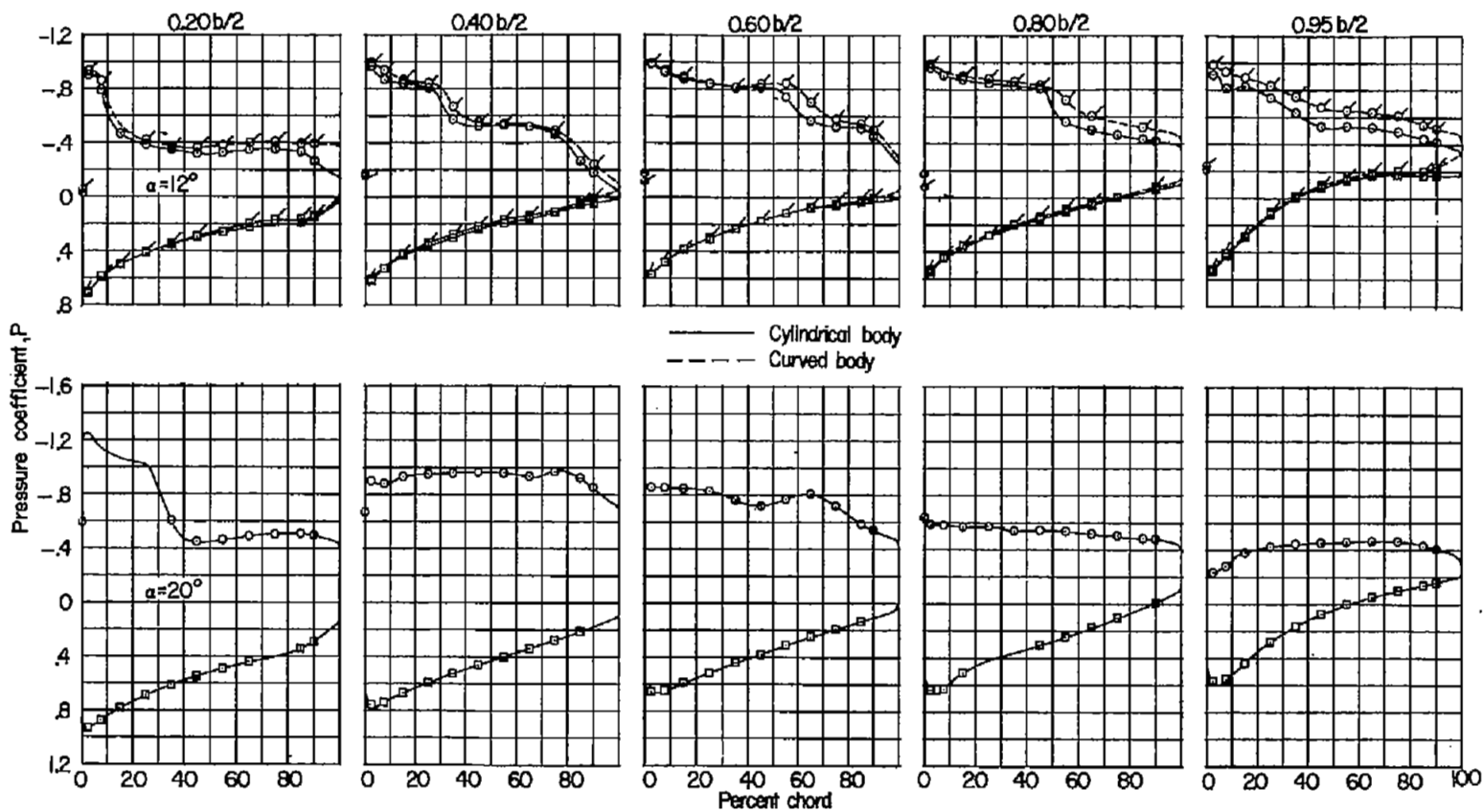
(i) $M = 1.10$; $\alpha = 8^\circ$ and 12° . Concluded.

Figure 5.- Continued.



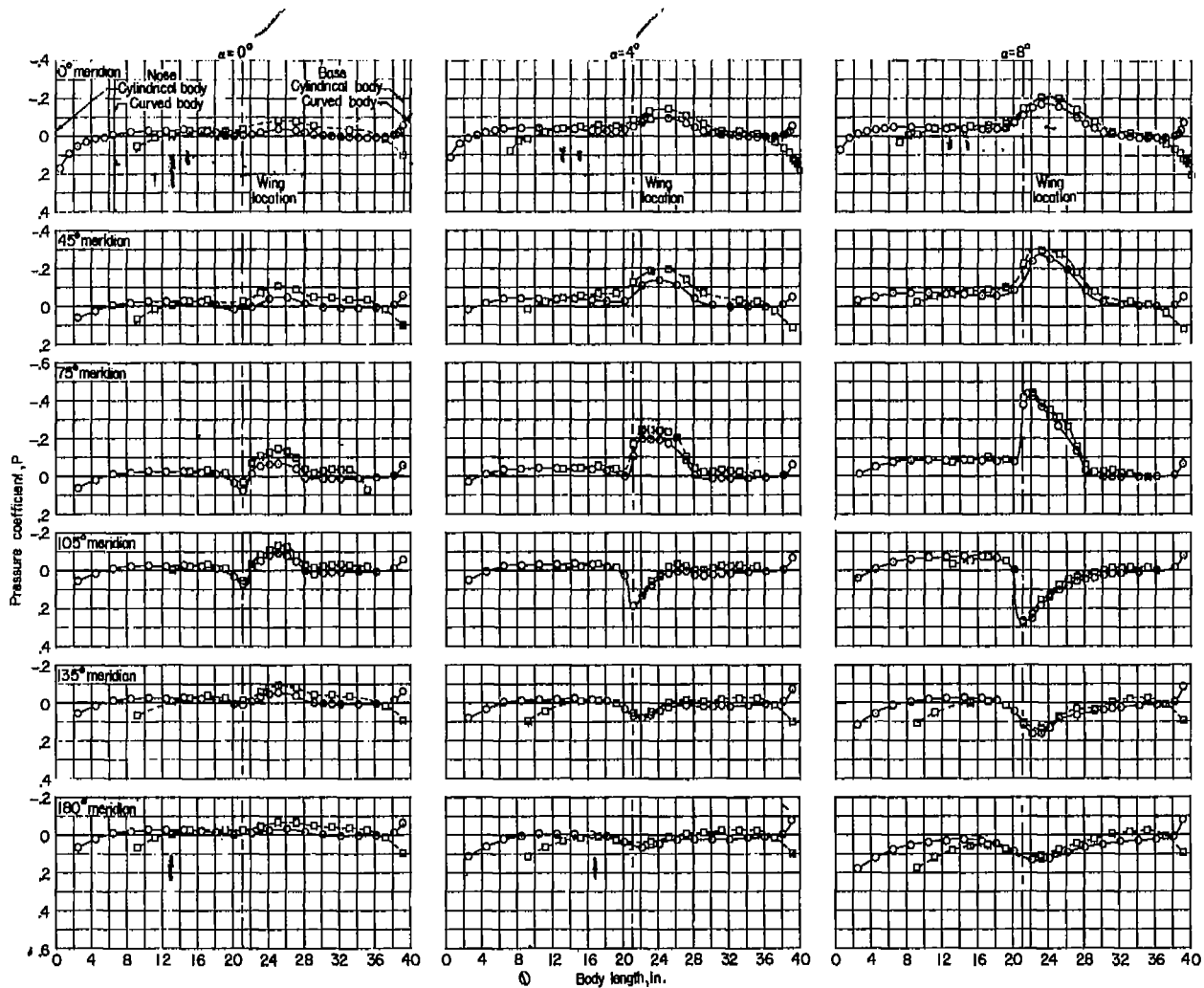
(j) $M = 1.13$; $\alpha = 0^\circ, 4^\circ, \text{ and } 8^\circ$.

Figure 5.- Continued.



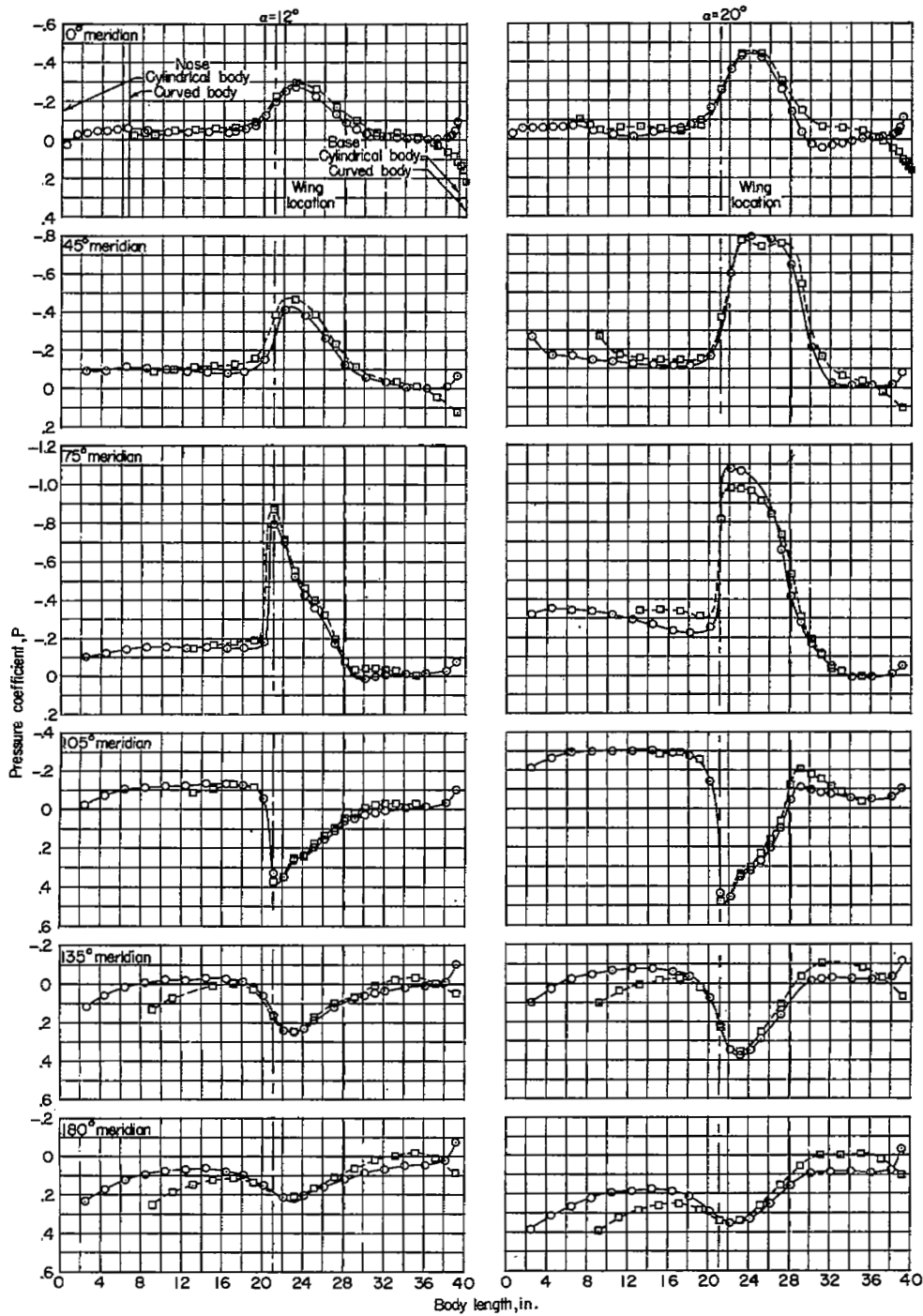
(j) $M = 1.13$; $\alpha = 12^\circ$ and 20° . Concluded.

Figure 5.- Concluded.



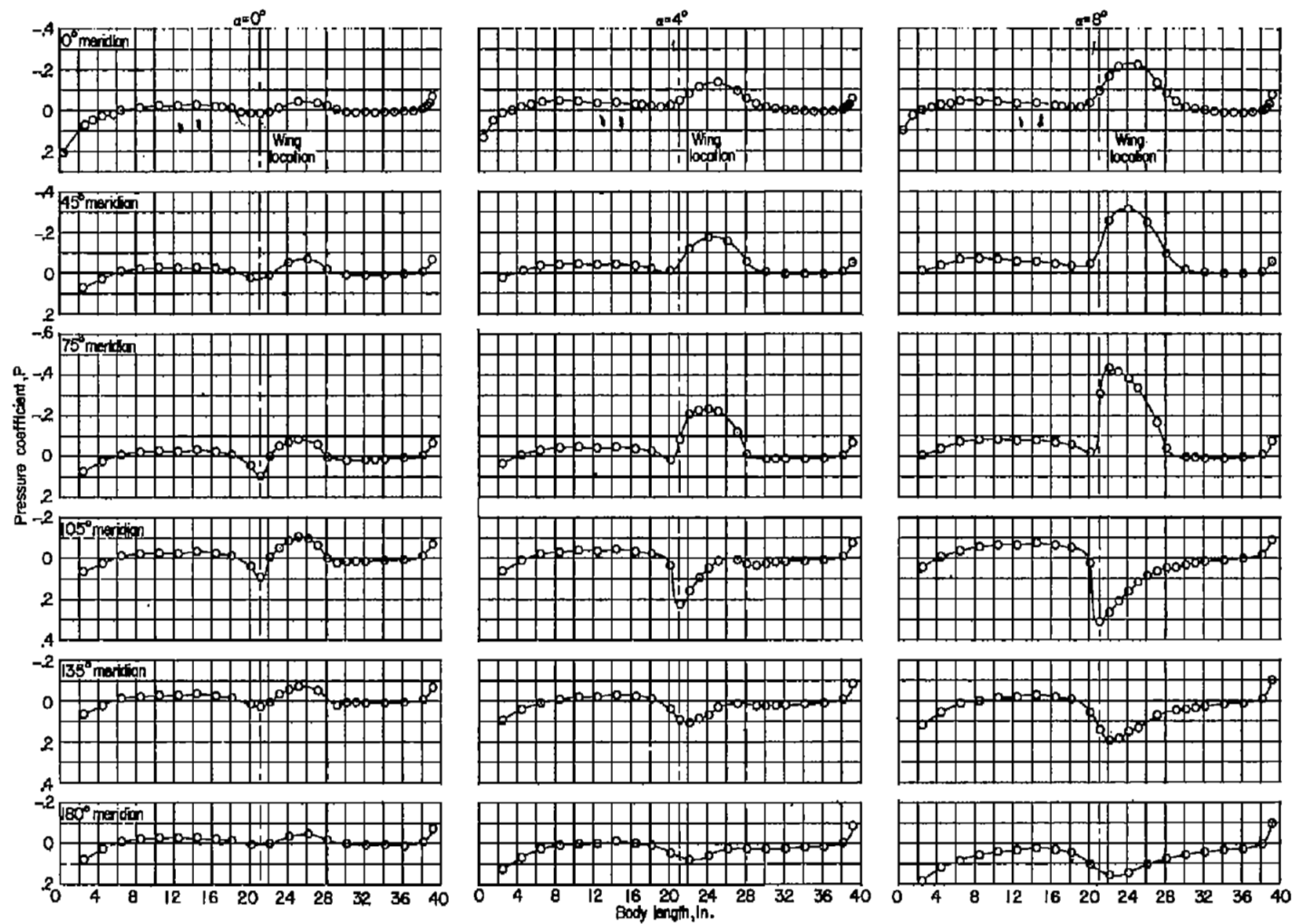
(a) $M = 0.60$; $\alpha = 0^\circ, 4^\circ, \text{ and } 8^\circ$.

Figure 6.- Longitudinal pressure distribution for six meridians on body with wing combination at various angles of attack.



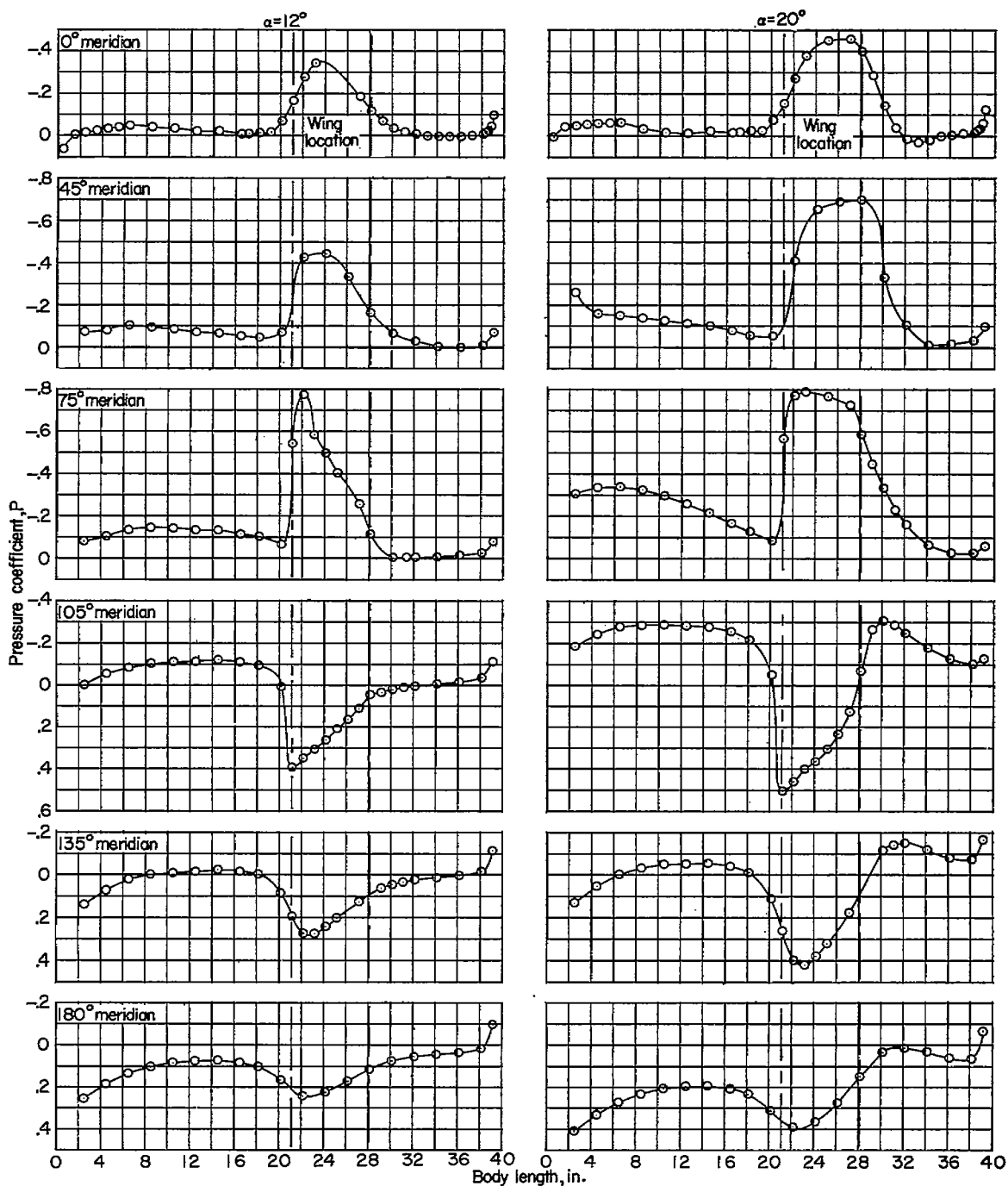
(a) $M = 0.60$; $\alpha = 12^\circ$ and 20° . Concluded.

Figure 6.- Continued.



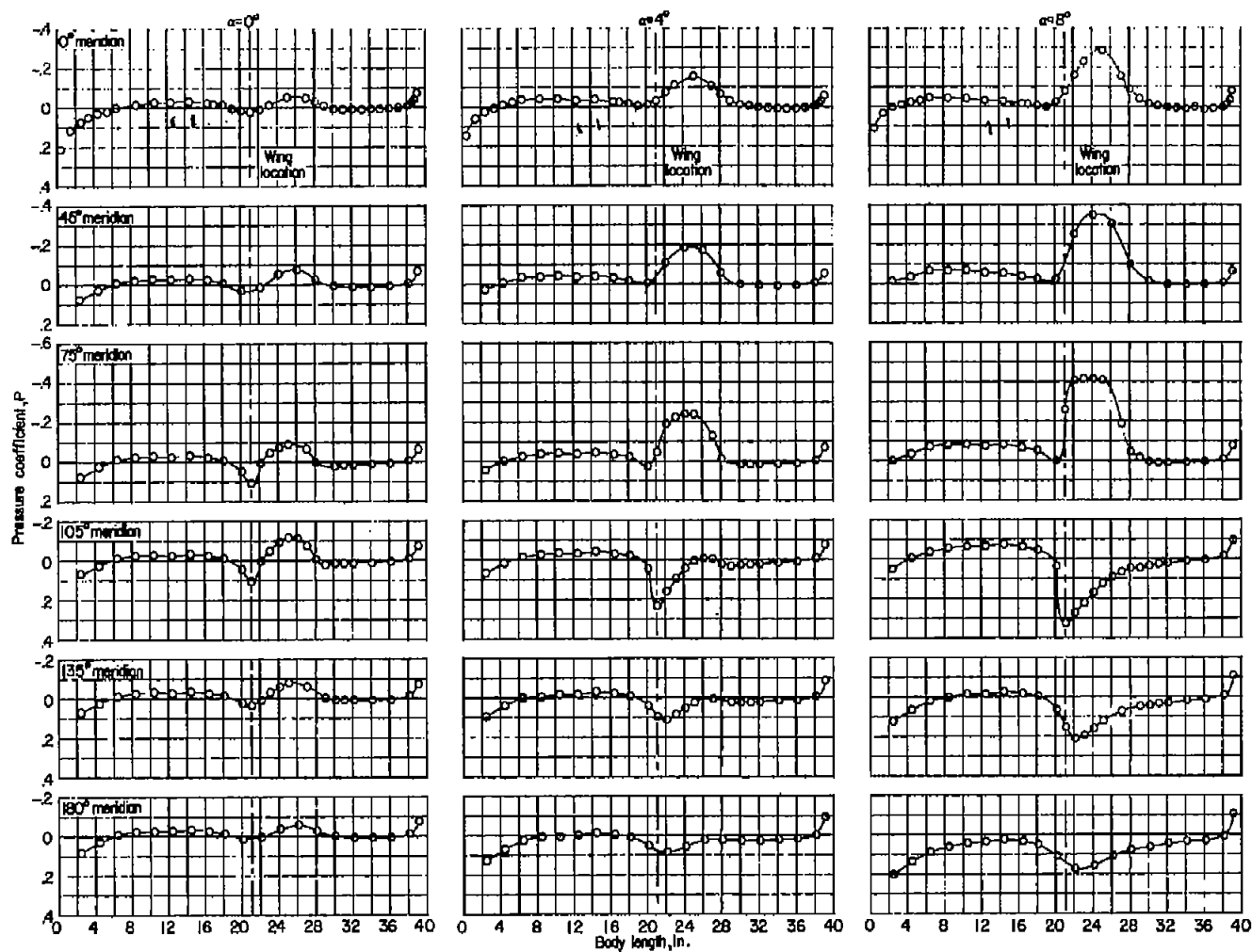
(b) $M = 0.80$; $\alpha = 0^\circ, 4^\circ, \text{ and } 8^\circ$.

Figure 6.- Continued.



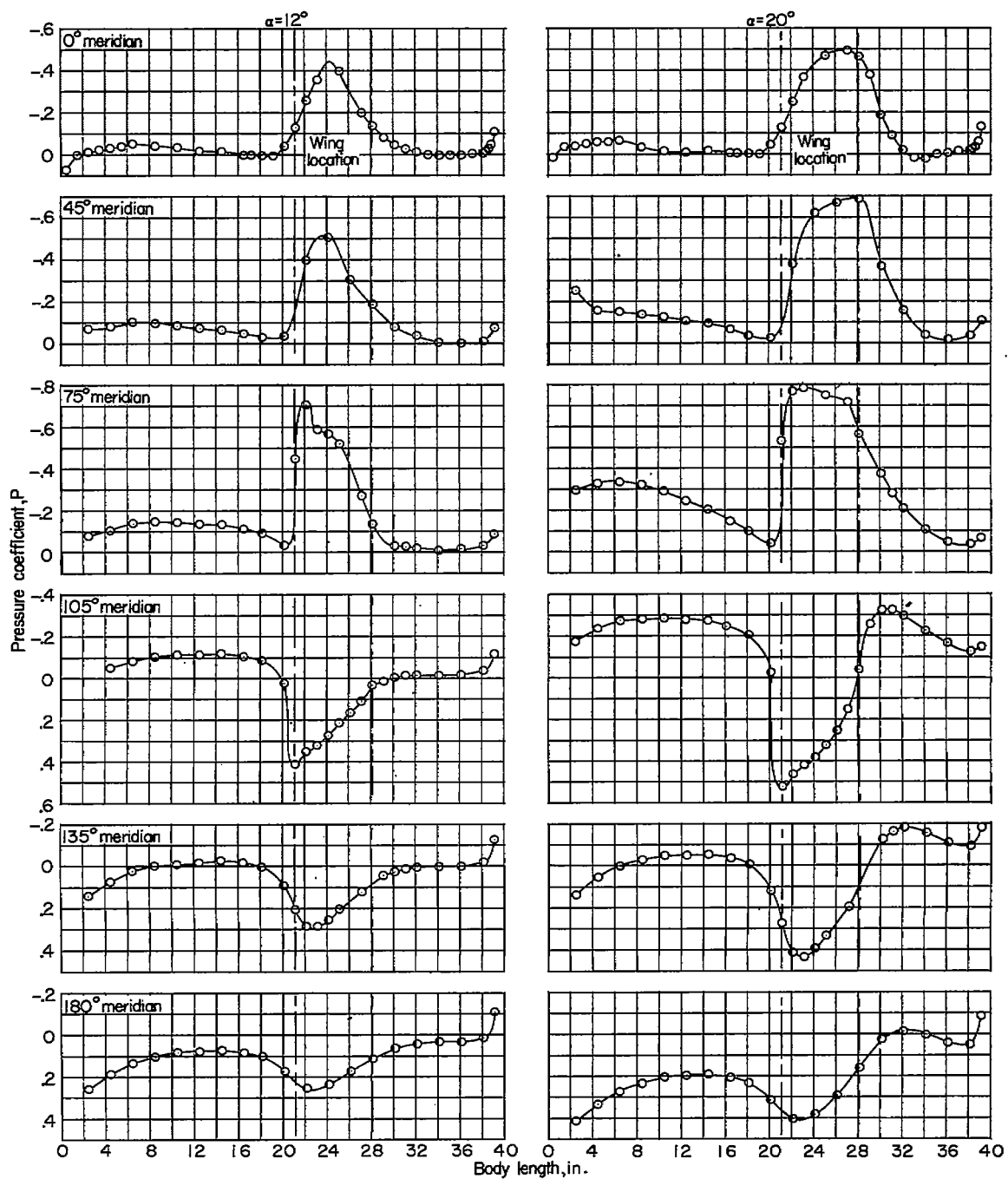
(b) $M = 0.80$; $\alpha = 12^\circ$ and 20° . Concluded.

Figure 6.- Continued.



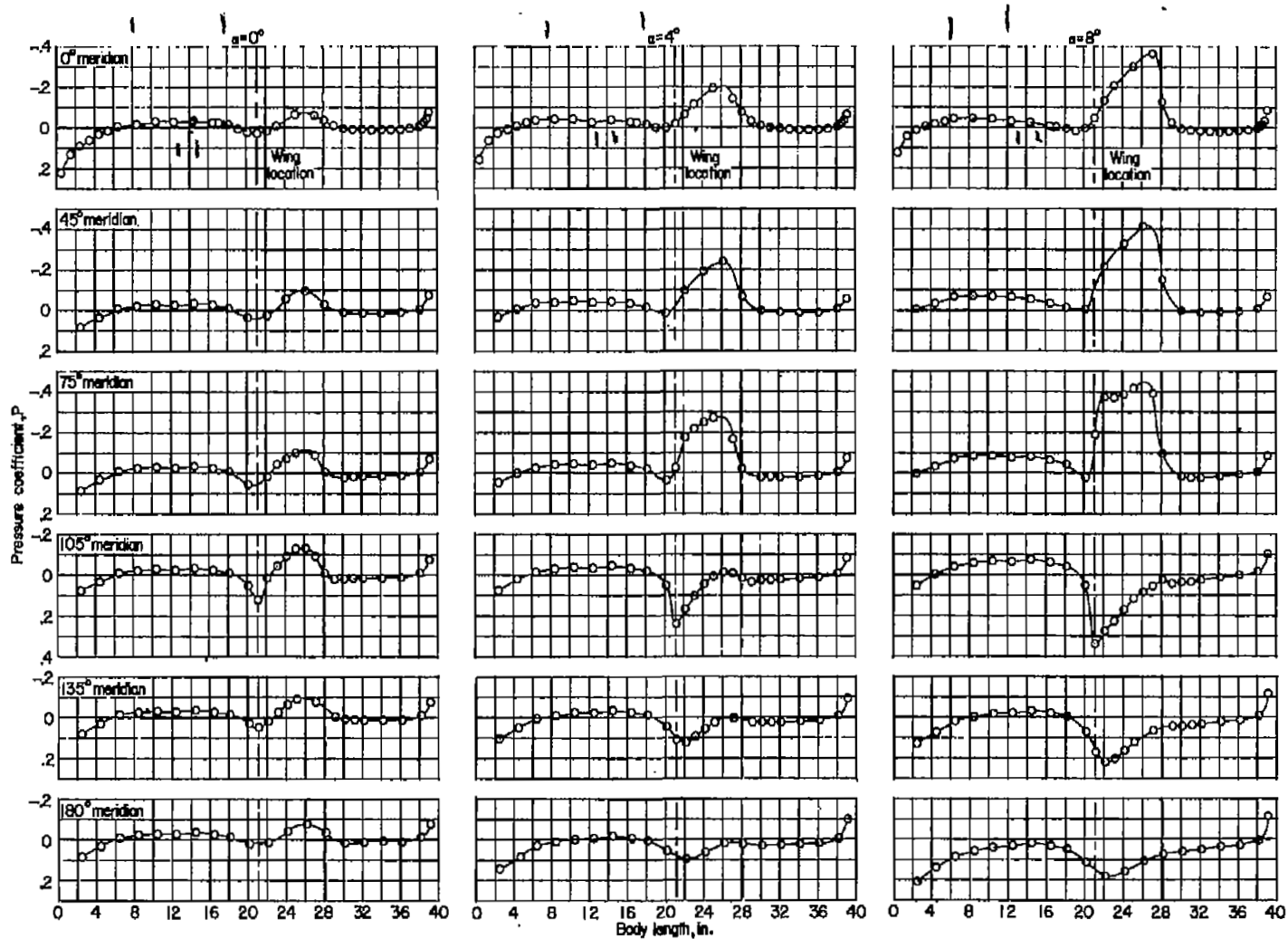
(c) $M = 0.85$; $\alpha = 0^\circ, 4^\circ, \text{ and } 8^\circ$.

Figure 6.- Continued.



(c) $M = 0.85$; $\alpha = 12^\circ$ and 20° . Concluded.

Figure 6.- Continued.



(a) $M = 0.90$; $\alpha = 0^\circ, 4^\circ, \text{ and } 8^\circ$.

Figure 6.- Continued.

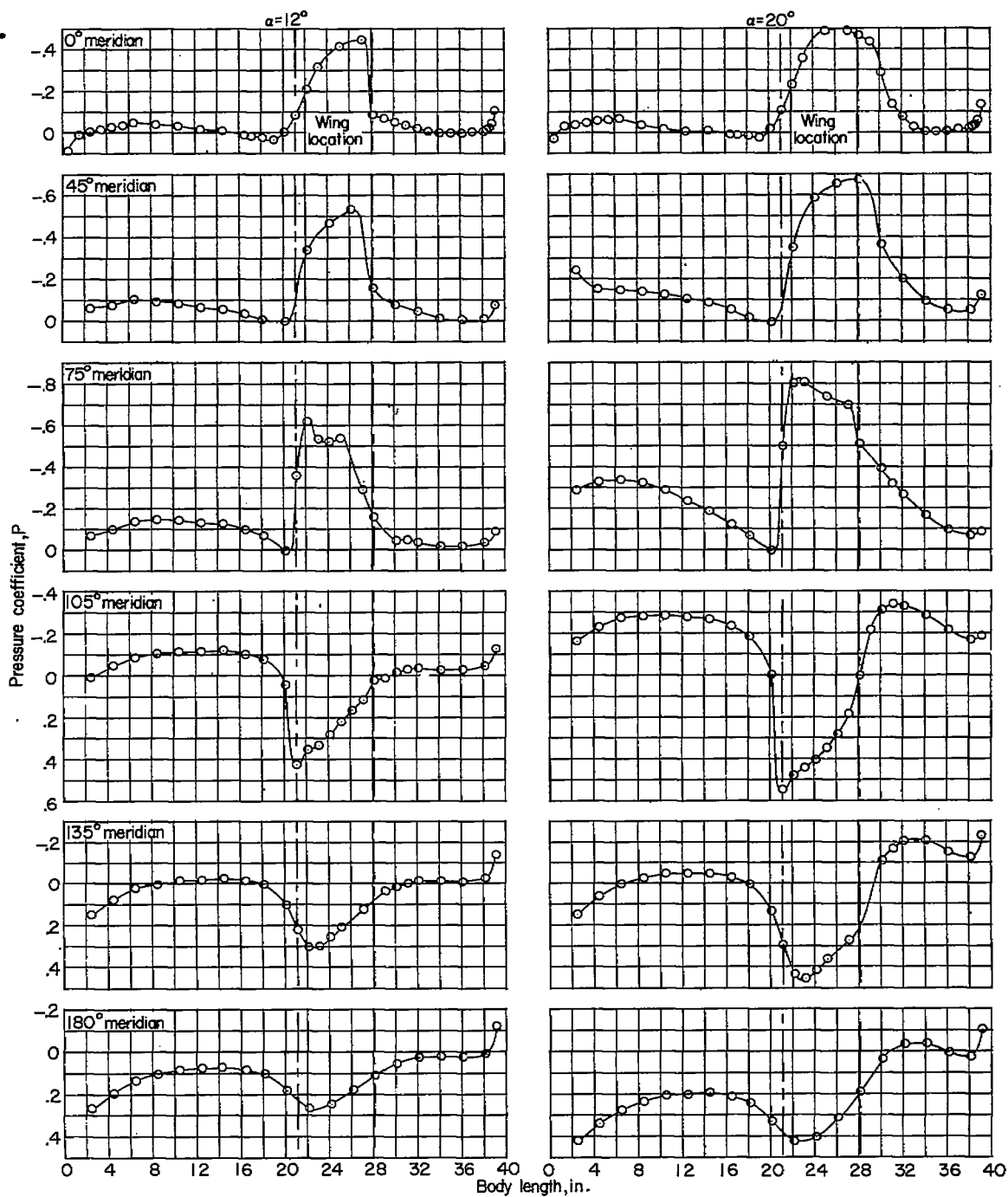
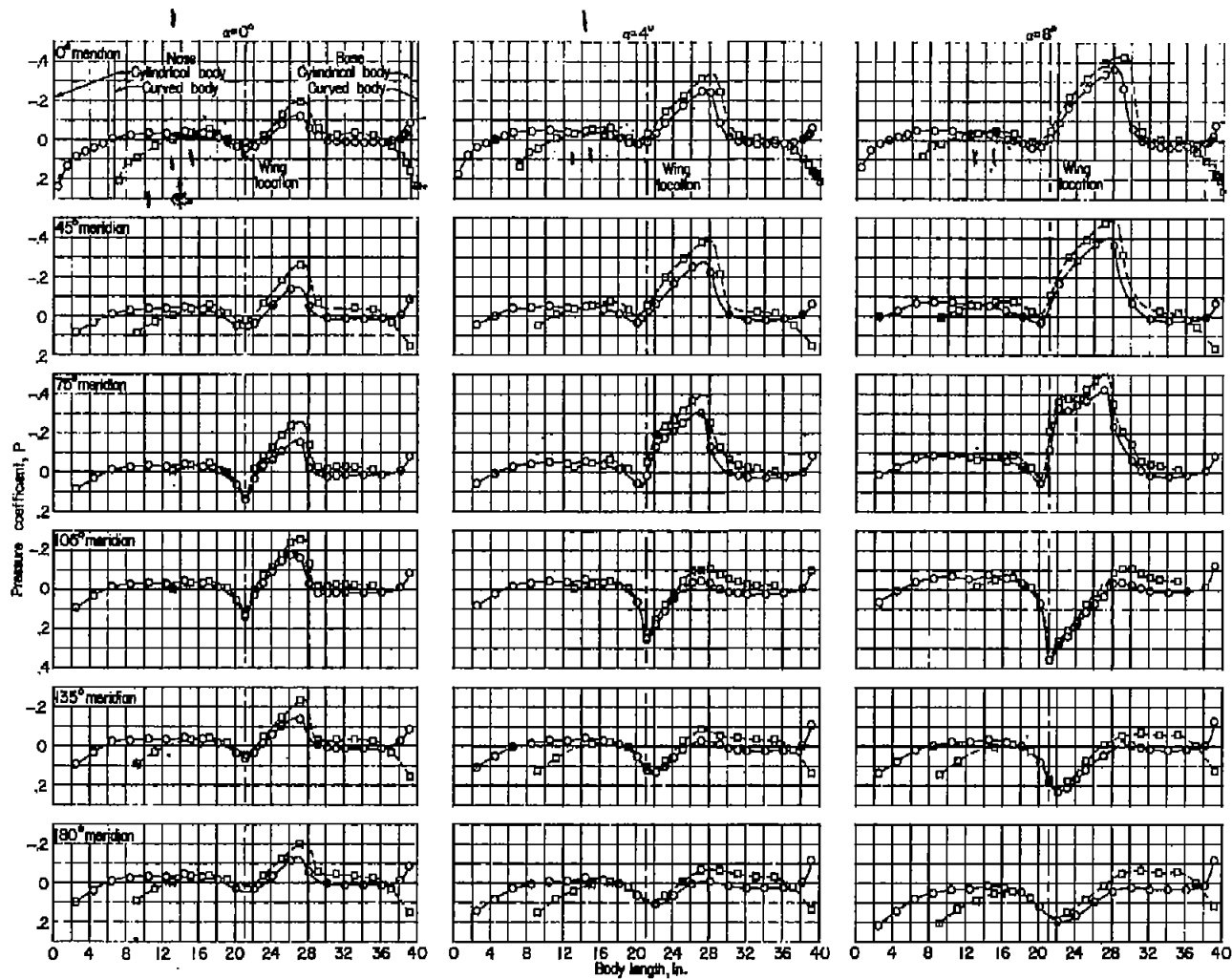
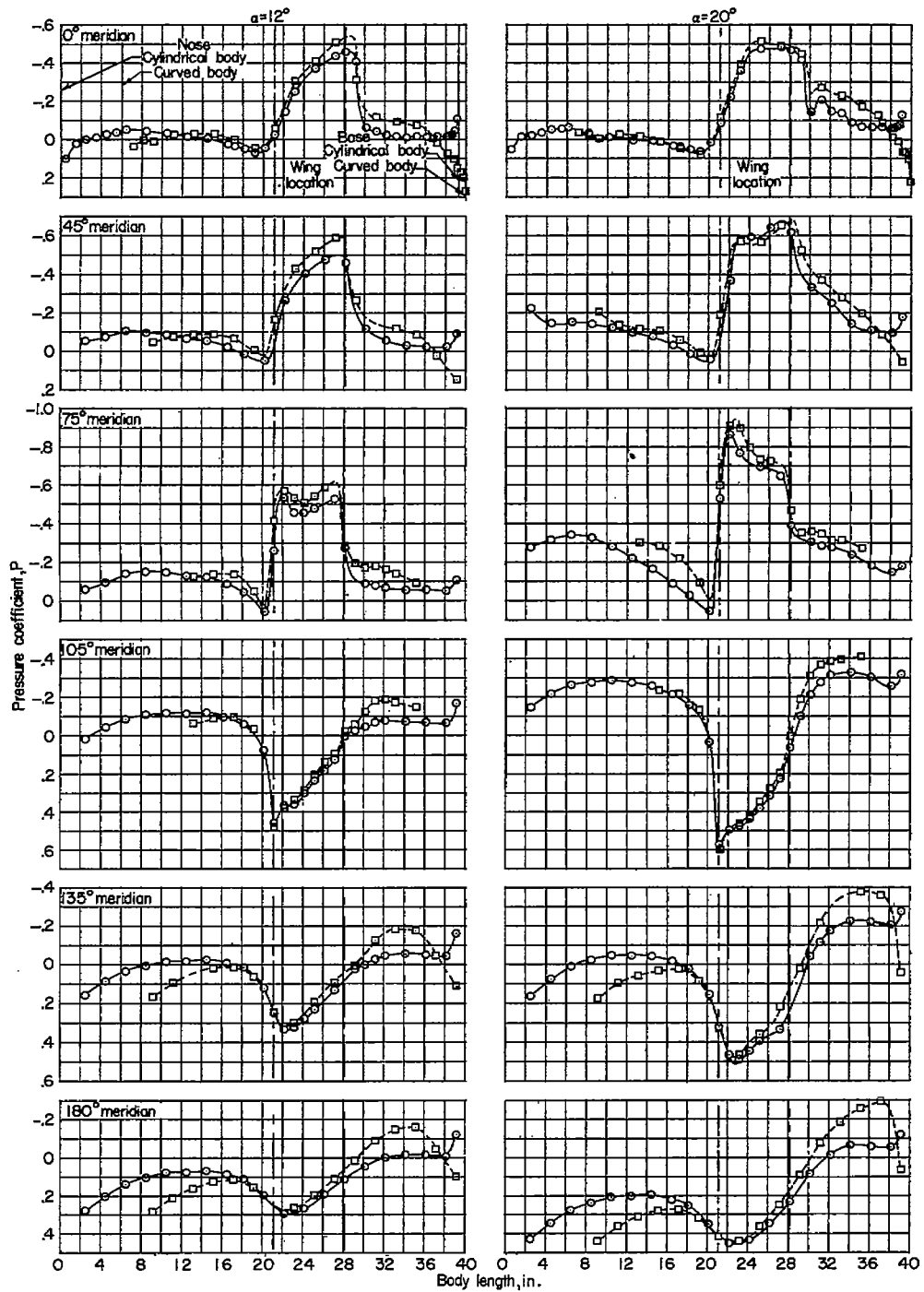
(d) $M = 0.90$; $\alpha = 12^\circ$ and 20° . Concluded.

Figure 6.- Continued.



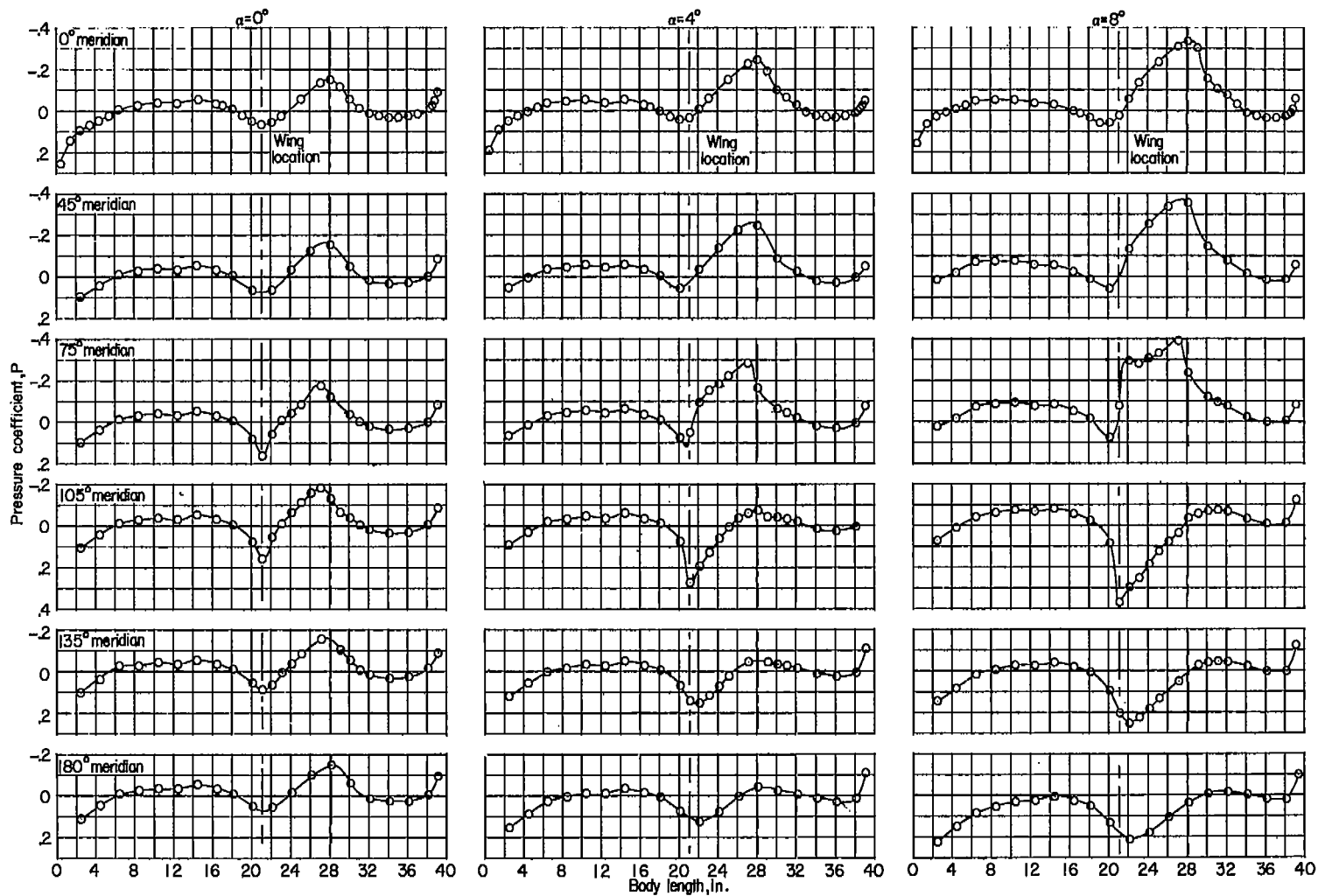
(e) Cylindrical body, $M = 0.95$; curved body, $M = 0.94$; $\alpha = 0^\circ, 4^\circ, \text{ and } 8^\circ$.

Figure 6.- Continued.



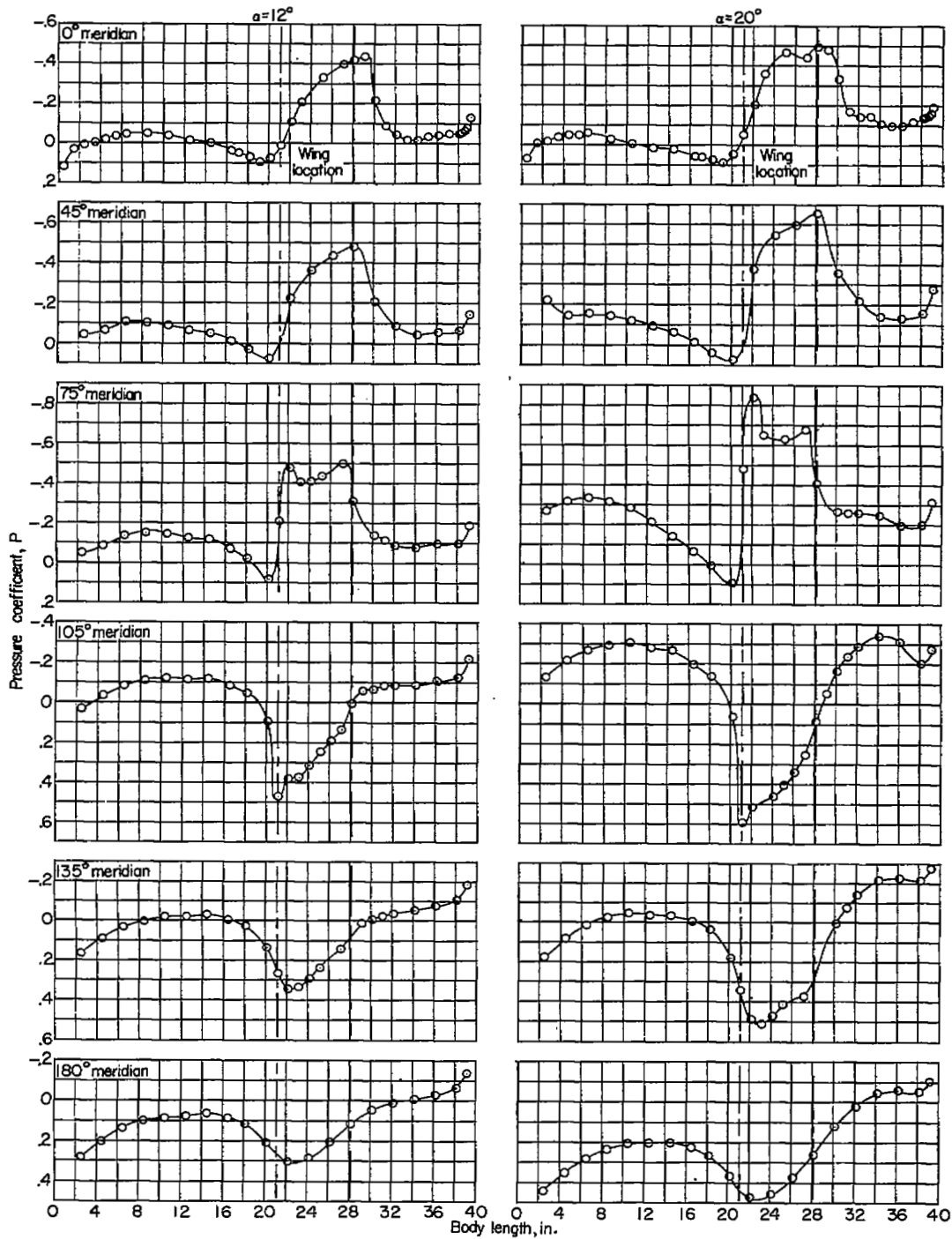
(e) Cylindrical body, $M = 0.95$; curved body, $M = 0.94$; $\alpha = 12^\circ$ and 20° .
Concluded.

Figure 6.- Continued.



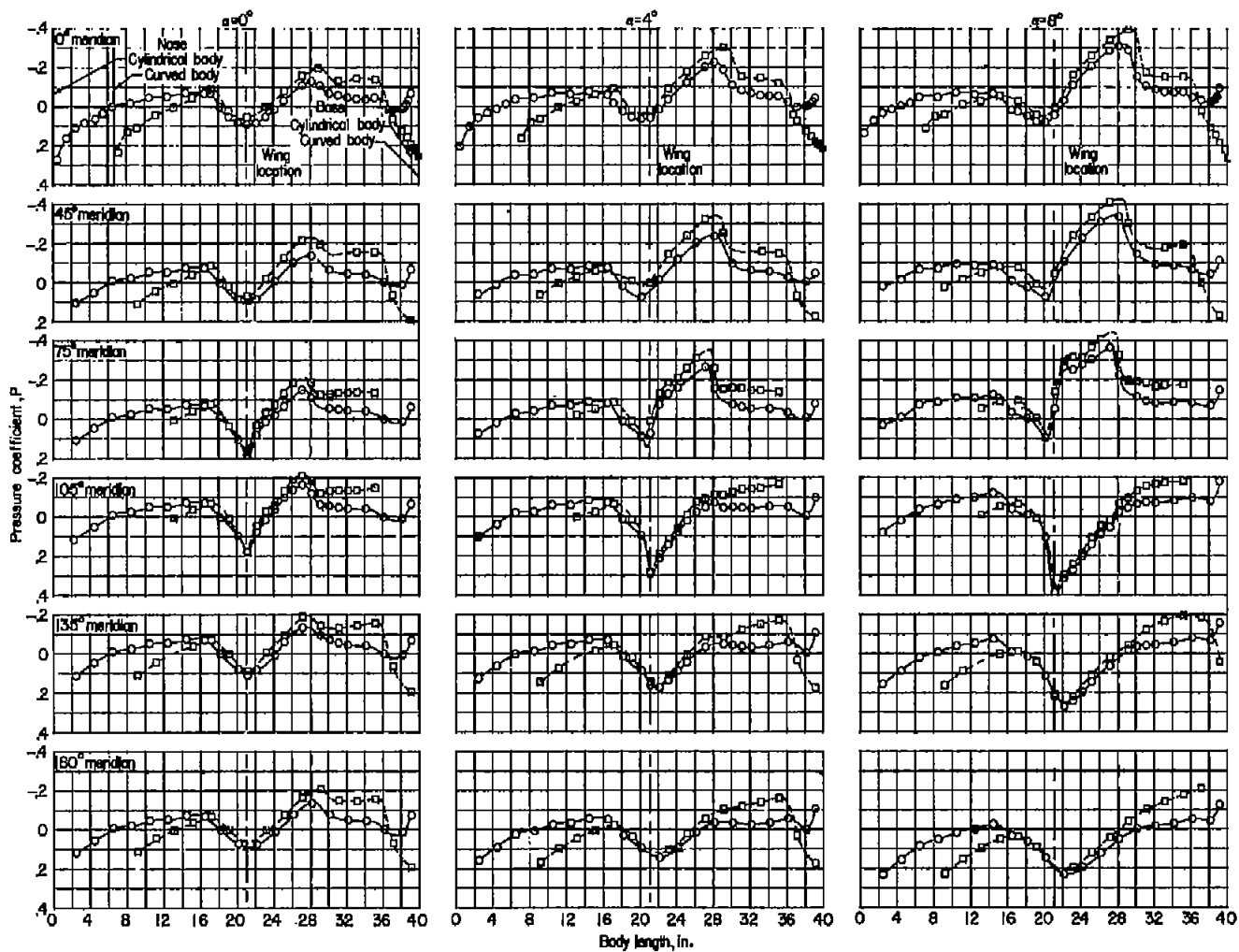
(f) $M = 0.98$; $\alpha = 0^\circ, 4^\circ, \text{ and } 8^\circ$.

Figure 6.- Continued.



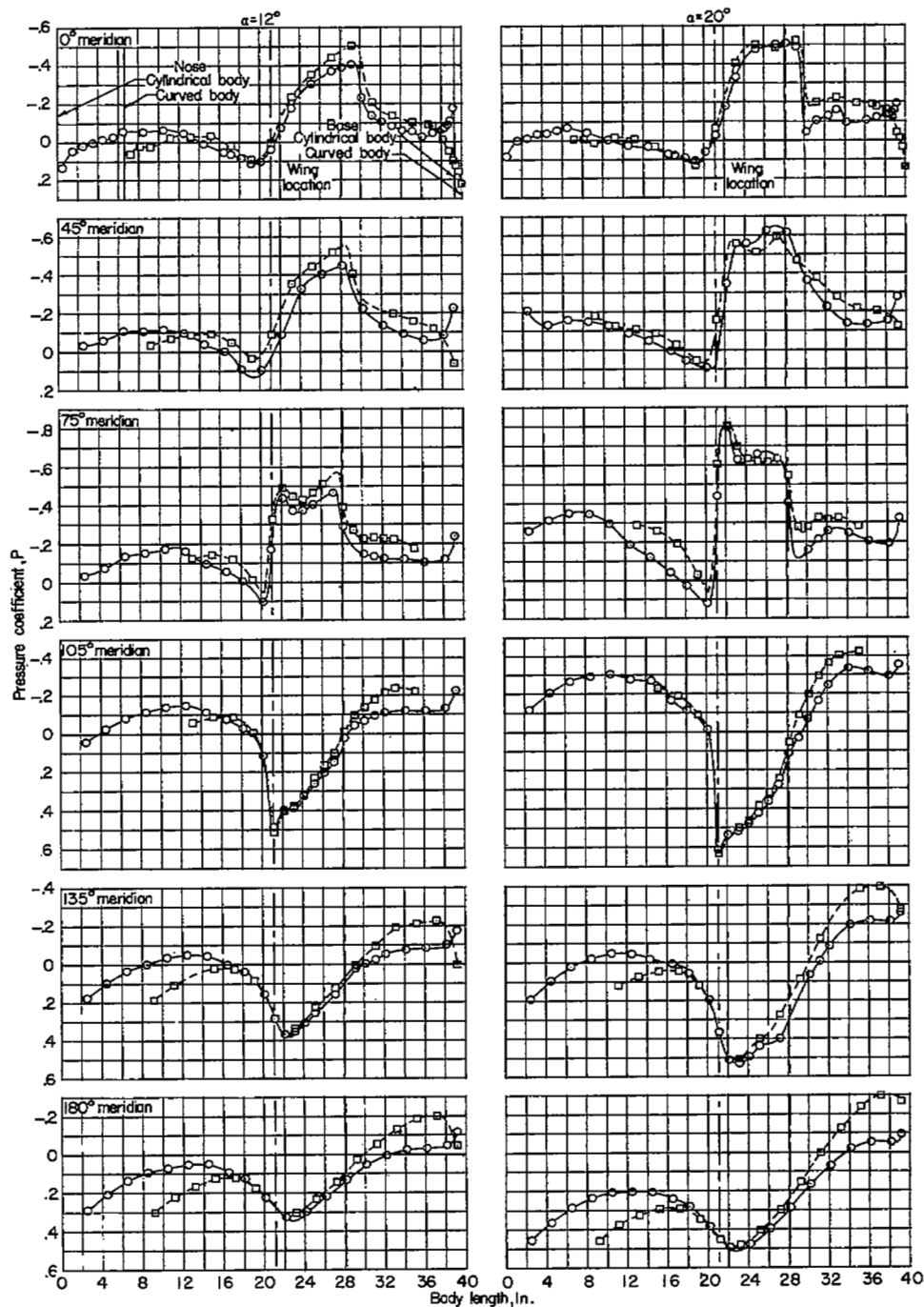
(f) $M = 0.98$; $\alpha = 12^\circ$ and 20° . Concluded.

Figure 6.- Continued.



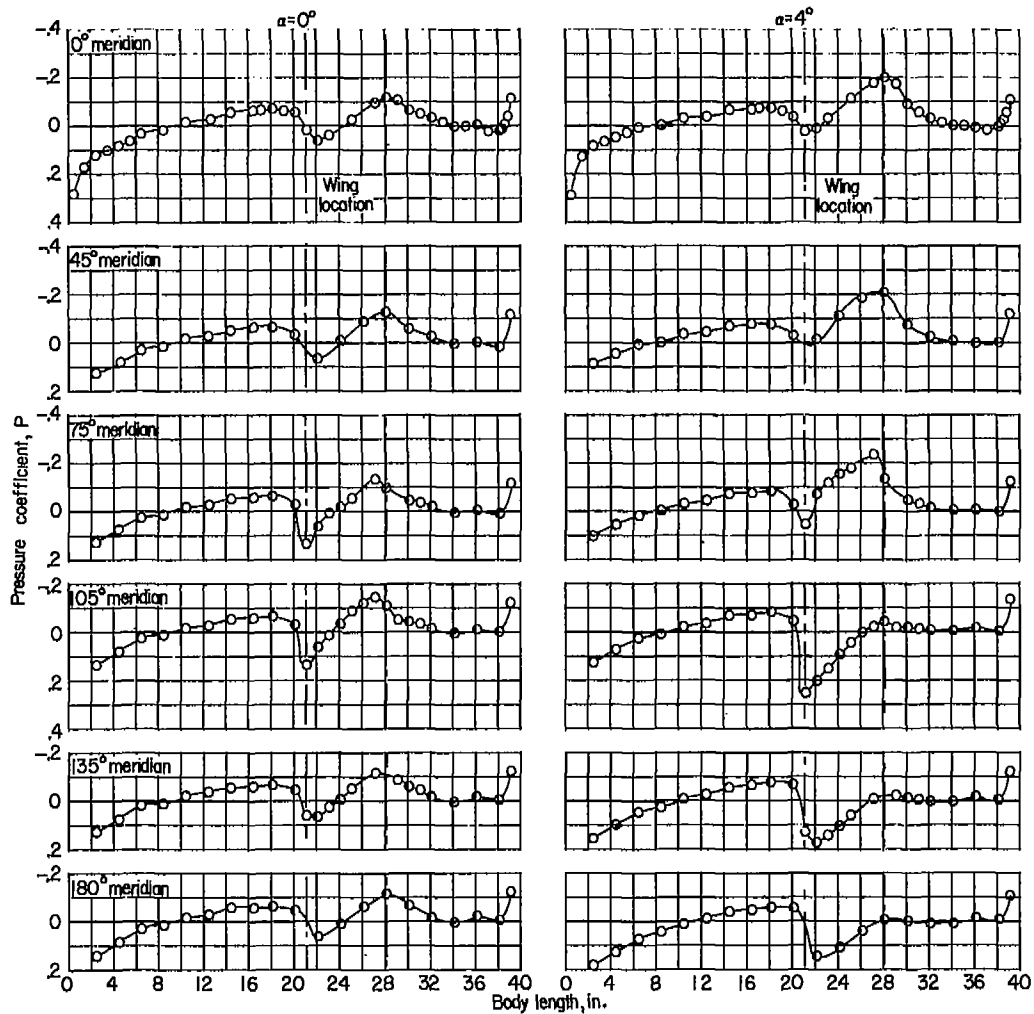
(g) Cylindrical body, $M = 1.00$; curved body, $M = 0.99$; $\alpha = 0^\circ, 4^\circ, \text{ and } 8^\circ$.

Figure 6.- Continued.



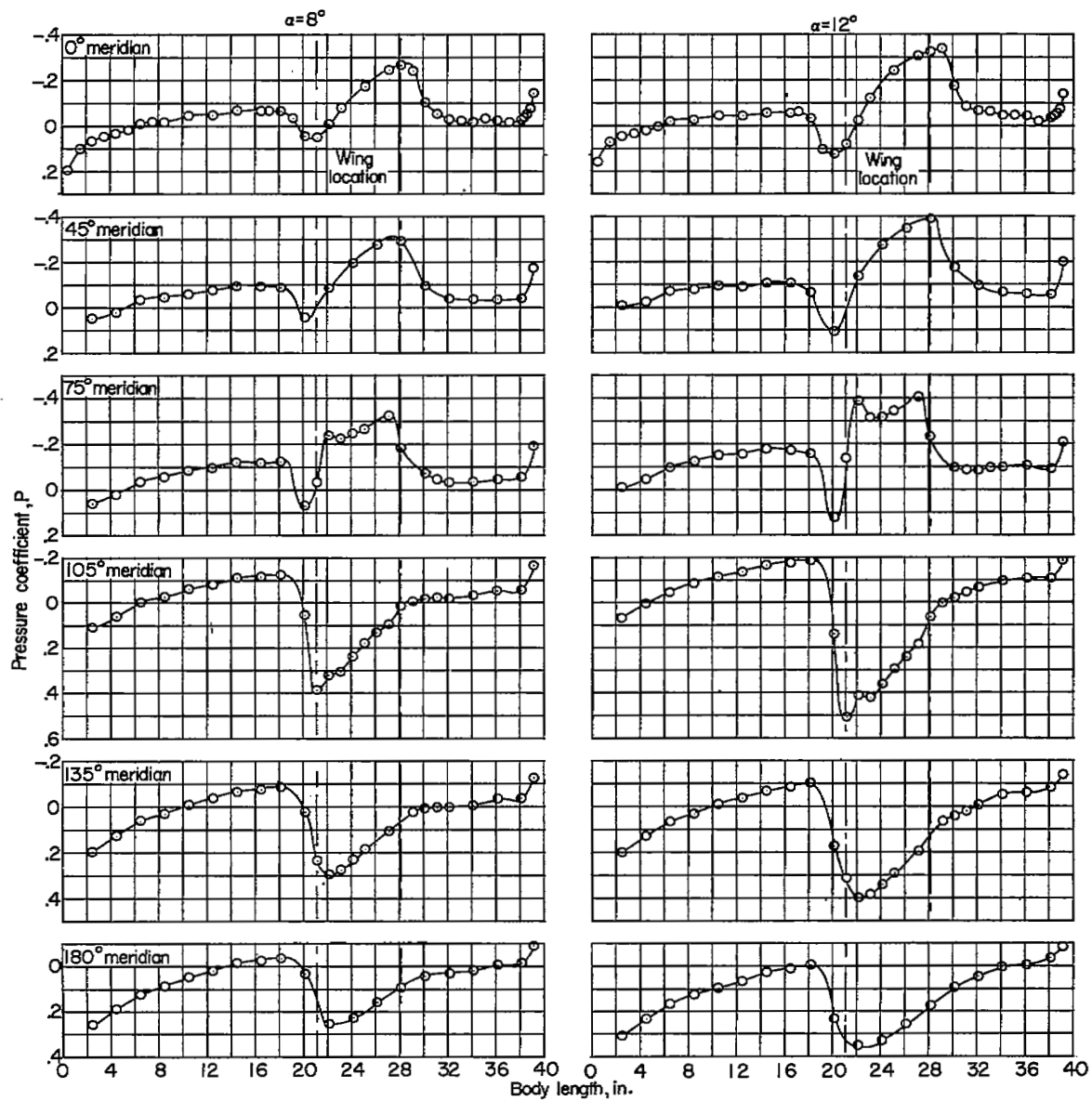
(g) Cylindrical body, $M = 1.00$; curved body, $M = 0.99$; $\alpha = 12^\circ$ and 20° .
Concluded.

Figure 6.- Continued.



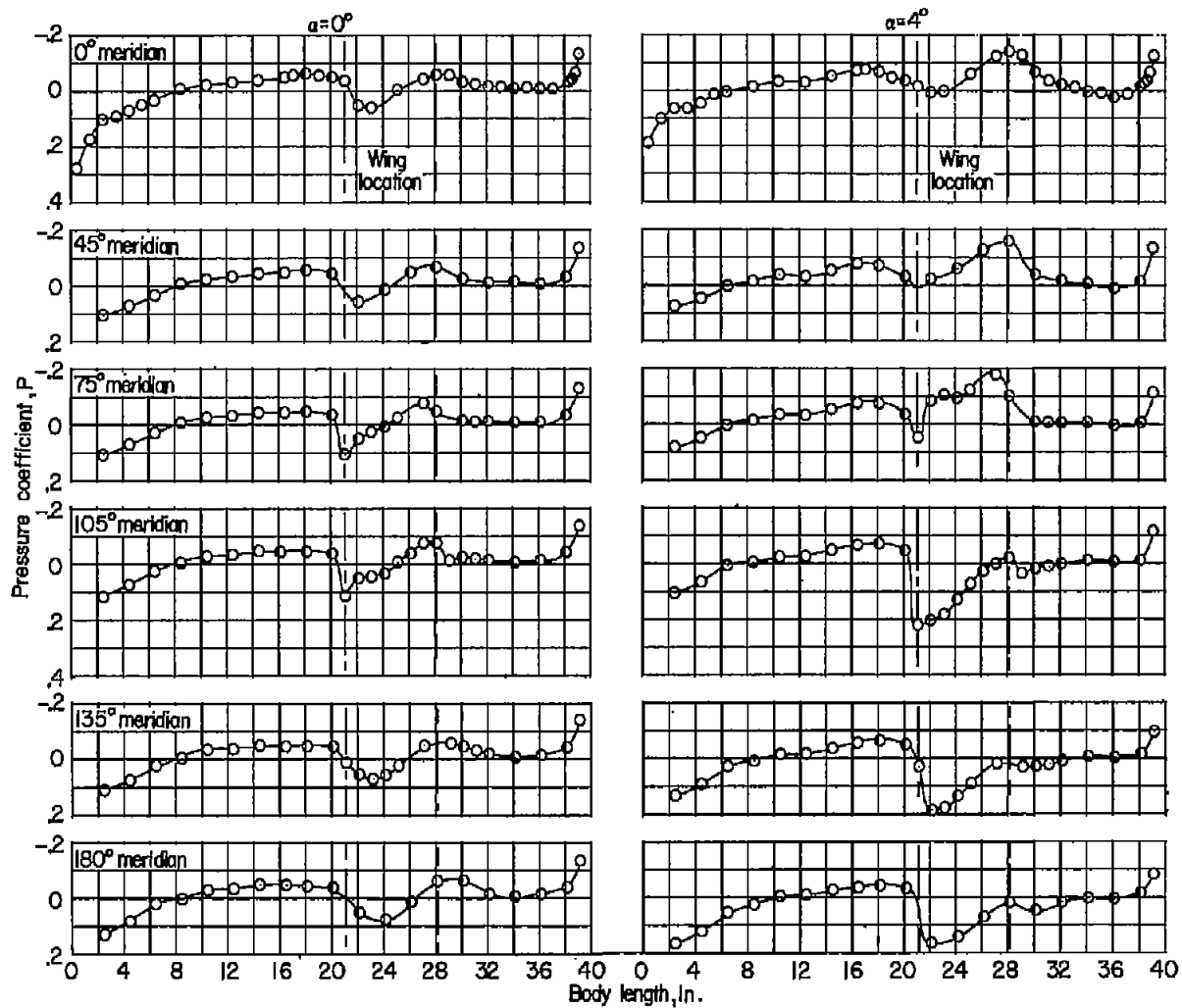
(h) $M = 1.03$; $\alpha = 0^\circ$ and 4° .

Figure 6.- Continued.



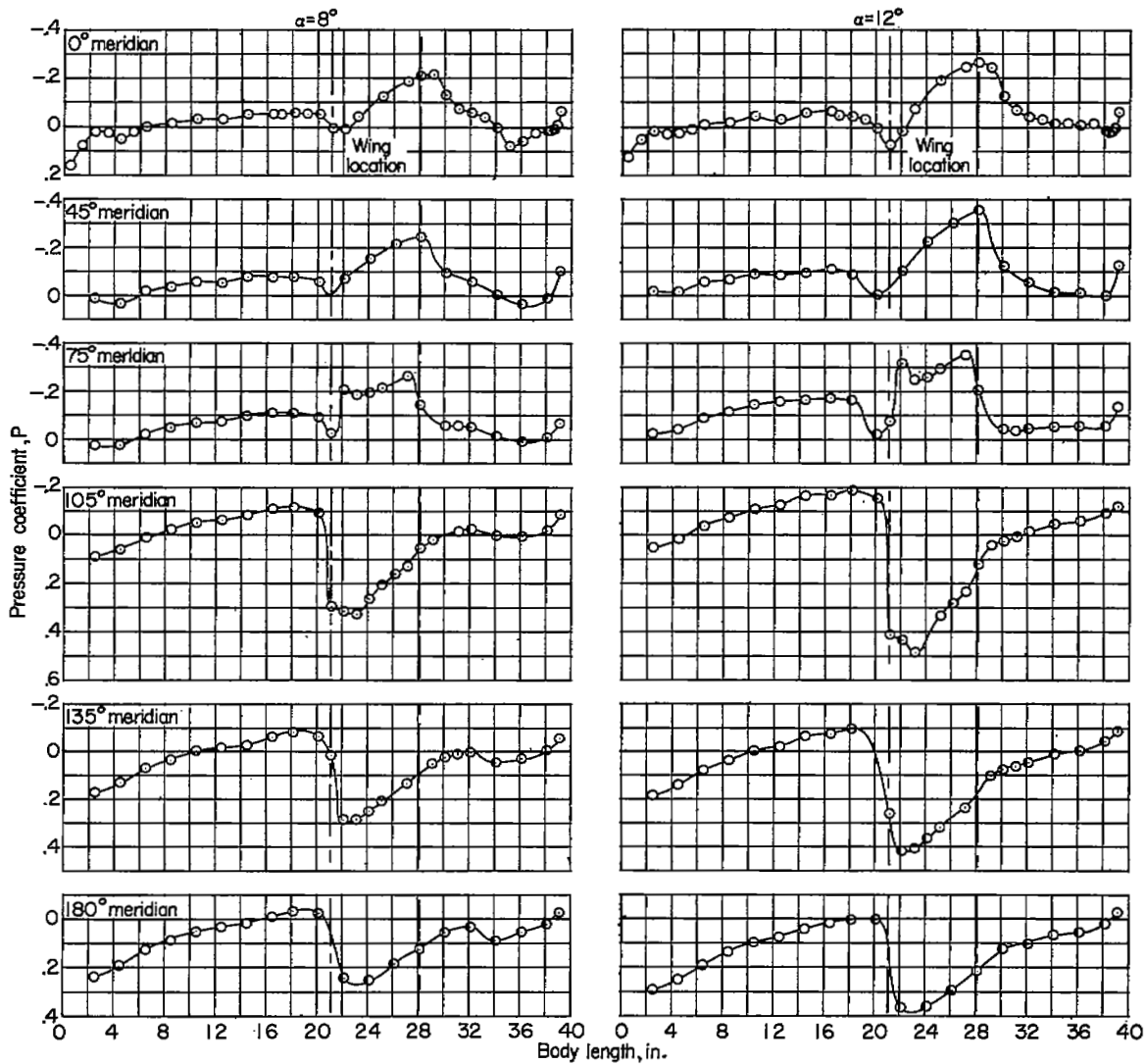
(h) $M = 1.03$; $\alpha = 8^\circ$ and 12° . Concluded.

Figure 6.- Continued.



(1) $M = 1.10$; $\alpha = 0^\circ$ and 4° .

Figure 6.- Continued.

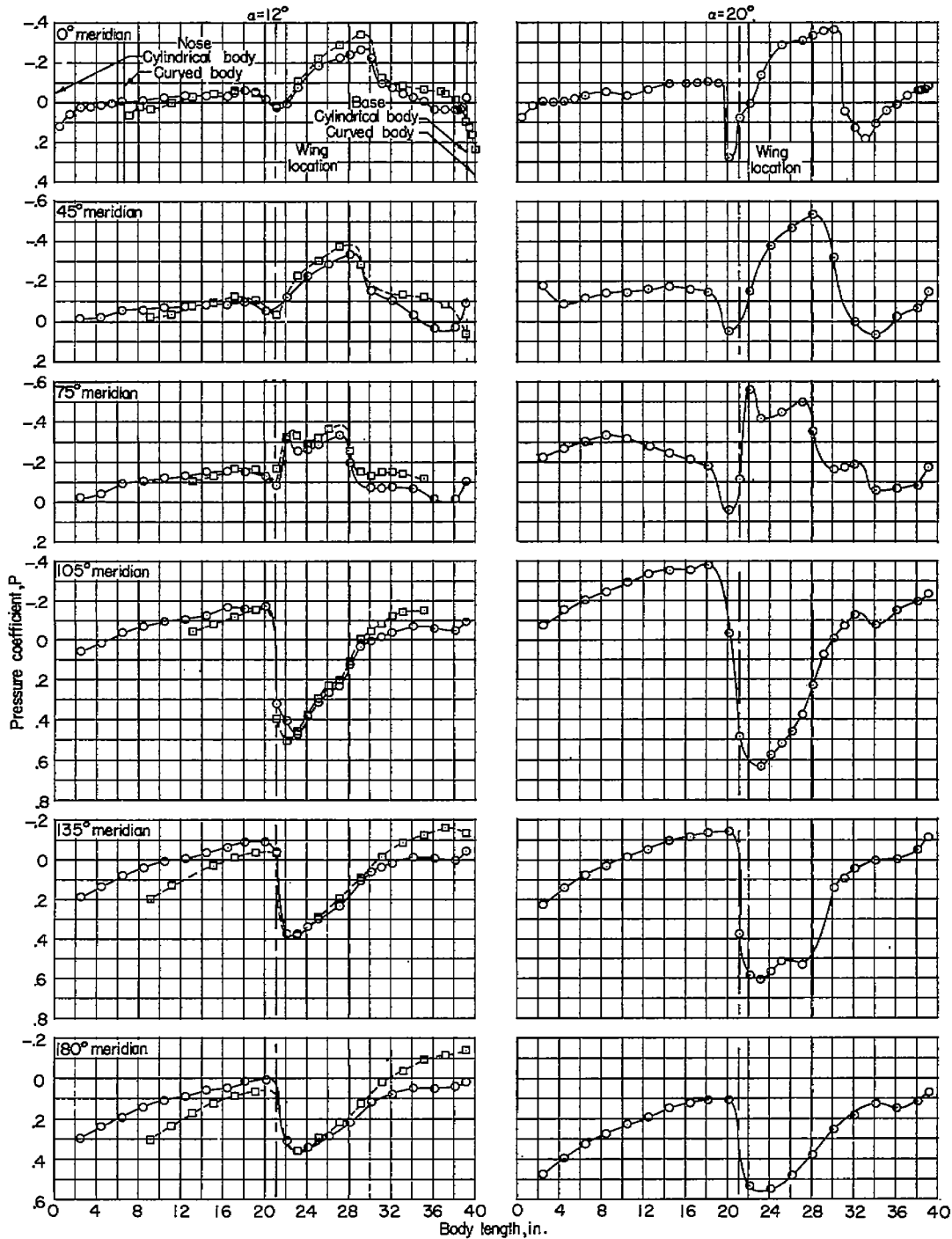


(i) $M = 1.10$; $\alpha = 8^\circ$ and 12° . Concluded.

Figure 6.- Continued.

Error

An error occurred while processing this page. See the system log for more details.



(j) $M = 1.13$; $\alpha = 12^\circ$ and 20° . Concluded.

Figure 6.- Concluded.

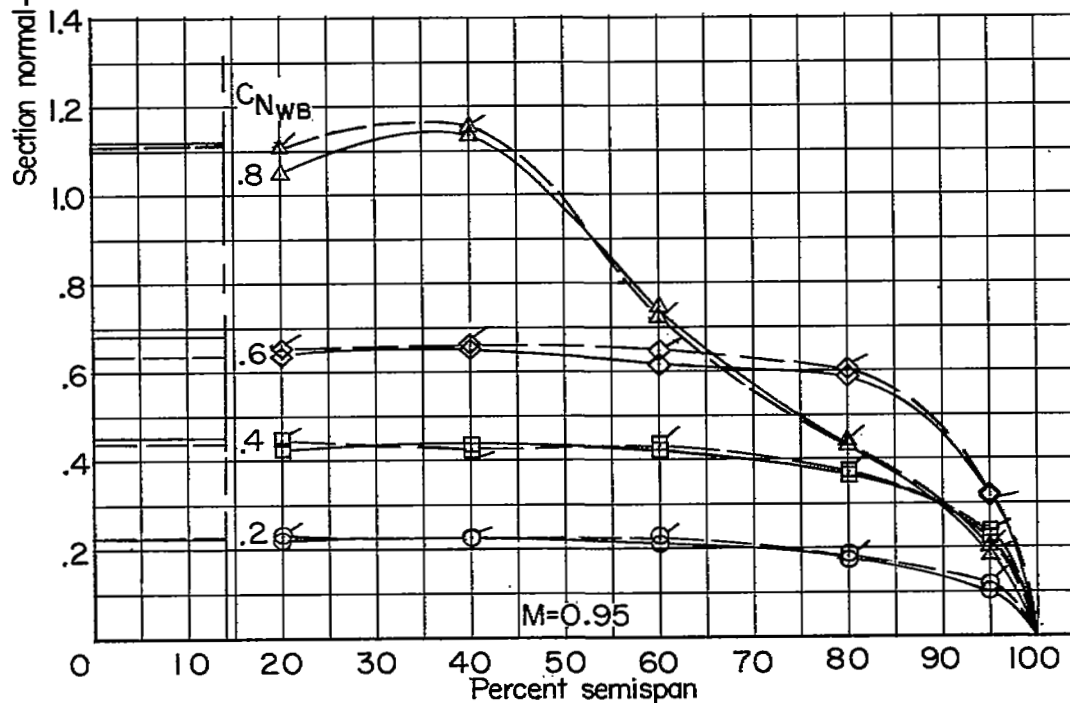
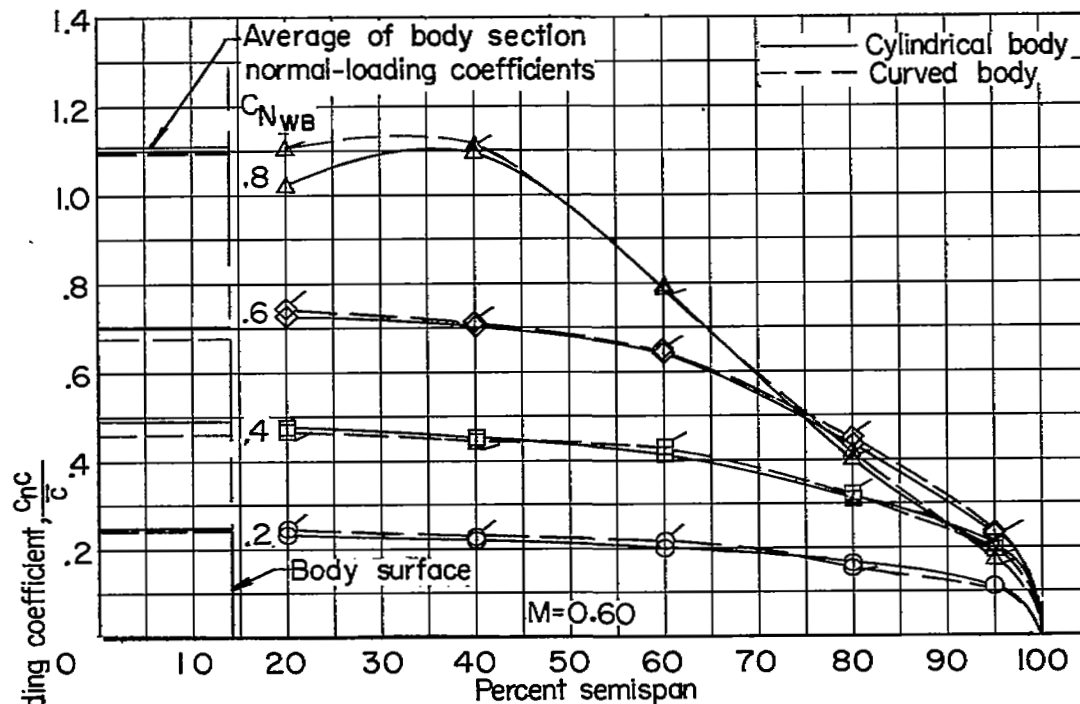


Figure 7.-- Spanwise distributions of section normal-loading coefficient at several total normal-force coefficients.

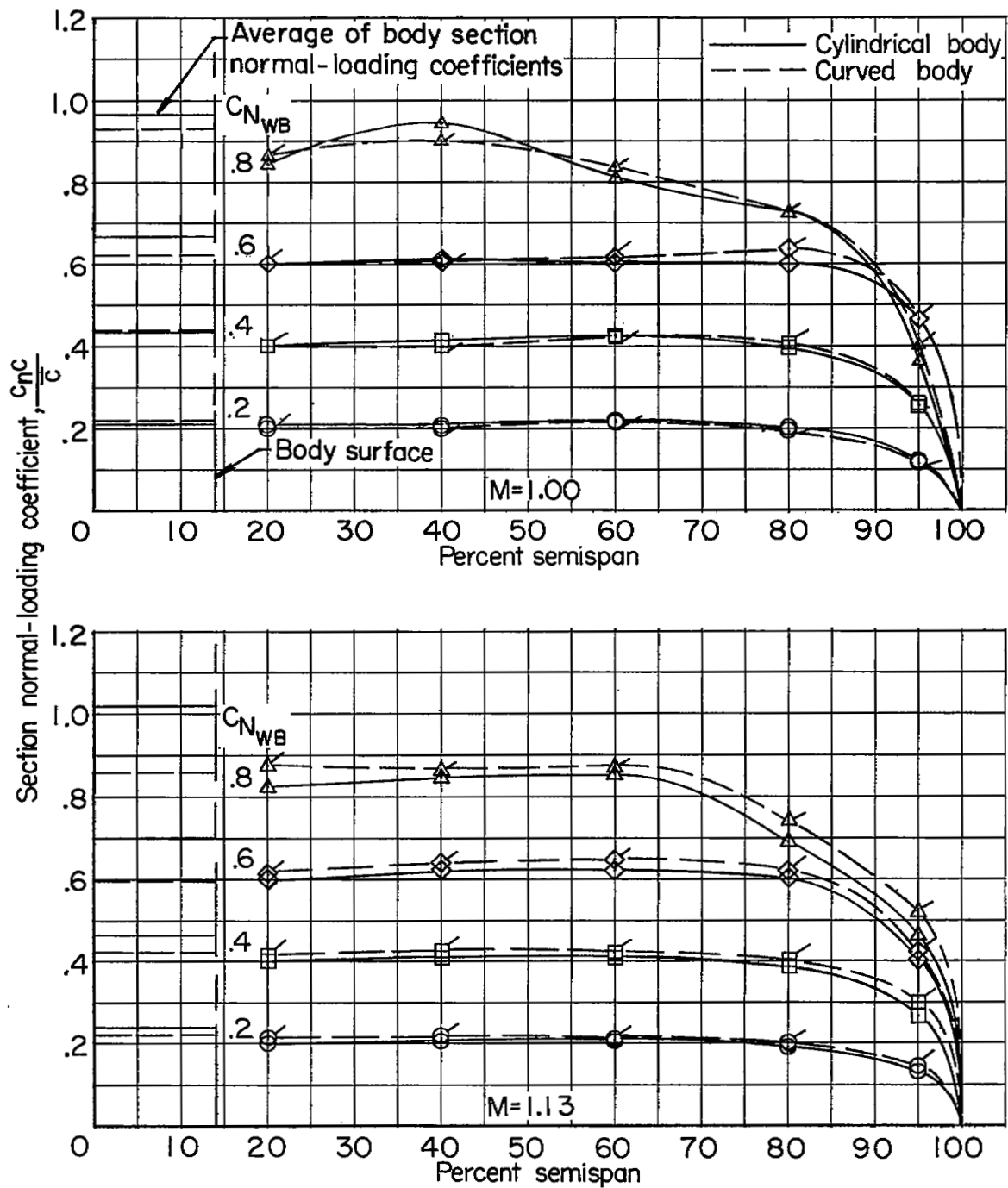


Figure 7.- Concluded.

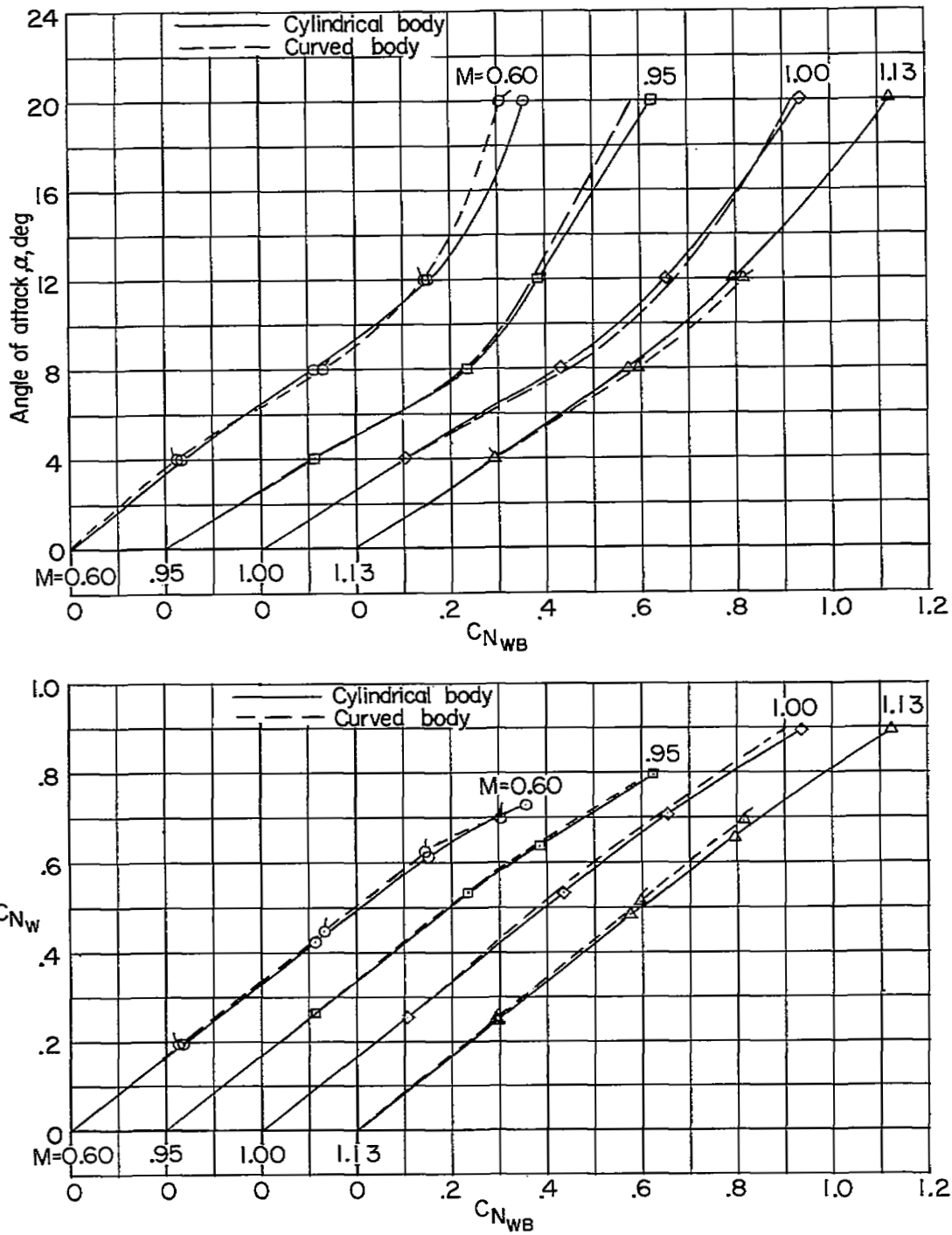


Figure 8.- Variation with total normal-force coefficient of angle of attack and exposed wing normal-force coefficient for several Mach numbers.

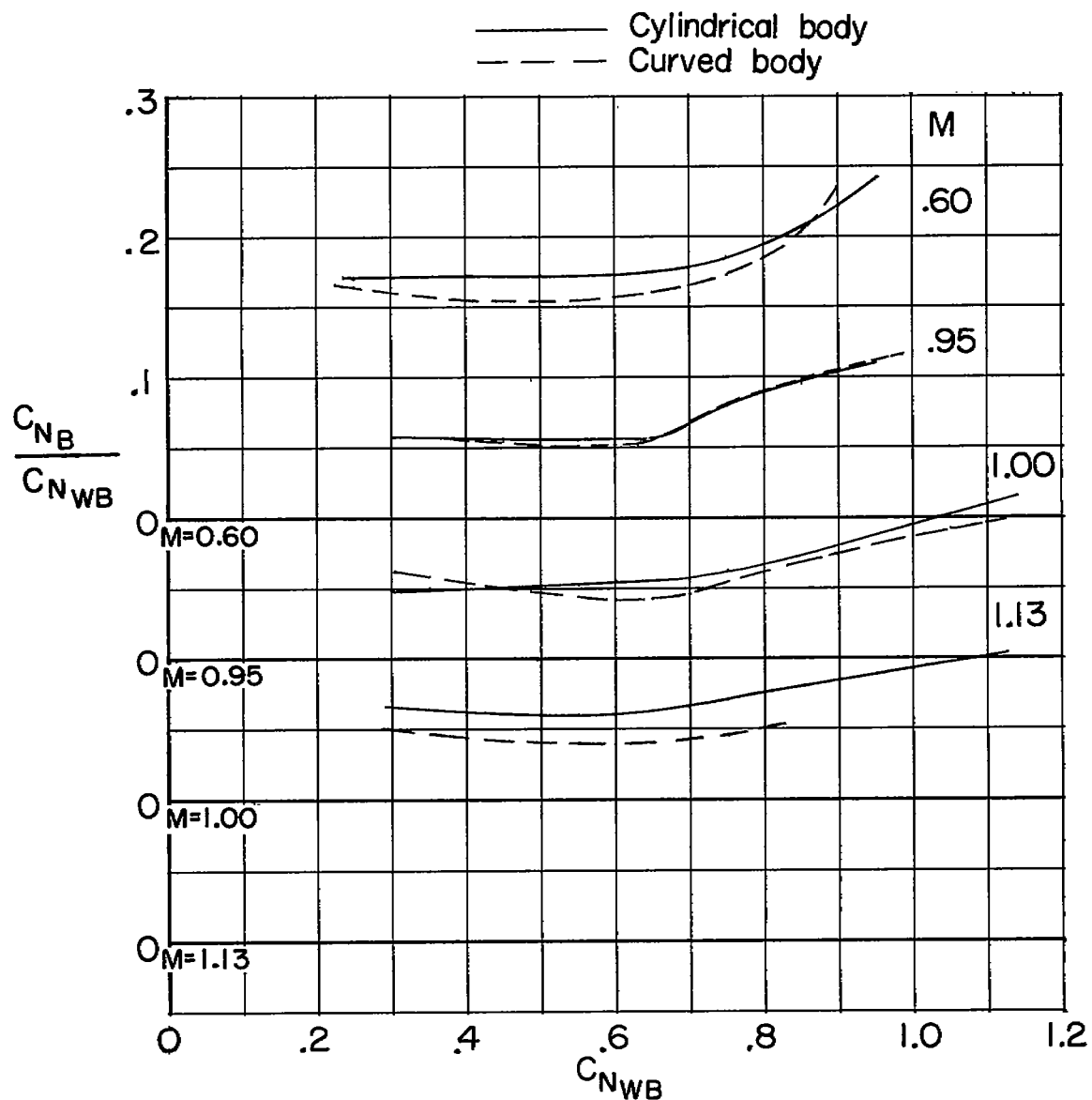


Figure 9.- Variation with total normal-force coefficient of load carried by body relative to load on wing-body combination at several Mach numbers.

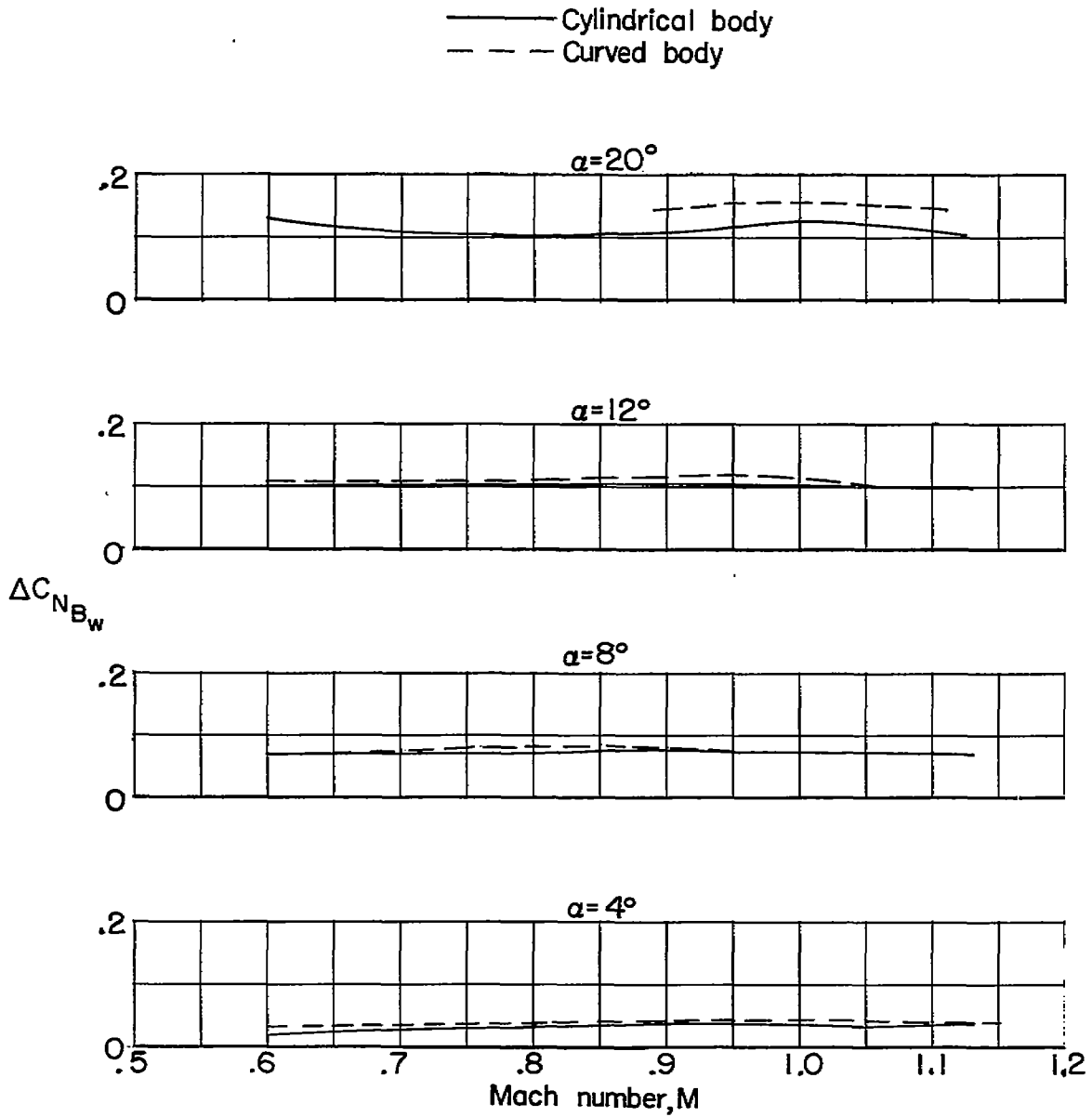


Figure 10.- Variation with Mach number of wing-body interference on load carried by body at several angles of attack.

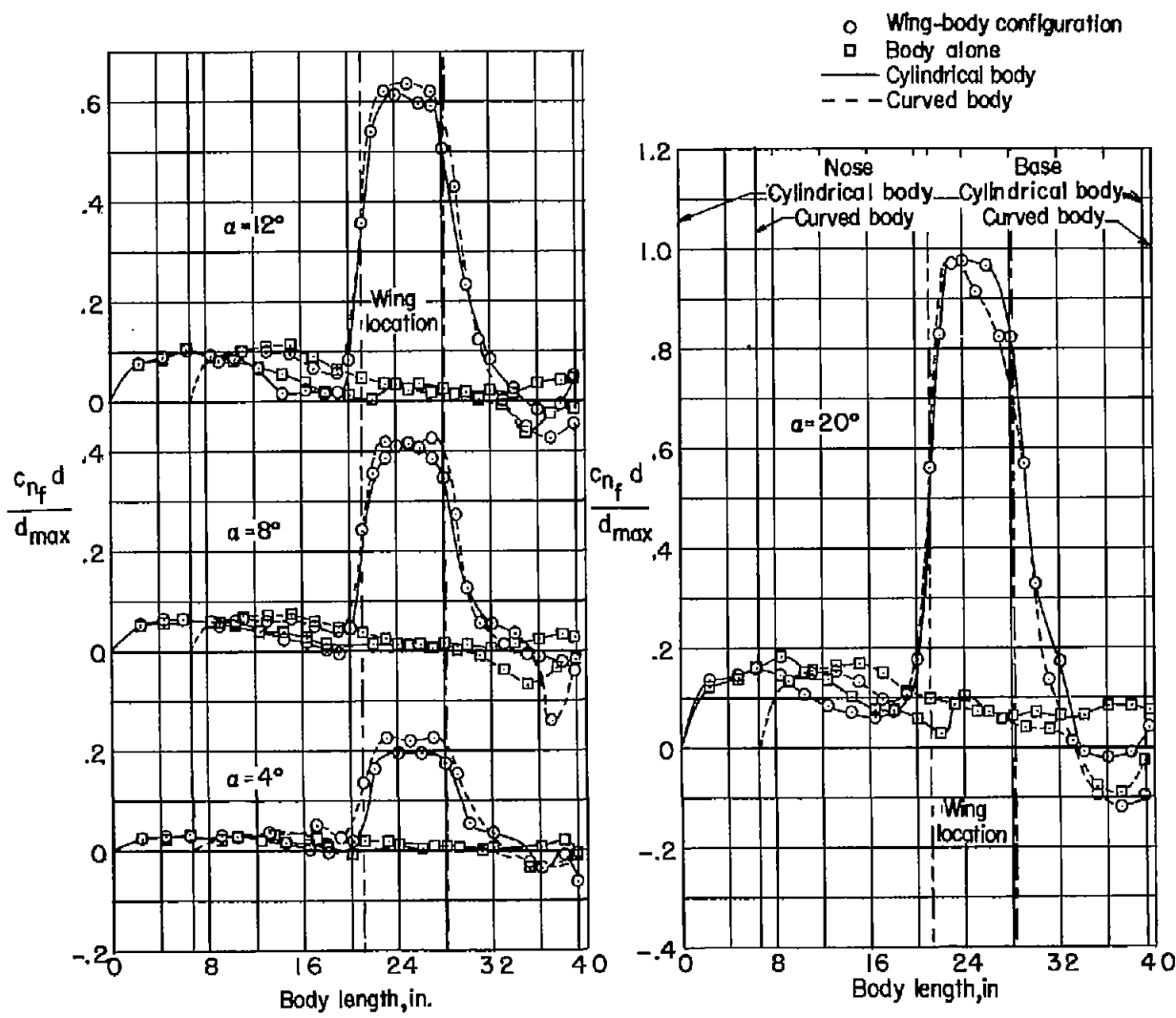


Figure 11.- Longitudinal distribution of loading over body and body with wing combination at several angles of attack. $M = 1.00$.

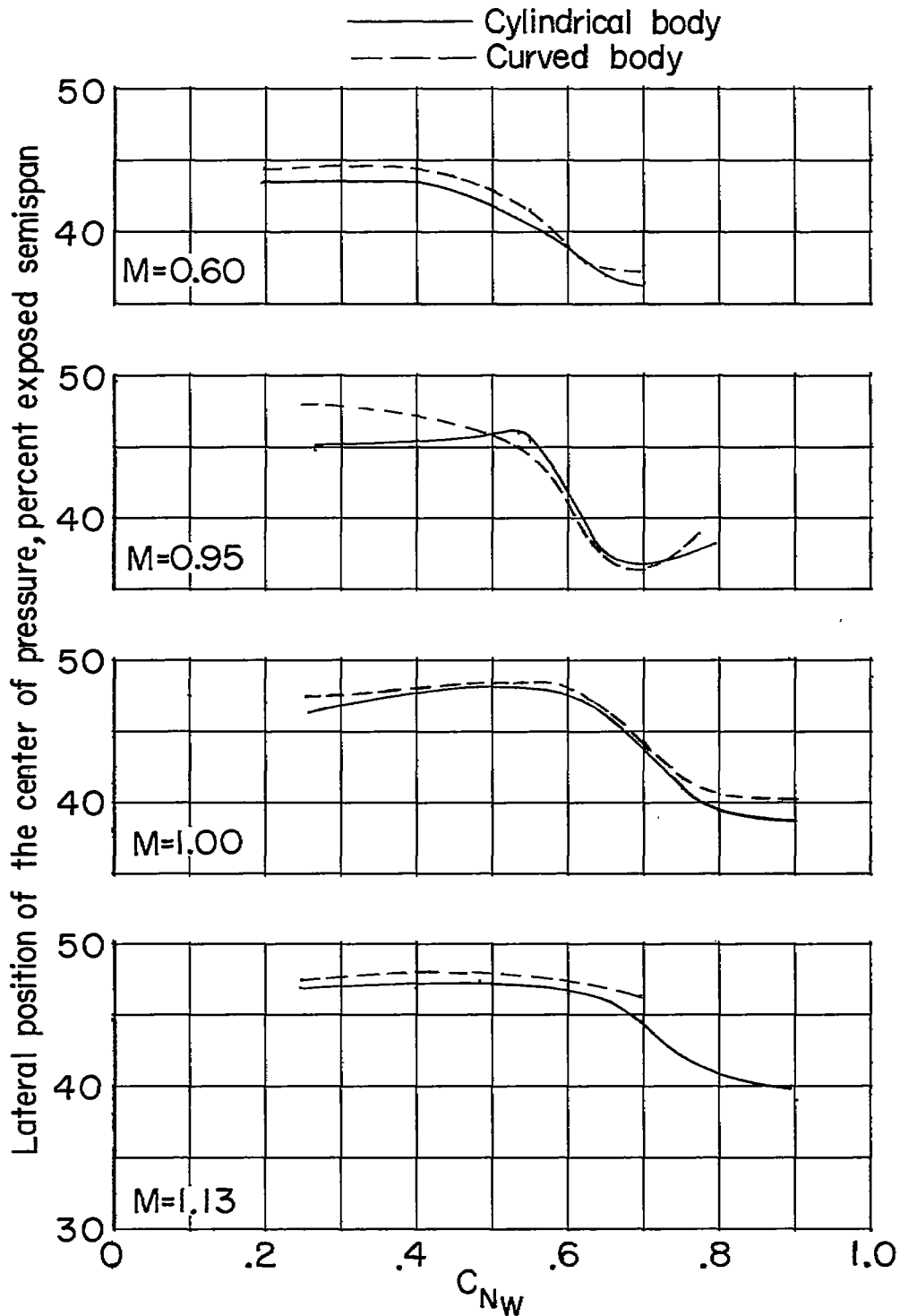


Figure 12.-- Variation with exposed wing normal-force coefficient of lateral position of center of pressure of exposed wing at several Mach numbers.

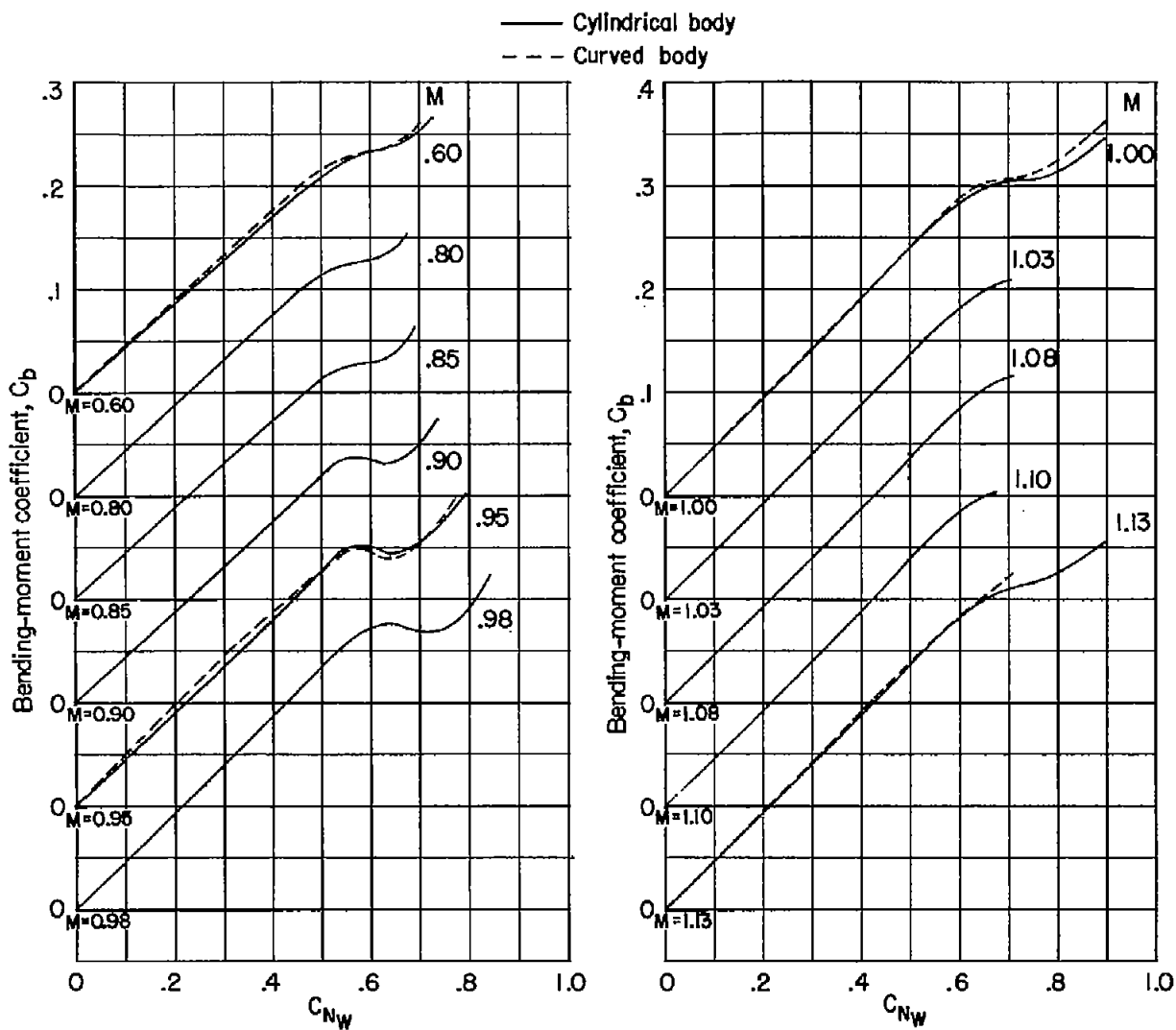


Figure 13.- Variation with exposed wing normal-force coefficient of bending-moment coefficient of exposed wing about wing-body juncture.

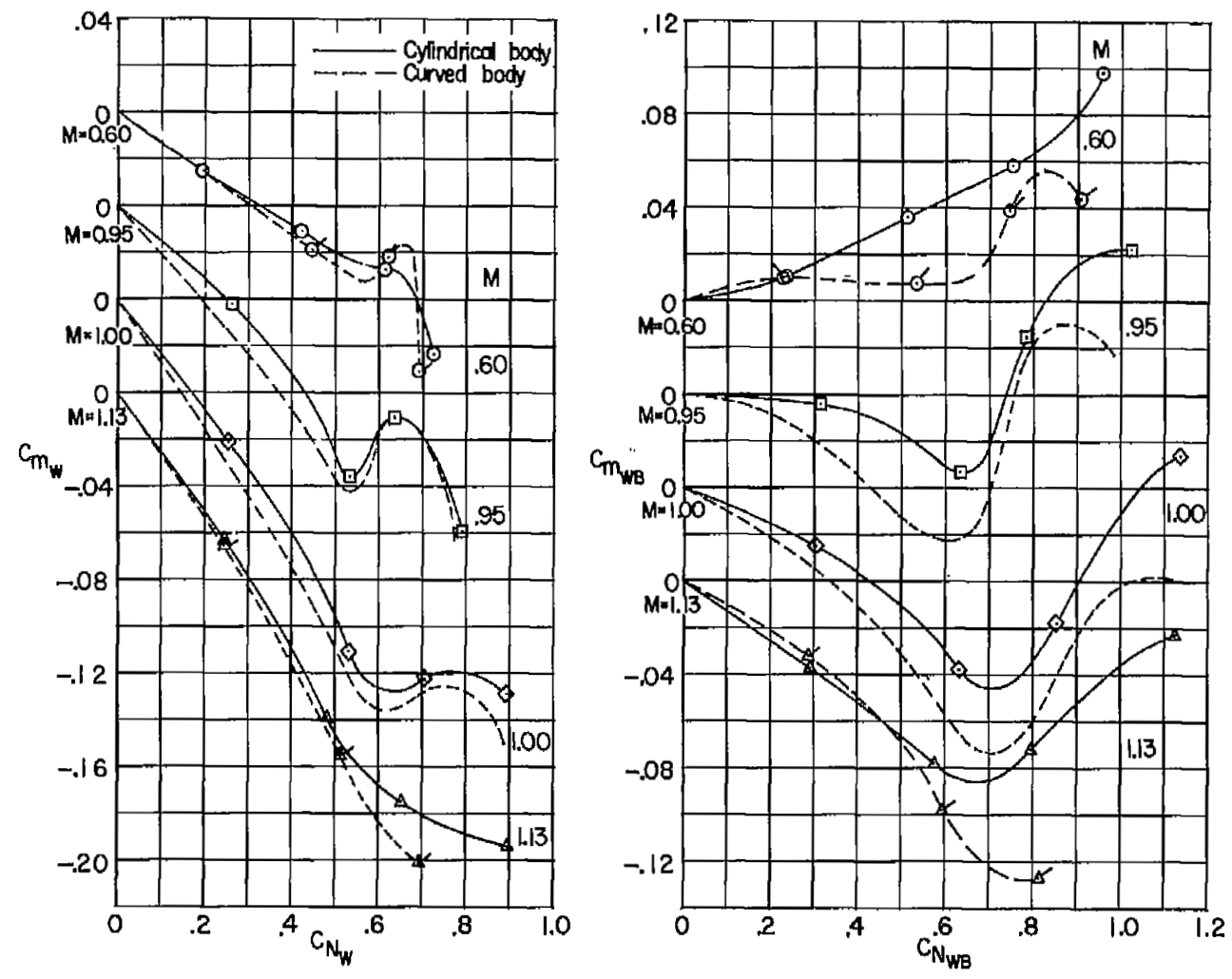


Figure 14.- Stability characteristics of exposed wing and wing-body combination at several Mach numbers.

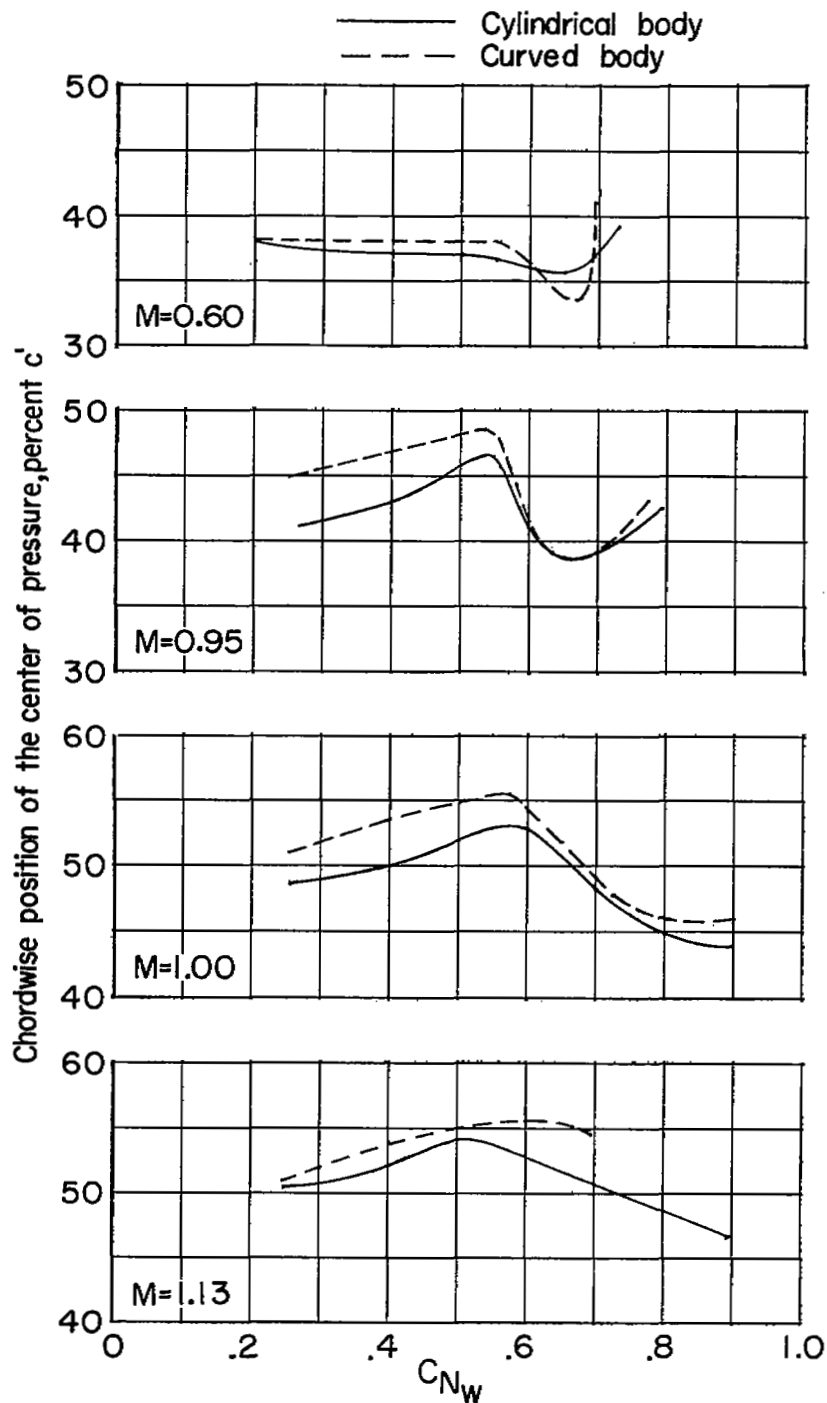


Figure 15.- Variation with exposed wing normal-force coefficient of chordwise position of center of pressure of exposed wing relative to leading edge of mean aerodynamic chord at several Mach numbers.

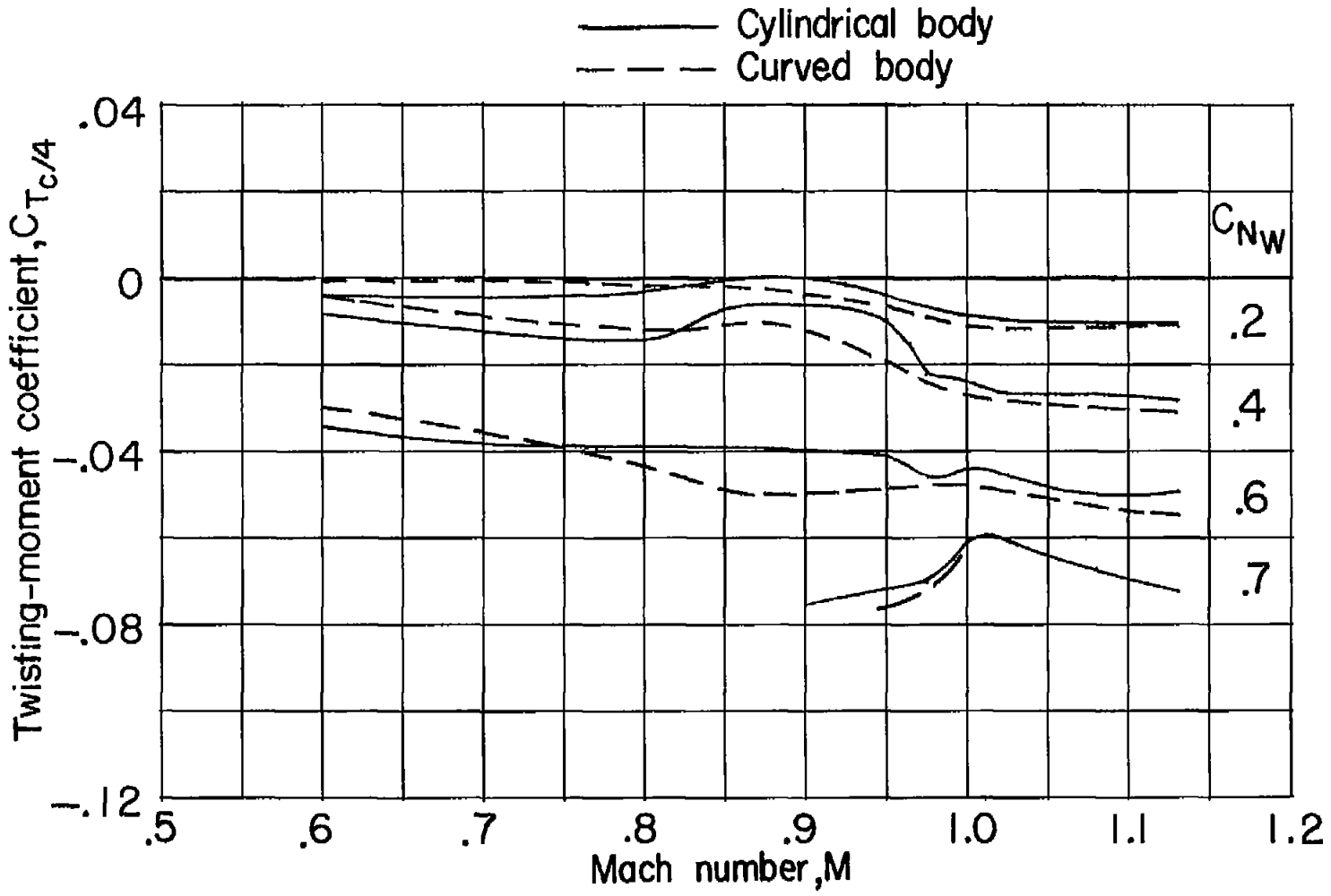


Figure 16.- Variation with Mach number of twisting-moment coefficient about the 0.25 chord of various wing stations at several exposed wing normal-force coefficients.



LANGLEY RESEARCH CENTER
3 1176 00516 9843

